TECHNISCHE UNIVERSITÄT MÜNCHEN

CRC110

QwG

Quarkonium:
exploring the QGP with
Effective Field Theories and Lattice

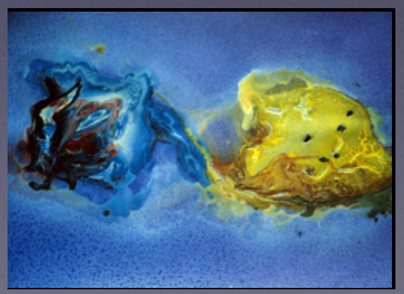

NORA BRAMBILLA

PHYSIK DEPARTMENT TUM
T30F

- EFTs and lattice are complementary tools for the study of Hard Probes in QGP

- EFTs and lattice are complementary tools for the study of Hard Probes in QGP

- EFTs allow to resum infinite class of diagrams related to the existence of a physical scale, to give a precise definition to objects of great phenomenological interest like the potential or transport coefficients, to factorize contributions of different scales, to give a systematical framework for calculation of observables

- Lattice can evaluate the nonperturbative correlators that appear in the EFT factorisation

Combinations of different EFTs and lattice allows us to use Hard Probes to test the QGP

- EFTs and lattice are complementary tools for the study of Hard Probes in QGP

- EFTs allow to resum infinite class of diagrams related to the existence of a physical scale, to give a precise definition to objects of great phenomenological interest like the potential or transport coefficients, to factorize contributions of different scales, to give a systematical framework for calculation of observables

- Lattice can evaluate the nonperturbative correlators that appear in the EFT factorisation

Combinations of different EFTs and lattice allows us to use Hard Probes to test the QGP

- Examples include: free energies, entropy, static potential at finite T, nonequilibrium quarkonium evolution in strongly coupled medium, transport coefficients

- EFTs and lattice are complementary tools for the study of Hard Probes in QGP

- EFTs allow to resum infinite class of diagrams related to the existence of a physical scale, to give a precise definition to objects of great phenomenological interest like the potential or transport coefficients, to factorize contributions of different scales, to give a systematical framework for calculation of observables

- Lattice can evaluate the nonperturbative correlators that appear in the EFT factorisation

Combinations of different EFTs and lattice allows us to use Hard Probes to test the QGP

- Examples include: free energies, entropy, static potential at finite T, nonequilibrium quarkonium evolution in strongly coupled medium, transport coefficients

- To boost EFT and lattice interface we founded the TUMQCD lattice collaboration
- We need the help of the lattice community in a structured effort to calculate all the needed correlators

- We focus on quarkonium
- Quarkonium suppression identified as a probe of QGP by Matsui and Satz in 1986 in relation to screening

- We focus on quarkonium
- Quarkonium suppression identified as a probe of QGP by Matsui and Satz in 1986 in relation to screening
- Quarkonium is a nonrelativistic quantum bound system, i.e. a multiscale system
- To treat Quarkonium in QFT is necessary to develop appropriate nonrelativistic effective field theories (NREFTs)—> potential Nonrelativistic QCD-pNRQCD
- Quarkonium (spectrum, decay, production) is well understood at T=0 on the basis of pNRQCD and lattice

- We focus on quarkonium
- Quarkonium suppression identified as a probe of QGP by Matsui and Satz in 1986 in relation to screening
- Quarkonium is a nonrelativistic quantum bound system, i.e. a multiscale system
- To treat Quarkonium in QFT is necessary to develop appropriate nonrelativistic effective field theories (NREFTs)—> potential Nonrelativistic QCD-pNRQCD
- Quarkonium (spectrum, decay, production) is well understood at T=0 on the basis of pNRQCD and lattice
- Using pNRQCD at finite T to determine quarkonium interaction in medium we get a change of paradigm: suppression not driven by screening but by the imaginary parts in the potentials which have a physical interpretation

- We focus on quarkonium
- Quarkonium suppression identified as a probe of QGP by Matsui and Satz in 1986 in relation to screening
- Quarkonium is a nonrelativistic quantum bound system, i.e. a multiscale system
- To treat Quarkonium in QFT is necessary to develop appropriate nonrelativistic effective field theories (NREFTs)—> potential Nonrelativistic QCD-pNRQCD
- Quarkonium (spectrum, decay, production) is well understood at T=0 on the basis of pNRQCD and lattice
- Using pNRQCD at finite T to determine quarkonium interaction in medium we get a change of paradigm: suppression not driven by screening but by the imaginary parts in the potentials which have a physical interpretation
- Quarkonium quantum nonequilibrium propagation in medium can be addressed using pNRQCD at finite T, open quantum systems and Lattice
- The QGP is characterized by two transport coefficients defined in terms of nonperturbative correlators calculated on the lattice->no free parameter

- We focus on quarkonium
- Quarkonium suppression identified as a probe of QGP by Matsui and Satz in 1986 in relation to screening
- Quarkonium is a nonrelativistic quantum bound system, i.e. a multiscale system
- To treat Quarkonium in QFT is necessary to develop appropriate nonrelativistic effective field theories (NREFTs)—> potential Nonrelativistic QCD-pNRQCD
- Quarkonium (spectrum, decay, production) is well understood at T=0 on the basis of pNRQCD and lattice
- Using pNRQCD at finite T to determine quarkonium interaction in medium we get a change of paradigm: suppression not driven by screening but by the imaginary parts in the potentials which have a physical interpretation
- Quarkonium quantum nonequilibrium propagation in medium can be addressed using pNRQCD at finite T, open quantum systems and Lattice
- The QGP is characterized by two transport coefficients defined in terms of nonperturbative correlators calculated on the lattice->no free parameter
- I will discuss the type of lattice correlators needed and methods to calculate them

NOTICE for what concerns the nonequilibrium medium evolution:

NOTICE for what concerns the nonequilibrium medium evolution:

- What I discuss can be applied to jets using SCET and open quantum systems

NOTICE for what concerns the nonequilibrium medium evolution:

- What I discuss can be applied to jets using SCET and open quantum systems

- It can be generalised to X Y Z using BOEFT (Born-Oppenheimer EFT that we developed) and open quantum systems

NOTICE for what concerns the nonequilibrium medium evolution:

- What I discuss can be applied to jets using SCET and open quantum systems

- It can be generalised to X Y Z using BOEFT (Born-Oppenheimer EFT that we developed) and open quantum systems

- It is not depending on the medium : it can be a hot medium or a dense medium, weakly or strongly coupled

in what I will present T may be substituted as the inverse of a correlation length characterising the system—> does not need to be a thermal medium can be e.g. cold nuclear matter. It may be useful to treat processes at non vanishing chemical potential at EIC

Material for discussion/references

N. Brambilla, M. A. Escobedo, J. Soto and A. Vairo, Phys. Rev. D **96** (2017) no.3, 034021 [arXiv:1612.07248 [hep-ph]].

N. Brambilla, M. A. Escobedo, J. Soto and A. Vairo, Phys. Rev. D **97** (2018) no.7, 074009 [arXiv:1711.04515 [hep-ph]].

N. Brambilla, M. A. Escobedo, A. Vairo and P. Vander Griend, Phys. Rev. D **100** (2019) no.5, 054025 [arXiv:1903.08063 [hep-ph]].

N. Brambilla, M. A. Escobedo, M. Strickland, A. Vairo, P. Vander Griend and J. H. Weber, [arXiv:2012.01240 [hep-ph]].

Non-equilibrium evolution in QGP

and arXiv: 2107 .06222

M. Escobedo *Phys.Rev.D* 103 (2021) 3, 034010 • e-Print: 2010.10424 [

N. Brambilla,J. Ghiglieri, A. Vairo, Peter Petreczky
Phys.Rev.D 78 (2008) 014017 • e-Print: 0804.0993 [hep-ph]

N. Brambilla, M. Escobedo, J. Ghiglieri, A. Vairo
JHEP 05 (2013) 130 • e-Print: 1303.6097 [hep-ph]

Potential and energies in medium

N. Brambilla, M. Escobedo, J. Ghiglieri, A. Vairo
JHEP 12 (2011) 116 • e-Print: 1109.5826 [hep-ph]

N. Brambilla, M. Escobedo, J. Ghiglieri, J. Soto, A. Vairo
JHEP 09 (2010) 038 • e-Print: 1007.4156 [hep-ph]

N. Brambilla, A. Pineda, J. Soto, A. Vairo
Rev. Mod . Phys 77 (2005) 1423 • hep-ph/0410047

pNRQCD

N. Brambilla, A. Pineda J. Soto, A. Vairo
Nucl. Phys. B566 (2000) 275• hep-ph/9907240

N. Brambilla, V. Leino, Peter Petreczky, A. Vairo
Phys.Rev.D102 (220) 074503 • e-Print 2007.100

Lattice calculation of the heavy quark transport coefficient

Heavy quarks are QGP probes

- heavy quark are produced at the beginning and remain up to the end
- The heavy-quark mass introduces one or more large scales, whose contributions may be factorized and computed in perturbation theory ($\alpha_{\rm s}(M) \ll 1$).
- Low-energy scales are sensitive to the temperature.
  Low-energy contributions may be accessible via lattice calculations.

Heavy quarks are QGP probes

- heavy quark are produced at the beginning and remain up to the end
- The heavy-quark mass introduces one or more large scales, whose contributions may be factorized and computed in perturbation theory ($\alpha_{\rm s}(M) \ll 1$).
- Low-energy scales are sensitive to the temperature.
  Low-energy contributions may be accessible via lattice calculations.

Quarkonia are better hard probes
because they are multi scale systems

NR bound states formed by heavy quarks offer a privileged access to strong interactions

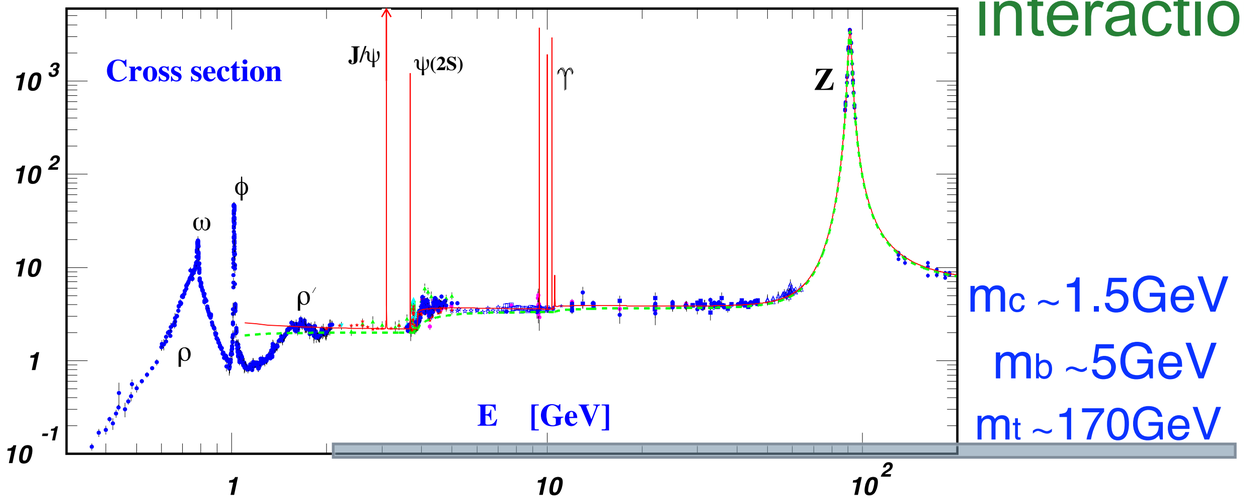

$m_c \sim 1.5\text{GeV}$

$m_b \sim 5\text{GeV}$

$m_t \sim 170\text{GeV}$

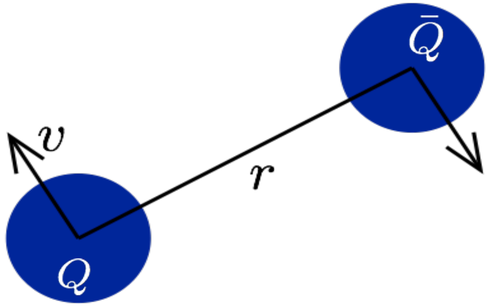

with $Q, \bar{Q} = c, b, t$

NR bound states formed by heavy quarks offer a privileged access to strong interactions

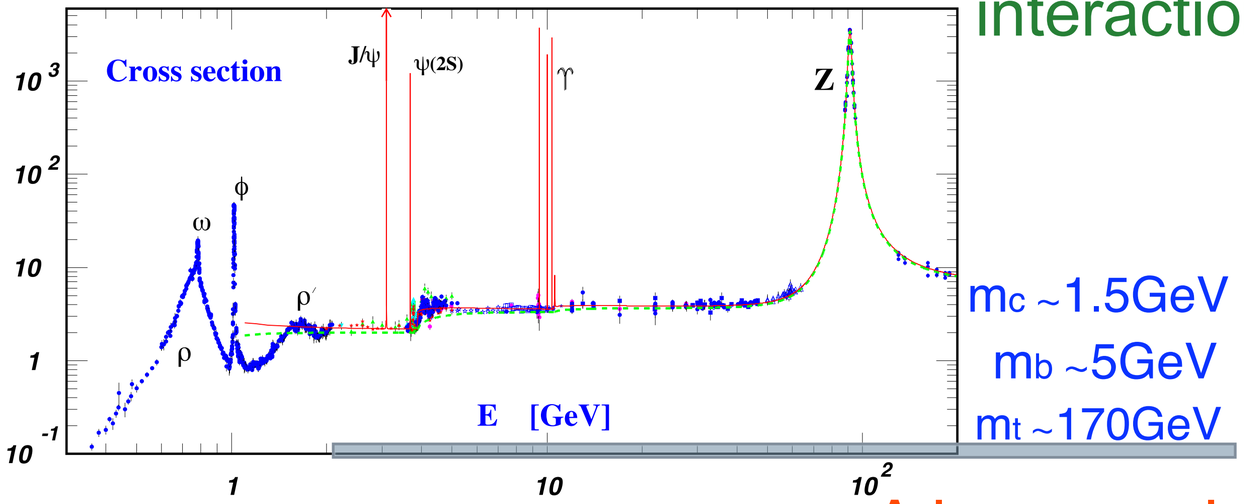

$m_c \sim 1.5\text{GeV}$

$m_b \sim 5\text{GeV}$

$m_t \sim 170\text{GeV}$

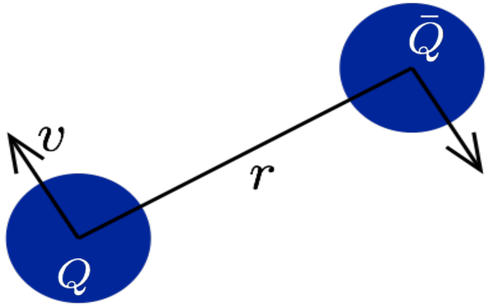

with $Q, \bar{Q} = c, b, t$

A large scale $m_Q \gg \Lambda_{\rm QCD}$ $\alpha_s(m_Q) \ll 1$

NR bound states formed by heavy quarks offer a privileged access to strong interactions

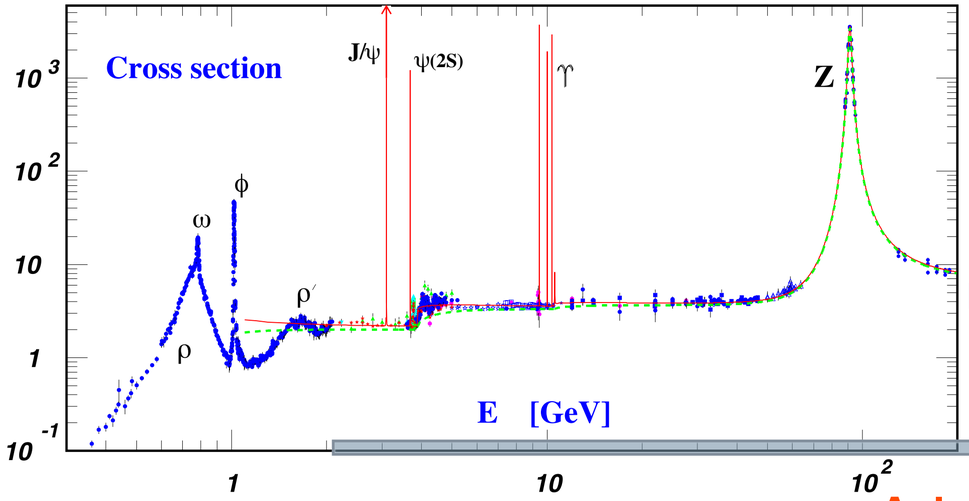

$m_c \sim 1.5\text{GeV}$

$m_b \sim 5\text{GeV}$

$m_t \sim 170\text{GeV}$

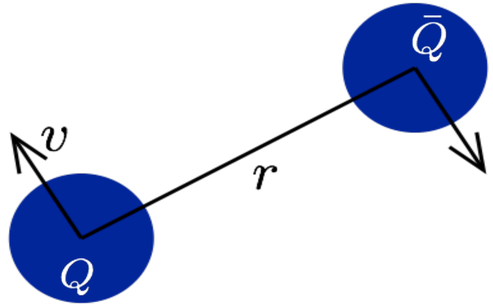

with $Q, \bar{Q} = c, b, t$

A large scale $m_Q \gg \Lambda_{\rm QCD}$ $\alpha_s(m_Q) \ll 1$

Heavy quarkonium is very different from heavy-light hadrons

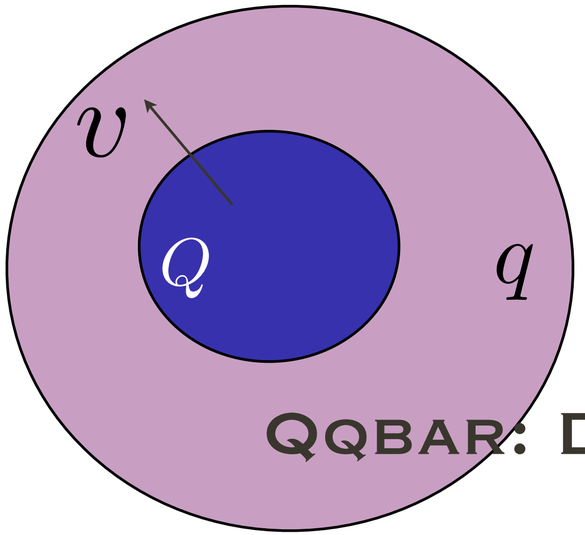

different physics from the heavy light meson where only two scales exist m and Λ_{QCD}

QQBAR: D, B MESONS

NR bound states formed by heavy quarks offer a privileged access to strong interactions

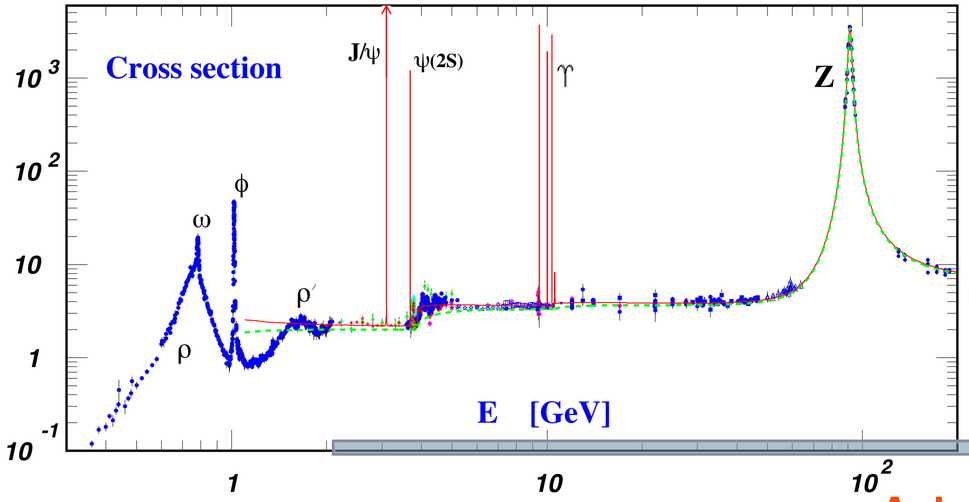

$m_c \sim 1.5\text{GeV}$

$m_b \sim 5\text{GeV}$

$m_t \sim 170\text{GeV}$

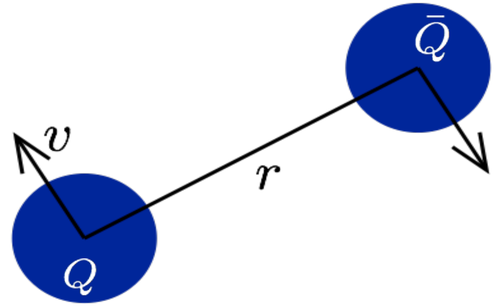

with $Q, \bar{Q} = c, b, t$

A large scale $m_Q \gg \Lambda_{\rm QCD}$ $\alpha_s(m_Q) \ll 1$

Heavy quarkonium is very different from heavy-light hadrons

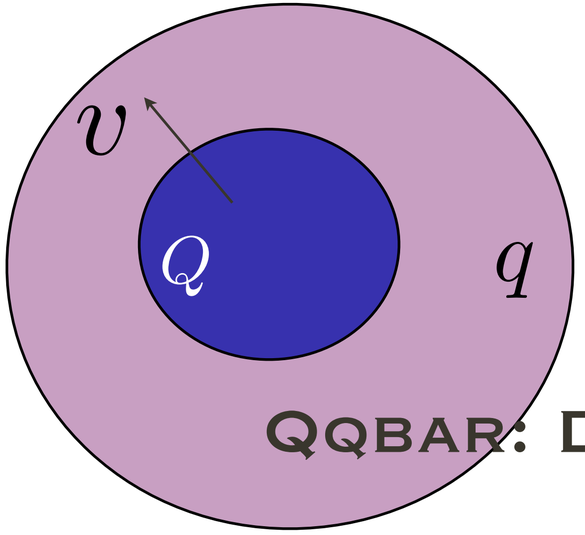

different physics from the heavy light meson where only two scales exist m and Λ_{QCD}

for heavy-light the EFT is HQET (Heavy Quark Effective Theory)

QQBAR: D, B MESONS

Quarkonium scales

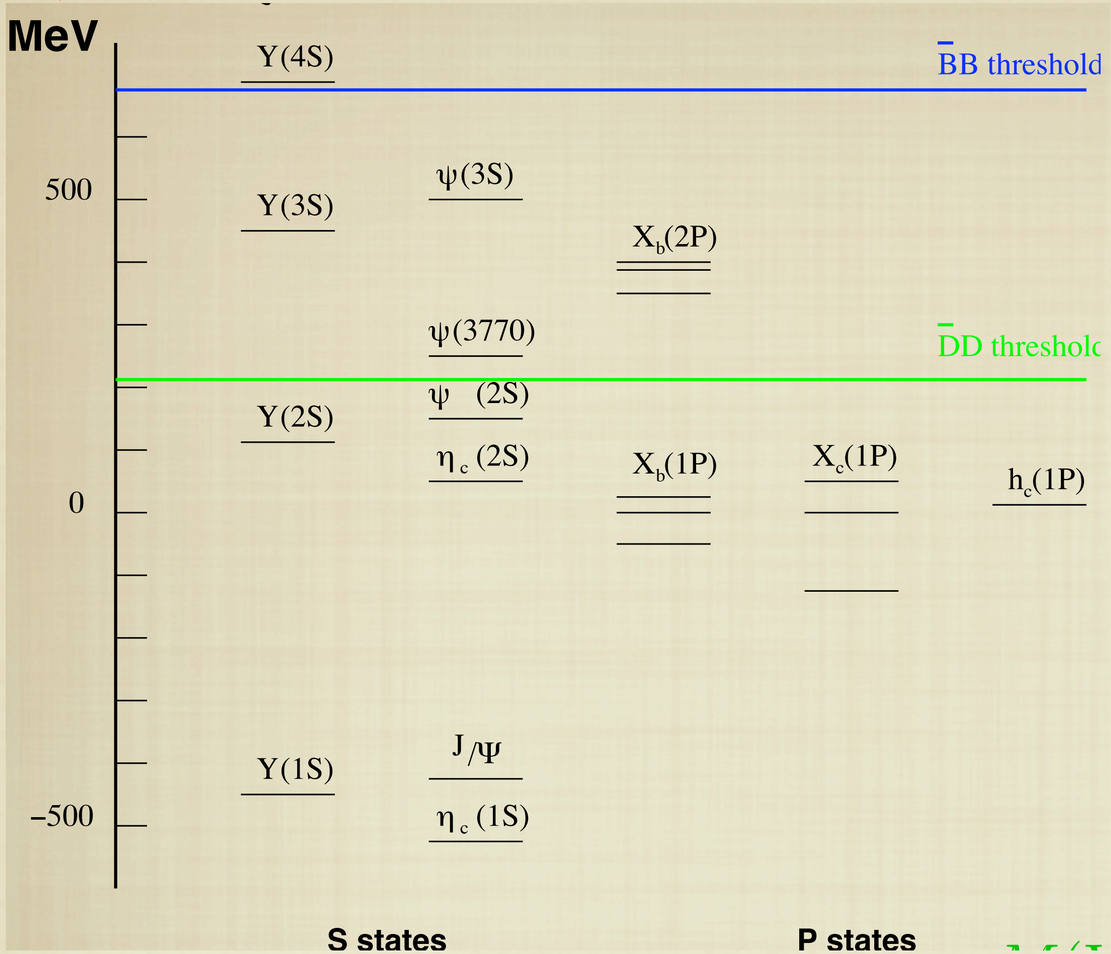

Normalized with respect to $\chi_b(1P)$ and $\chi_c(1P)$

$^{2S+1}L_J$

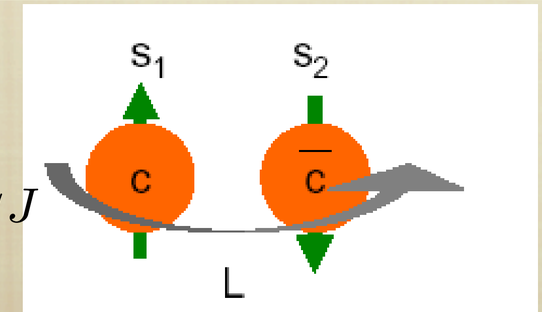

The mass scale is perturbative

$$m_Q \gg \Lambda_{\rm QCD}$$

$$m_b \simeq 5\,\text{GeV}; m_c \simeq 1.5\,\text{GeV}$$

$$M(Y(1S)) = 9460\,\text{GeV}$$

$$M(J/\Psi) = 3097\,\text{GeV}$$

Quarkonium scales

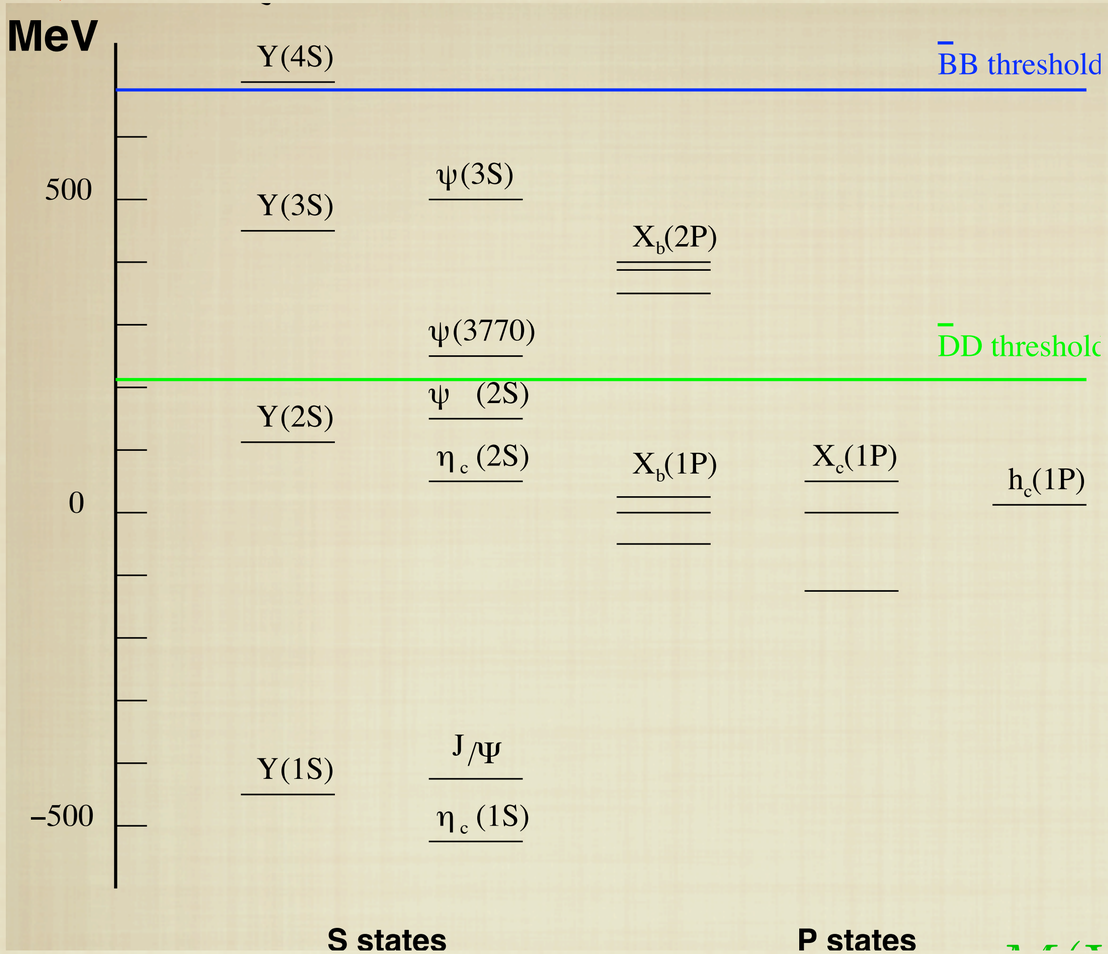

Normalized with respect to $\chi_b(1P)$ and $\chi_c(1P)$

$^{2S+1}L_J$

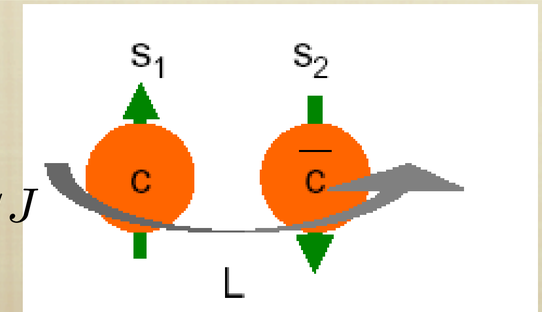

The system is nonrelativistic(NR)

$$\Delta E \sim mv^2, \Delta_{fs} E \sim mv^4$$

$$v_b^2 \sim 0.1, v_c^2 \sim 0.3$$

The mass scale is perturbative

$$m_Q \gg \Lambda_{\rm QCD}$$

$$m_b \simeq 5\,{\rm GeV}; m_c \simeq 1.5\,{\rm GeV}$$

$$M(Y(1S)) = 9460\,{\rm GeV}$$

$$M(J/\Psi) = 3097\,{\rm GeV}$$

Quarkonium scales

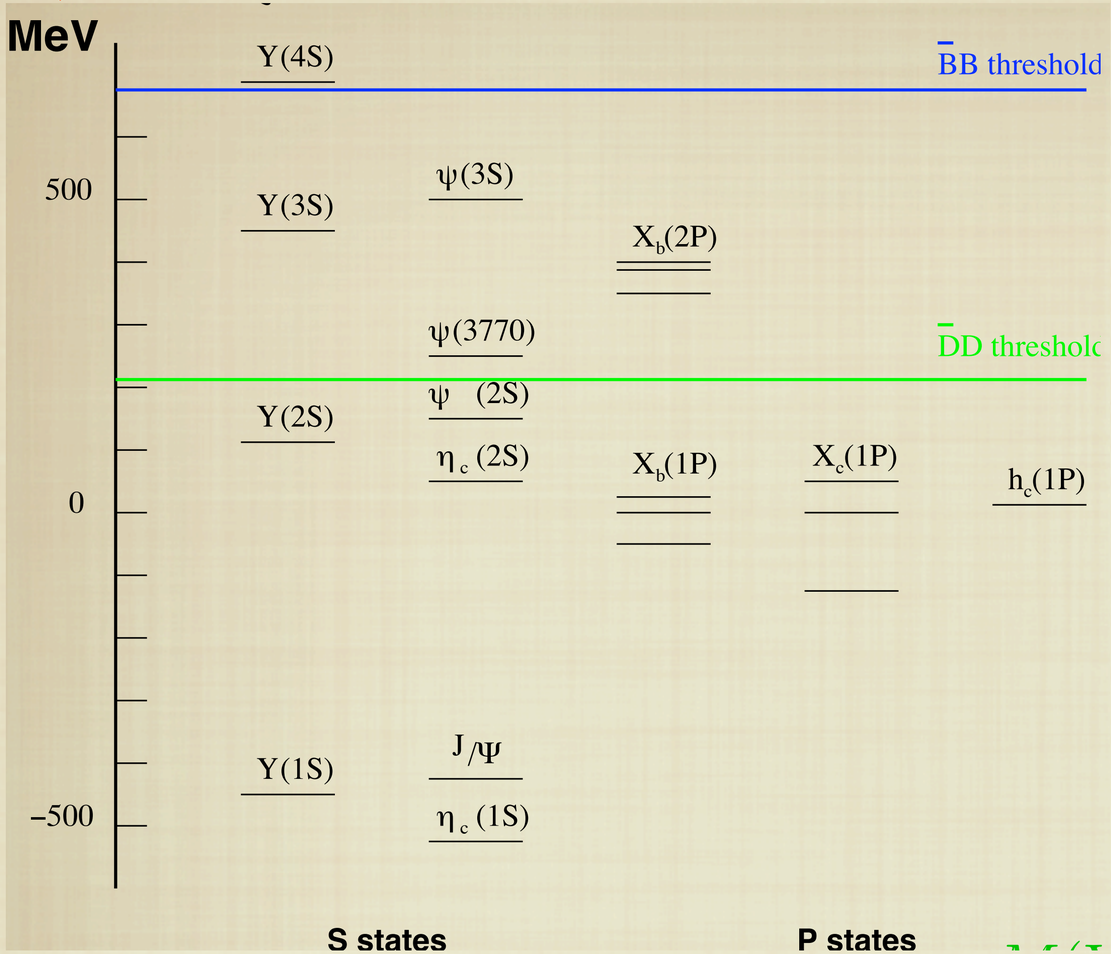

Normalized with respect to $\chi_b(1P)$ and $\chi_c(1P)$

$^{2S+1}L_J$

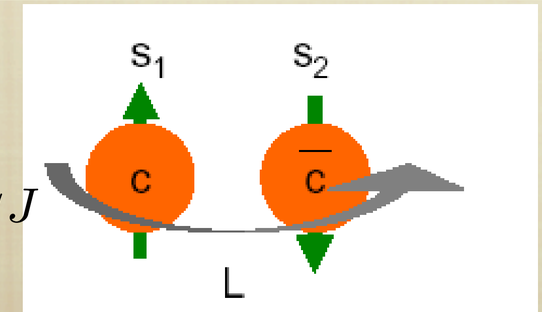

NR bound states have at least 3 scales

$$m \gg mv \gg mv^2 \quad v \ll 1$$

The system is nonrelativistic(NR)

$$\Delta E \sim mv^2, \Delta_{fs} E \sim mv^4$$

$$v_b^2 \sim 0.1, v_c^2 \sim 0.3$$

The mass scale is perturbative

$$m_Q \gg \Lambda_{\rm QCD}$$

$$m_b \simeq 5\,{\rm GeV}; m_c \simeq 1.5\,{\rm GeV}$$

$$M(Y(1S)) = 9460\,{\rm GeV}$$

$$M(J/\Psi) = 3097\,{\rm GeV}$$

Quarkonium scales

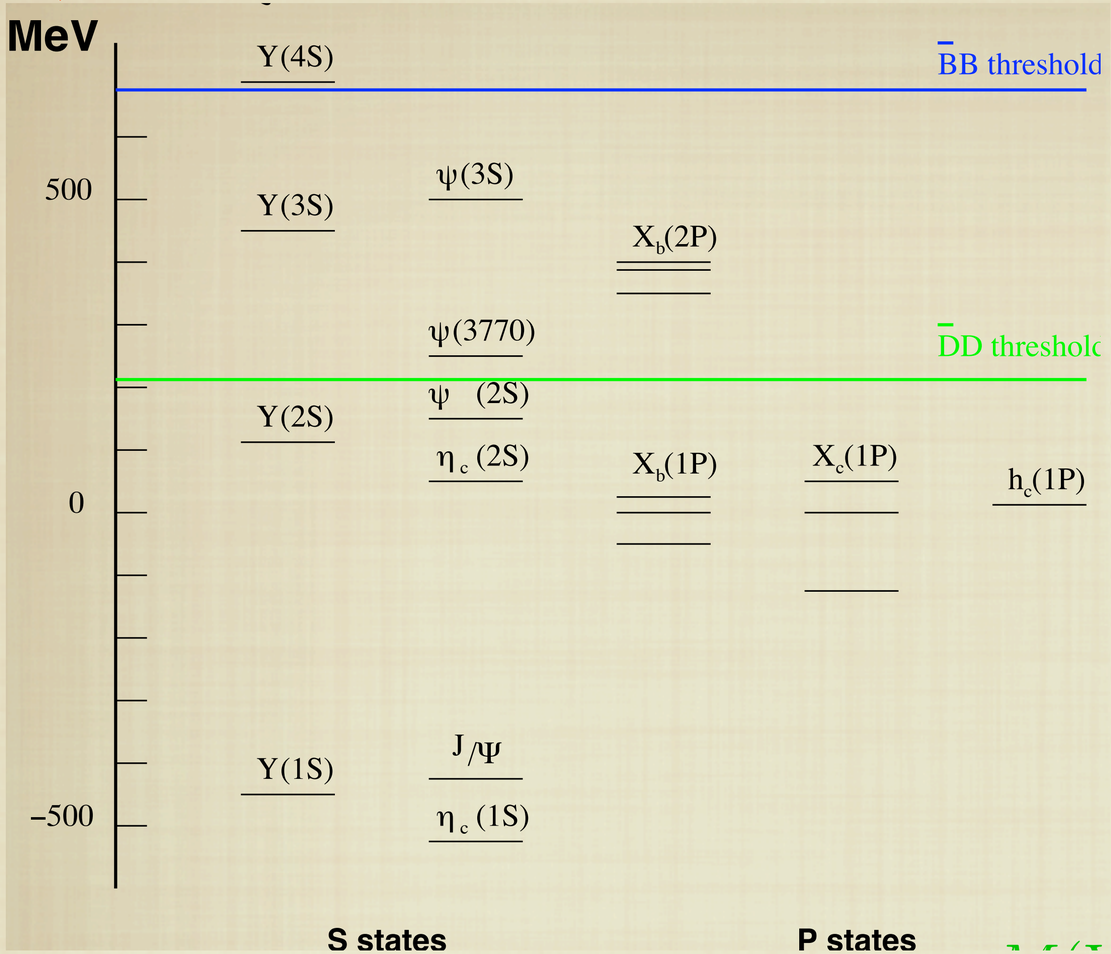

Normalized with respect to $\chi_b(1P)$ and $\chi_c(1P)$

$^{2S+1}L_J$

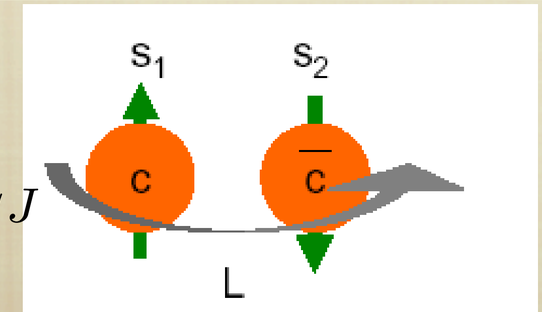

NR bound states have at least 3 scales

$$m \gg mv \gg mv^2 \quad v \ll 1$$

$$mv \sim r^{-1}$$

The system is nonrelativistic(NR)

$$\Delta E \sim mv^2, \Delta_{fs} E \sim mv^4$$

$$v_b^2 \sim 0.1, v_c^2 \sim 0.3$$

The mass scale is perturbative

$$m_Q \gg \Lambda_{\rm QCD}$$

$$m_b \simeq 5\,{\rm GeV}; m_c \simeq 1.5\,{\rm GeV}$$

$$M(Y(1S)) = 9460\,{\rm GeV}$$

$$M(J/\Psi) = 3097\,{\rm GeV}$$

Quarkonium scales

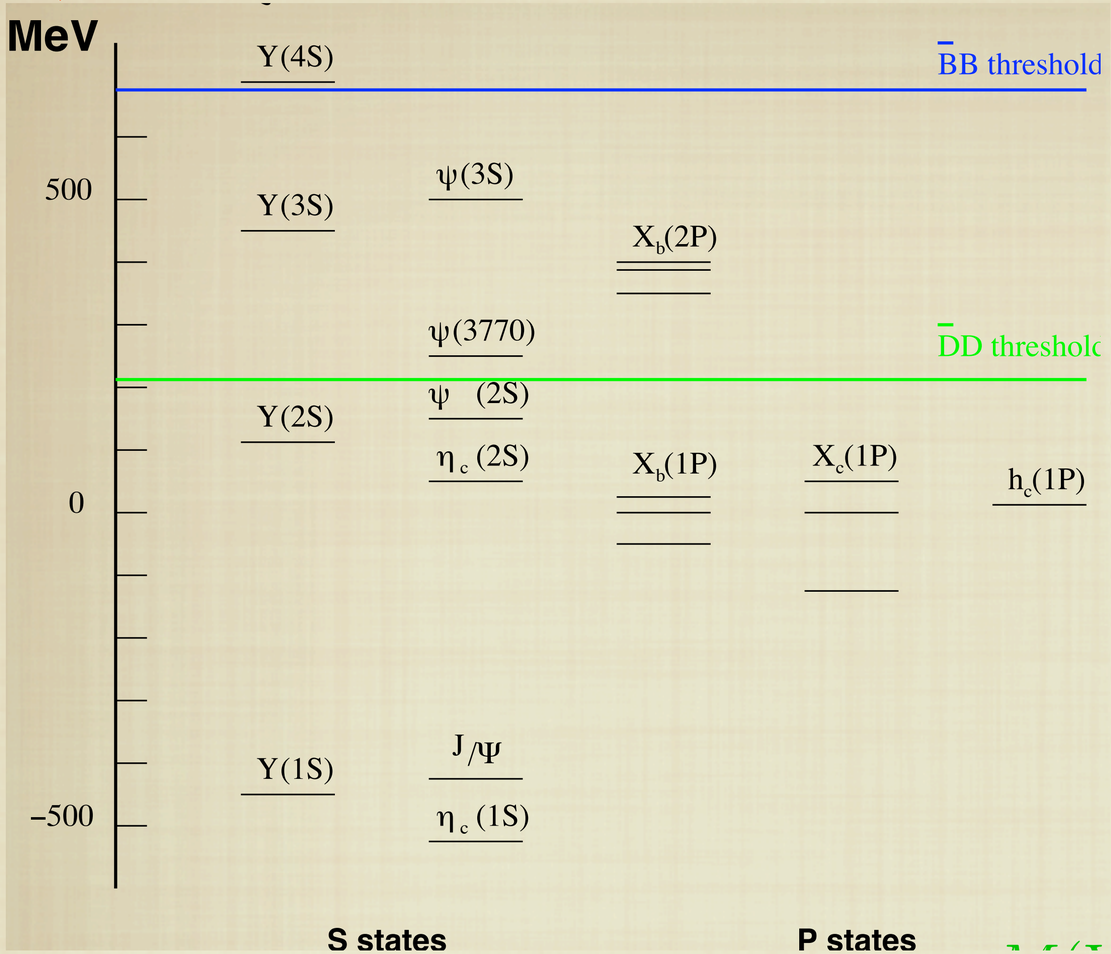

Normalized with respect to $\chi_b(1P)$ and $\chi_c(1P)$

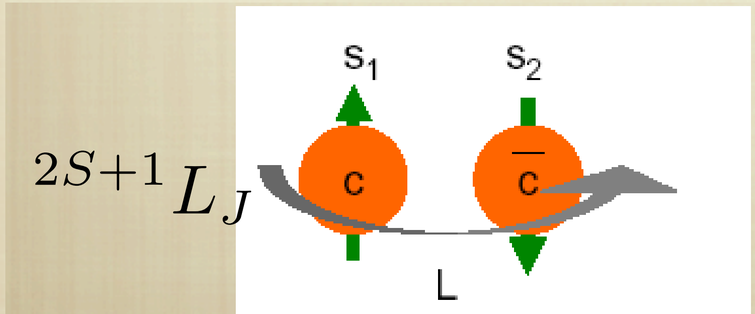

$M(Y(1S)) = 9460\,\mathrm{GeV}$

$M(J/\Psi) = 3097\,\mathrm{GeV}$

NR bound states have at least 3 scales

$$m \gg mv \gg mv^2 \quad v \ll 1$$

$$mv \sim r^{-1}$$

and Λ_{QCD}

The system is nonrelativistic(NR)

$$\Delta E \sim mv^2, \Delta_{fs} E \sim mv^4$$

$$v_b^2 \sim 0.1, v_c^2 \sim 0.3$$

The mass scale is perturbative

$$m_Q \gg \Lambda_{\mathrm{QCD}}$$

$$m_b \simeq 5\,\mathrm{GeV}; m_c \simeq 1.5\,\mathrm{GeV}$$

Quarkonium as a confinement probe

The rich structure of separated energy scales makes QQbar an ideal probe

At zero temperature

- The different quarkonium radii provide different measures of the transition from a Coulombic to a confined bound state.

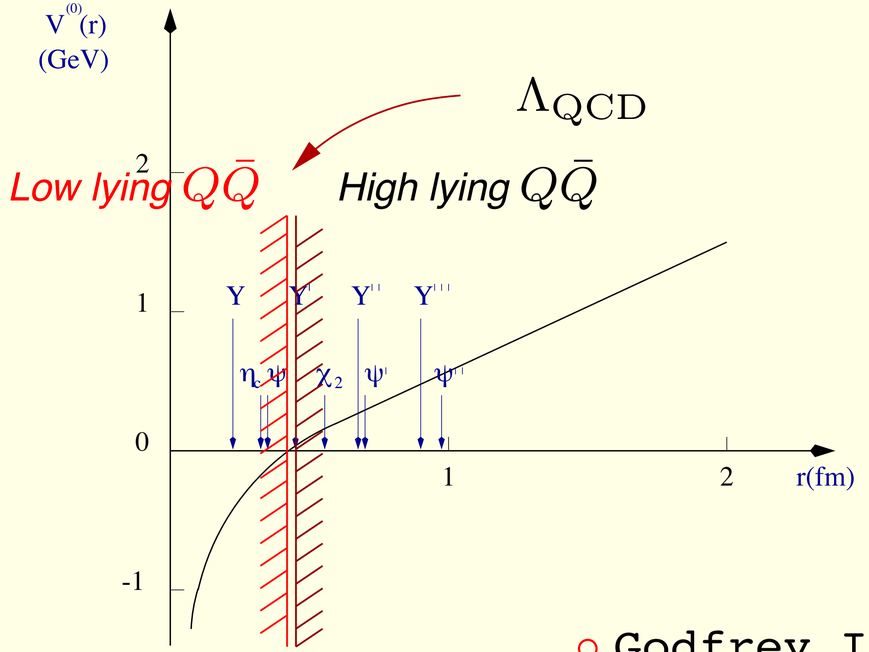

- Godfrey Isgur PRD 32(85)189

quarkonia probe the perturbative (high energy) and non perturbative region (low energy) as well as the transition region in dependence of their radius r

Quarkonium as a confinement probe

The rich structure of separated energy scales makes QQbar an ideal probe

At zero temperature

- The different quarkonium radii provide different measures of the transition from a Coulombic to a confined bound state.

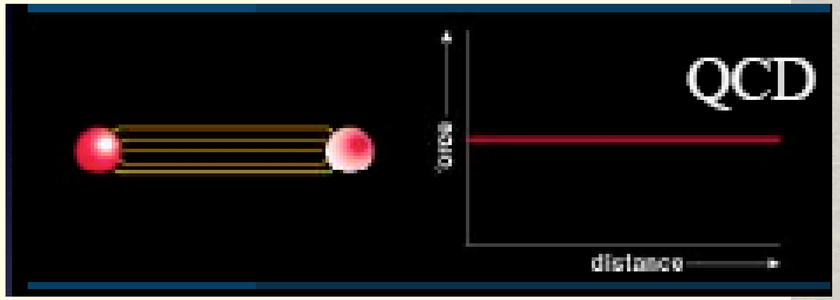

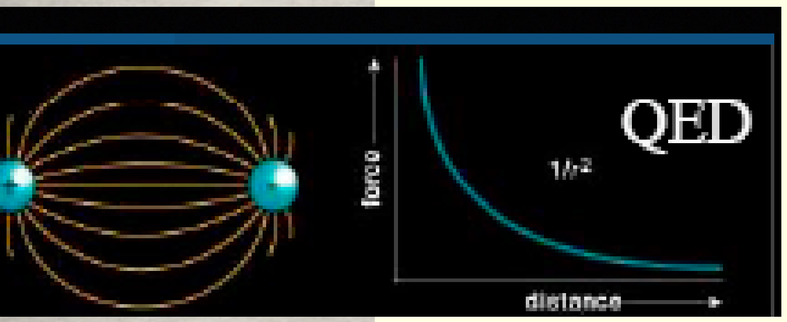

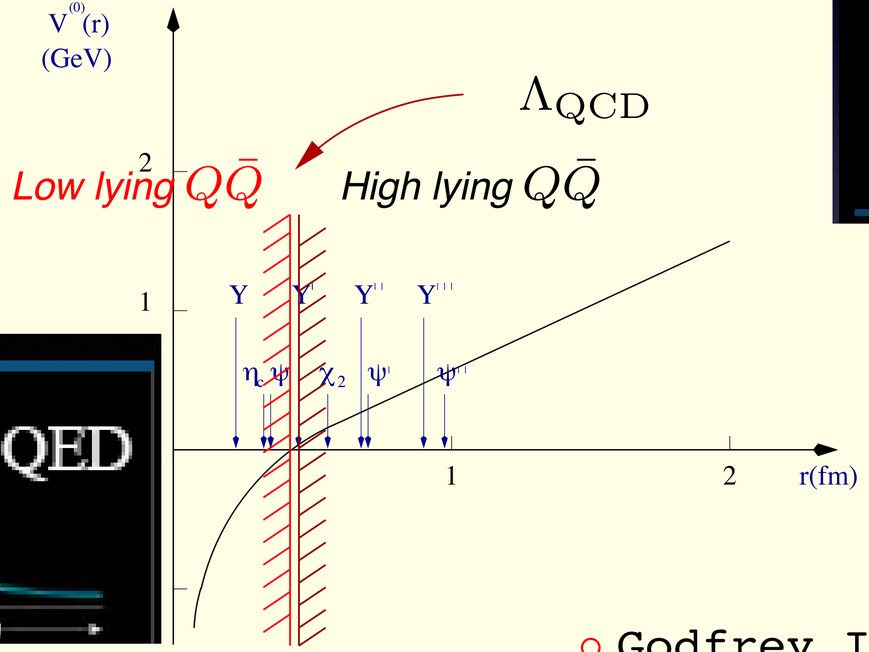

- Godfrey Isgur PRD 32(85)189

quarkonia probe the perturbative (high energy) and non perturbative region (low energy) as well as the transition region in dependence of their radius r

Quarkonium as a confinement and deconfinement probe

At finite temperature T they are sensitive to the formation of a quark gluon plasma via color screening

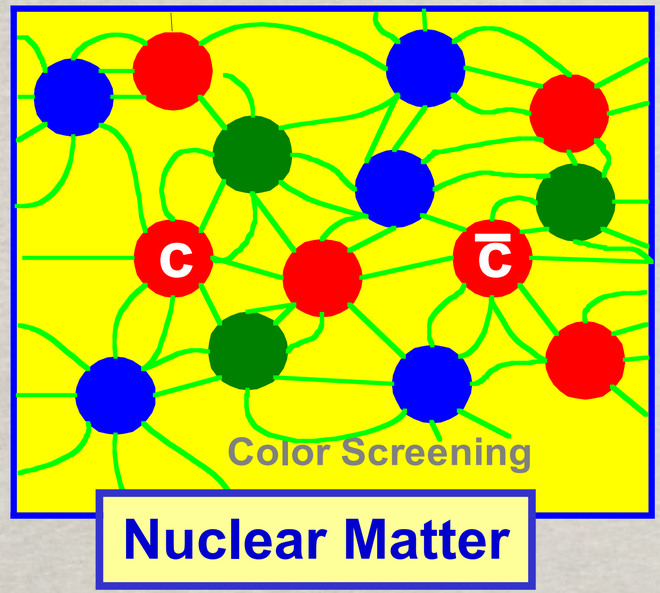

Debye charge screening $m_D \sim gT$

$$V(r) \sim -\alpha_s \frac{e^{-m_D r}}{r}$$

Matsui Satz 1986

A simulated collision of lead ions, courtesy the A
experiment at CERN

Quarkonium as a confinement and deconfinement probe

At finite temperature T they are sensitive to the formation of a quark gluon plasma via color screening

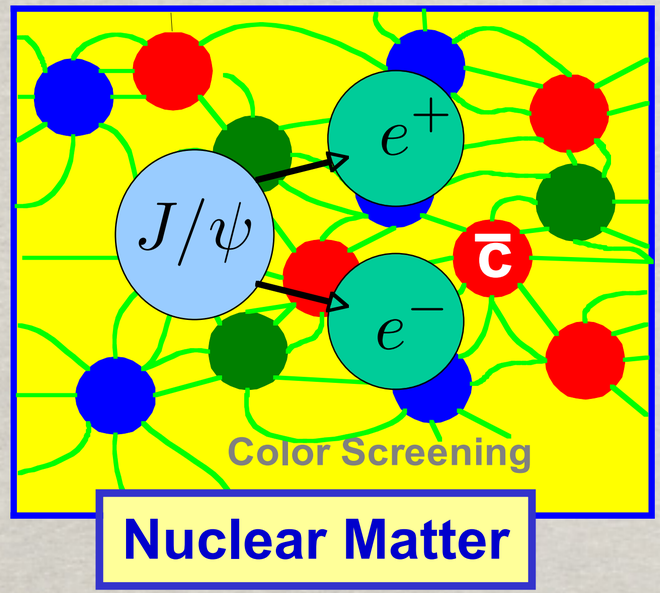

Debye charge screening $m_D \sim gT$

$$V(r) \sim -\alpha_s \frac{e^{-m_D r}}{r}$$

Matsui Satz 1986

A simulated collision of lead ions, courtesy the A
experiment at CERN

Quarkonium as a confinement and deconfinement probe

At finite temperature T they are sensitive to the formation of a quark gluon plasma via color screening

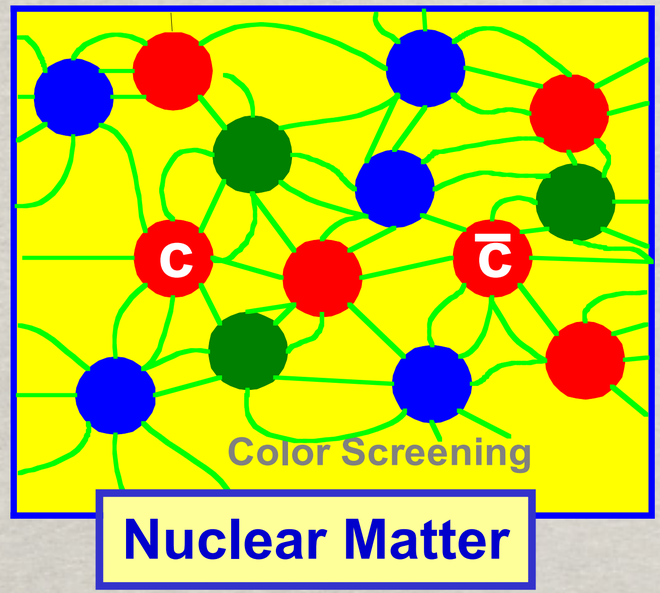

Debye charge screening $m_D \sim gT$

$$V(r) \sim -\alpha_s \frac{e^{-m_D r}}{r}$$

Matsui Satz 1986

A simulated collision of lead ions, courtesy the A
experiment at CERN

Quarkonium as a confinement and deconfinement probe

At finite temperature T they are sensitive to the formation of a quark gluon plasma via color screening

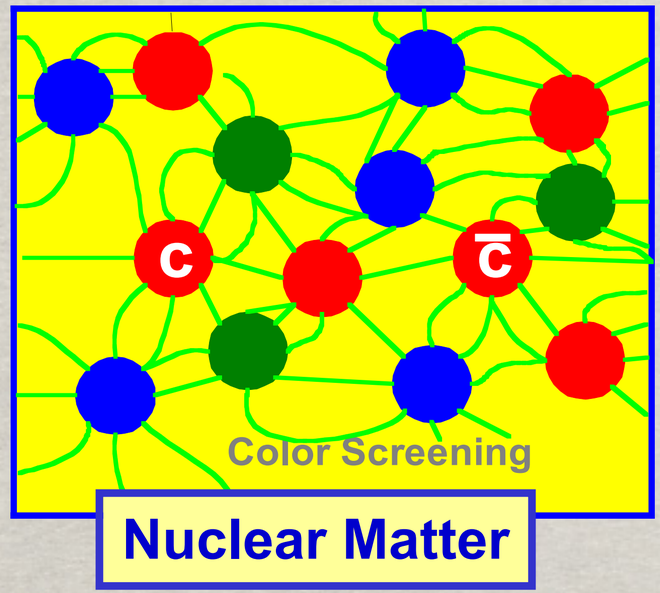

Debye charge screening $m_D \sim gT$

$$V(r) \sim -\alpha_s \frac{e^{-m_D r}}{r}$$

Matsui Satz 1986

$$r \sim \frac{1}{m_D} \longrightarrow$$ Bound state dissolves

A simulated collision of lead ions, courtesy the A
experiment at CERN

Quarkonium as a confinement and deconfinement probe

At finite temperature T they are sensitive to the formation of a quark gluon plasma via color screening

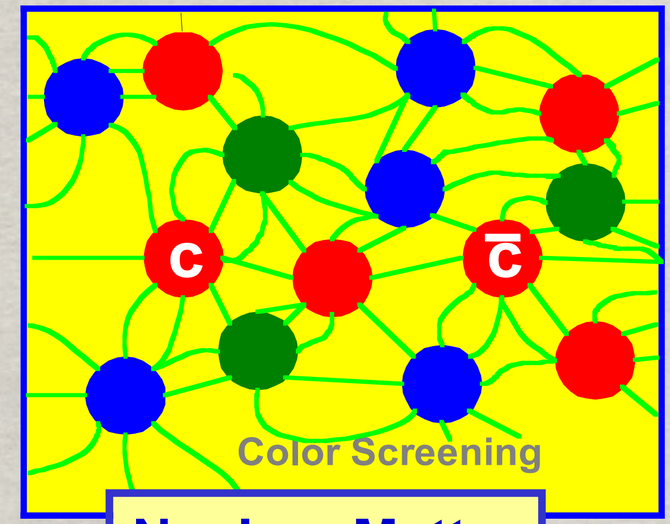

Debye charge screening $m_D \sim gT$

$$V(r) \sim -\alpha_s \frac{e^{-m_D r}}{r}$$

Matsui Satz 1986

$$r \sim \frac{1}{m_D} \longrightarrow$$ Bound state dissolves

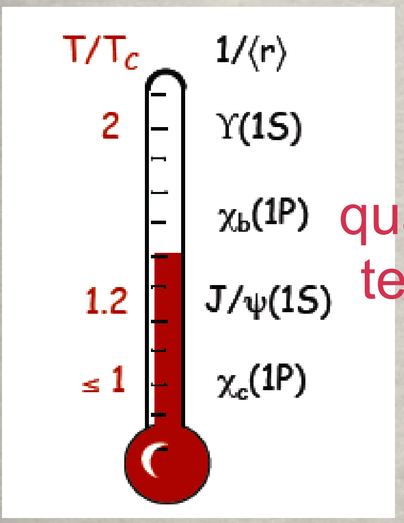

quarkonia dissociate at different temperature in dependence of their radius: they are a Quark Gluon Plasma thermometer

A simulated collision of lead ions, courtesy the A experiment at CERN

Quarkonium as a confinement and deconfinement probe

At finite temperature T they are sensitive to the formation of a quark gluon plasma via color screening

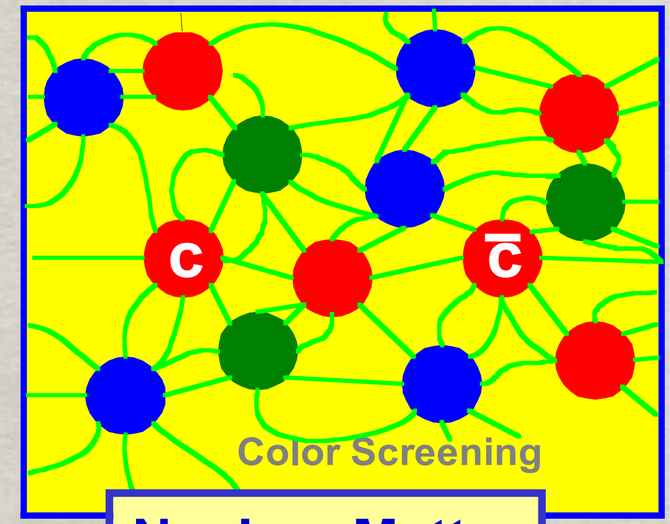

Debye charge screening $m_D \sim gT$

$$V(r) \sim -\alpha_s \frac{e^{-m_D r}}{r}$$

Matsui Satz 1986

$$r \sim \frac{1}{m_D} \longrightarrow$$ Bound state dissolves

nuclear modificatio

$$R_{AA} = \frac{Yield^{q\bar{q}}_{AA}}{\langle N_{coll} \rangle \times Yield^{q\bar{q}}_{pp}}$$

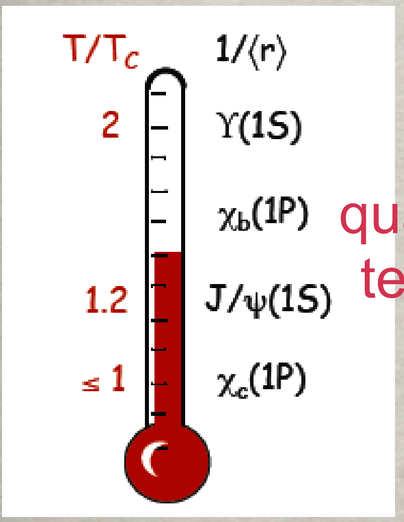

quarkonia dissociate at different temperature in dependence of their radius: they are a Quark Gluon Plasma thermometer

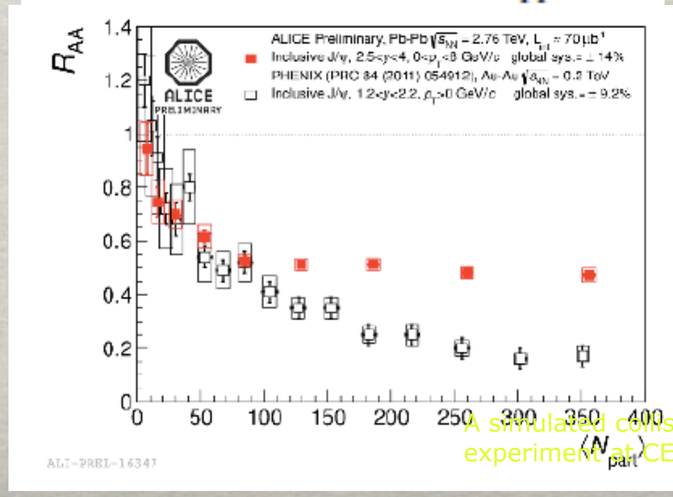

A simulated collision of lead ions, courtesy the ALICE experiment at CERN

nt and deconfinement probe

sitive to the formation of a quark gluon

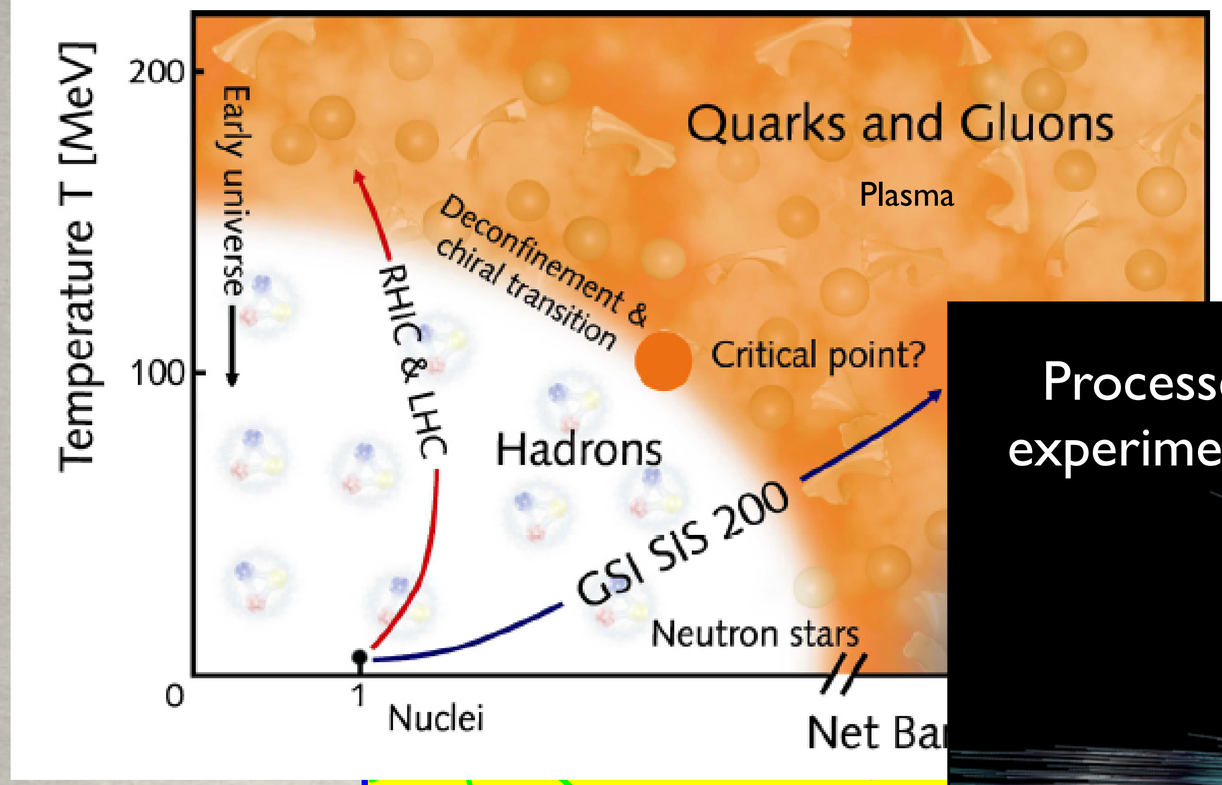

Nuclear Matter

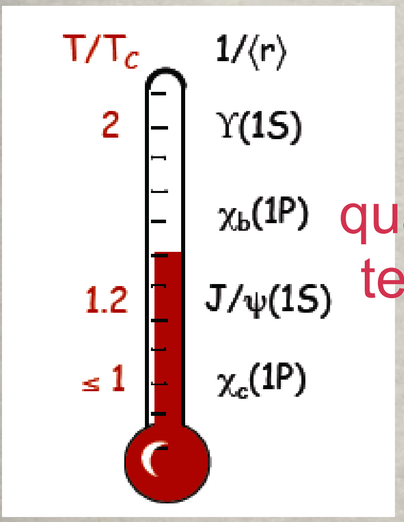

quarkonia dissociate at d
temperature in depende
their radius: they
are a Quark Gluon Pla
thermometer

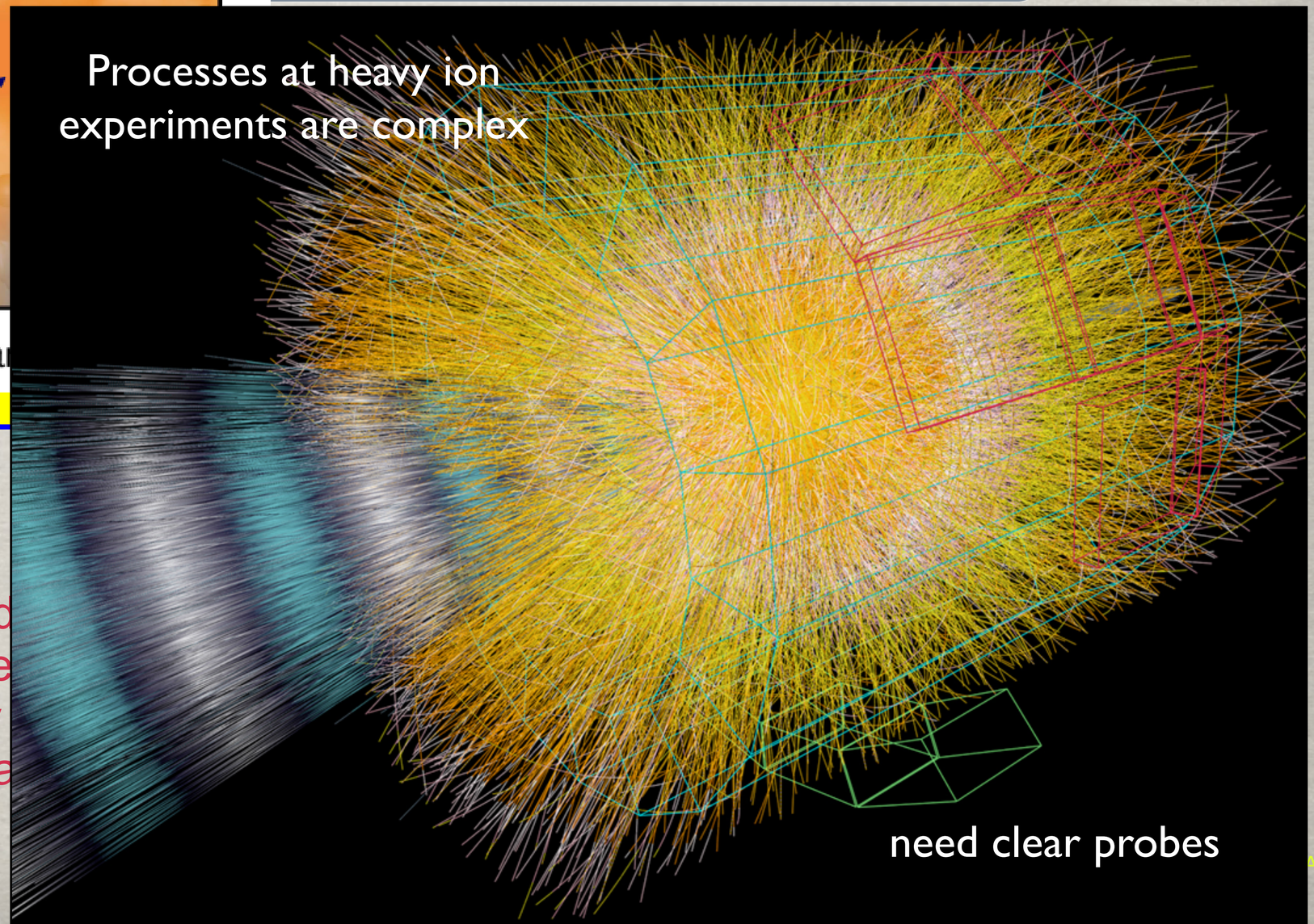

but what is the QCD potential?
and what are the other nonpotential effects to the spectrum and decay coming from QCD, i.e defined in QFT?

but what is the QCD potential?
and what are the other nonpotential effects to the spectrum and decay coming from QCD, i.e defined in QFT?

Nonrelativistic Effective Field Theories (NREFTs) can give an answer to this
in particular potential Nonrelativistic QCD (pNRQCD)

QCD theory of Quarkonium: a very hard problem even at T=0

QCD theory of Quarkonium: a very hard problem even at T=0

Close to the bound state $\alpha_s \sim v$

QCD theory of Quarkonium: a very hard problem even at T=0

Close to the bound state $\alpha_s \sim v$

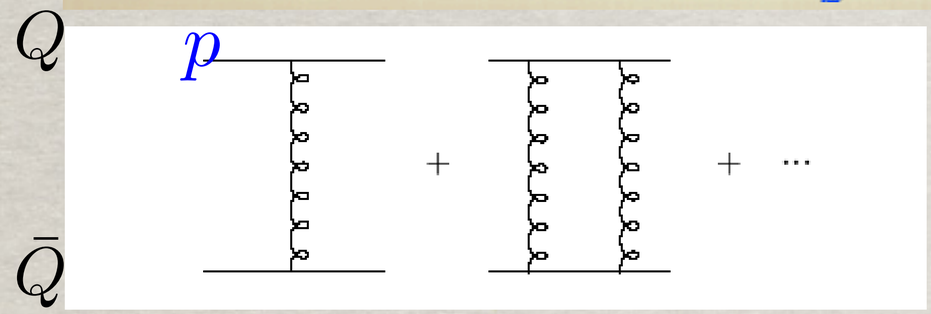

QCD theory of Quarkonium: a very hard problem even at T=0

Close to the bound state $\alpha_s \sim v$

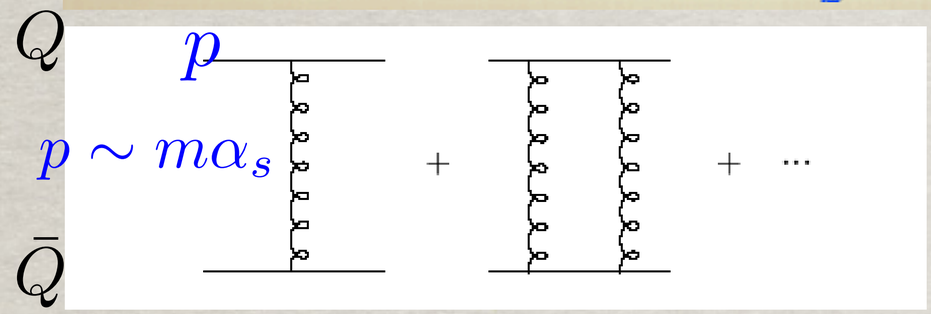

QCD theory of Quarkonium: a very hard problem even at T=0

Close to the bound state $\alpha_s \sim v$

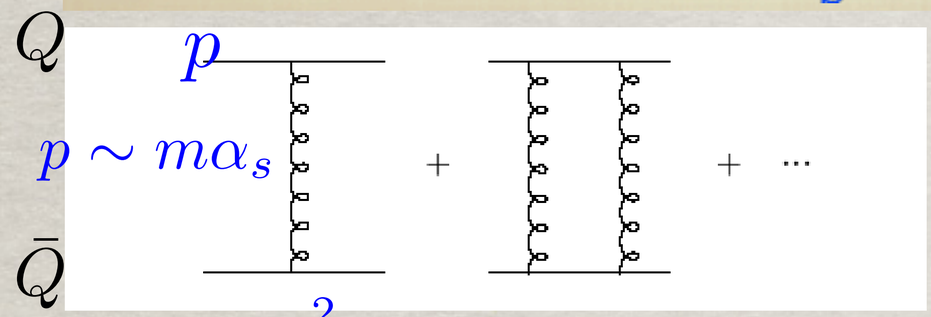

$$\frac{g^2}{p^2}(1 + \frac{m\alpha_s}{p})$$

QCD theory of Quarkonium: a very hard problem even at T=0

Close to the bound state $\alpha_s \sim v$

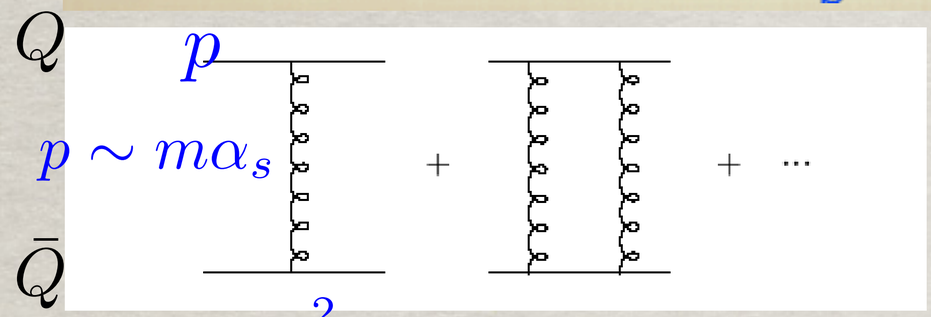

$$\frac{g^2}{p^2}(1+\frac{m\alpha_s}{p})$$

$$\sim \frac{1}{E-(\frac{p^2}{m}+V)}$$

QCD theory of Quarkonium: a very hard problem even at T=0

Close to the bound state $\alpha_s \sim v$

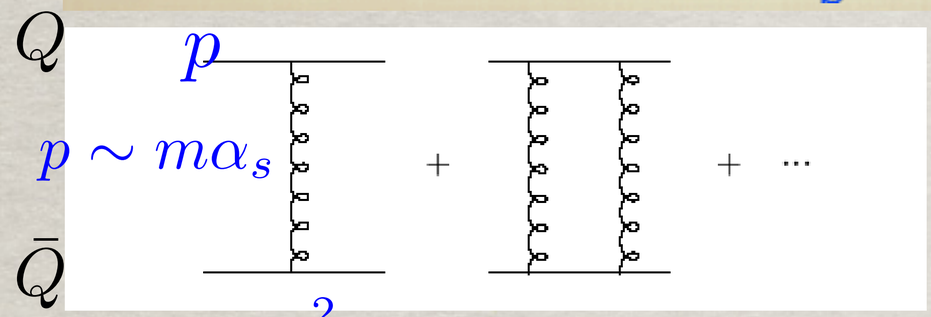

$$\frac{g^2}{p^2}(1+\frac{m\alpha_s}{p})$$

$$\sim \frac{1}{E-(\frac{p^2}{m}+V)}$$

- From $(\frac{p^2}{m}+V)\phi = E\phi \rightarrow p \sim mv$ and $E = \frac{p^2}{m} + V \sim mv^2$.

QCD theory of Quarkonium: a very hard problem even at T=0

Close to the bound state $\alpha_s \sim v$

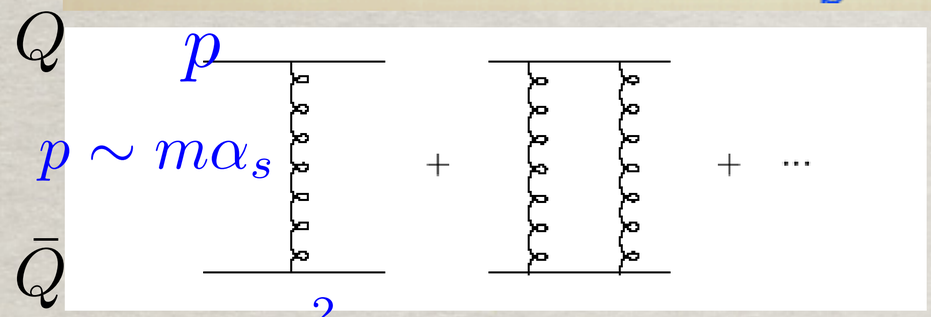

$$\frac{g^2}{p^2}(1+\frac{m\alpha_s}{p})$$

$$\sim \frac{1}{E-(\frac{p^2}{m}+V)}$$

- From $(\frac{p^2}{m}+V)\phi = E\phi \rightarrow p \sim mv$ and $E = \frac{p^2}{m}+V \sim mv^2$.

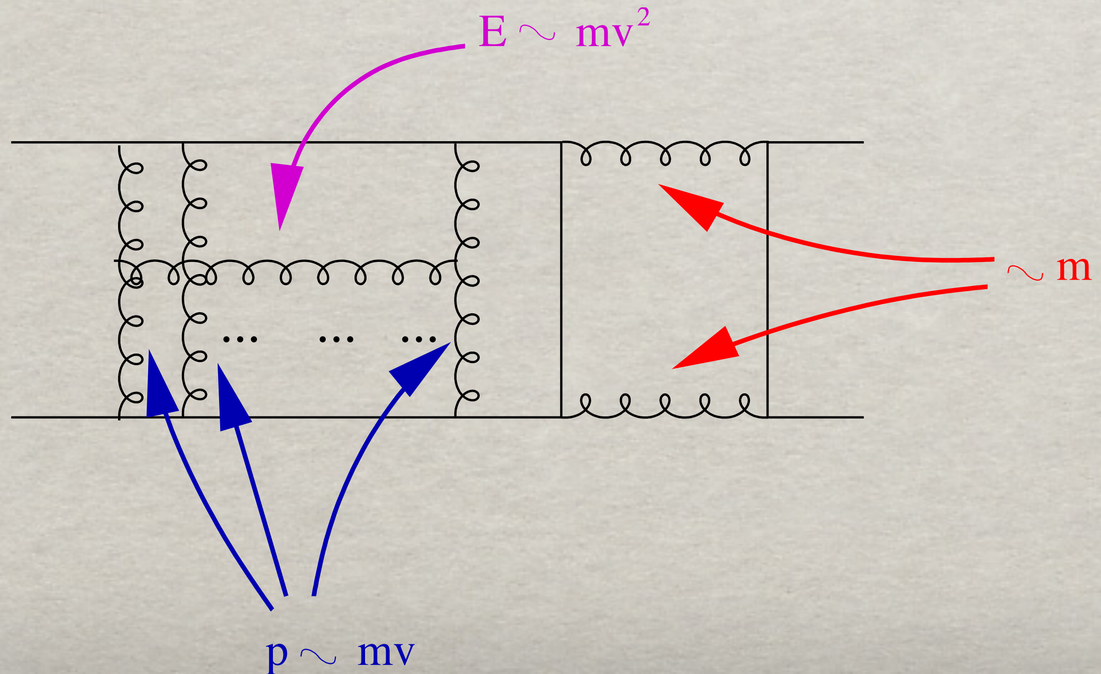

QCD theory of Quarkonium: a very hard problem even at T=0

Close to the bound state $\alpha_s \sim v$

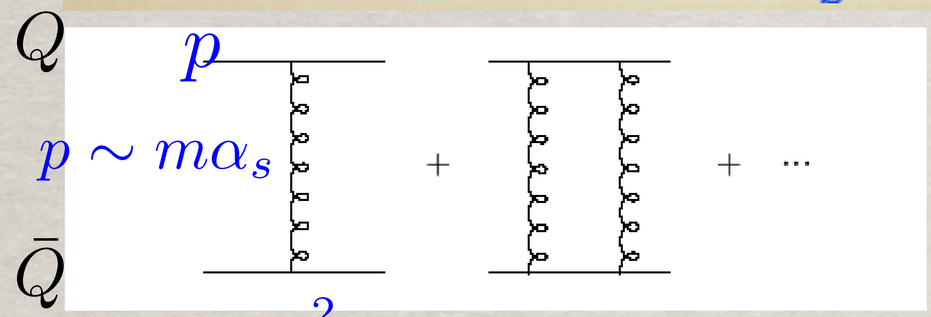

$$\frac{g^2}{p^2}(1+\frac{m\alpha_s}{p})$$

$$\sim \frac{1}{E-(\frac{p^2}{m}+V)}$$

- From $(\frac{p^2}{m}+V)\phi = E\phi \rightarrow p \sim mv$ and $E = \frac{p^2}{m}+V \sim mv^2$.

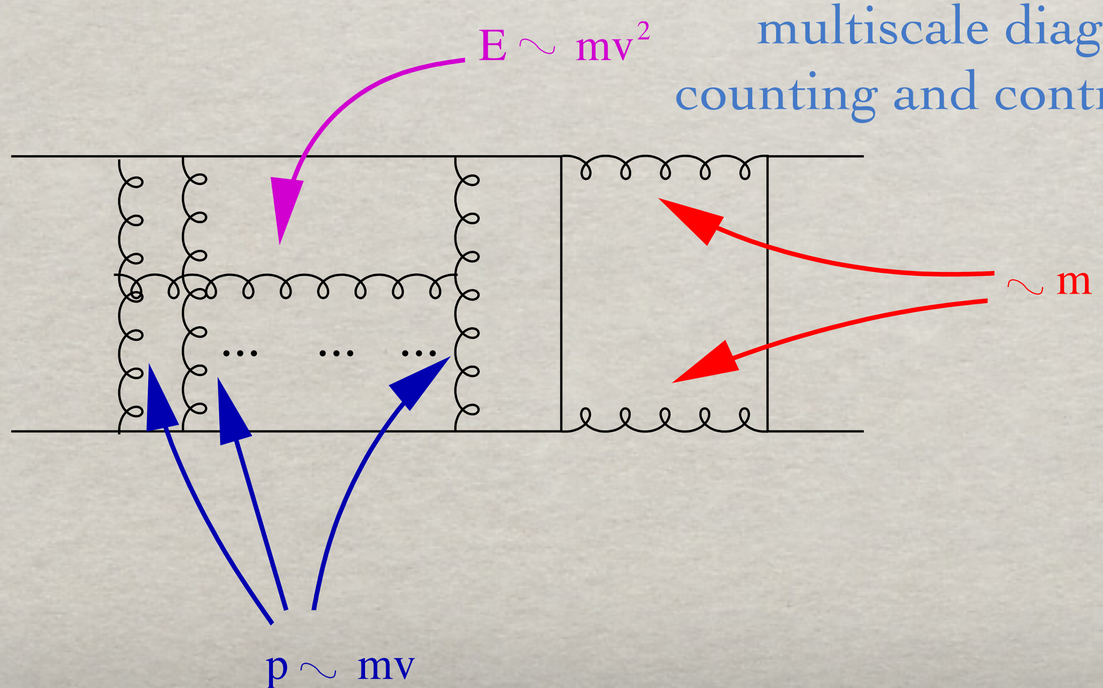

multiscale diagrams have a complicate power counting and contribute to all orders in the coupling

QCD theory of Quarkonium: a very hard problem even at T=0

Close to the bound state $\alpha_s \sim v$

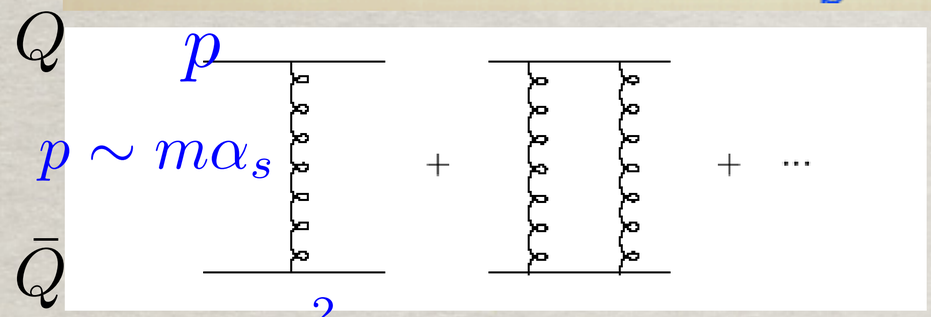

$$\frac{g^2}{p^2}\left(1+\frac{m\alpha_s}{p}\right)$$

$$\sim \frac{1}{E-\left(\frac{p^2}{m}+V\right)}$$

- From $\left(\frac{p^2}{m}+V\right)\phi = E\phi \rightarrow p \sim mv$ and $E = \frac{p^2}{m}+V \sim mv^2$.

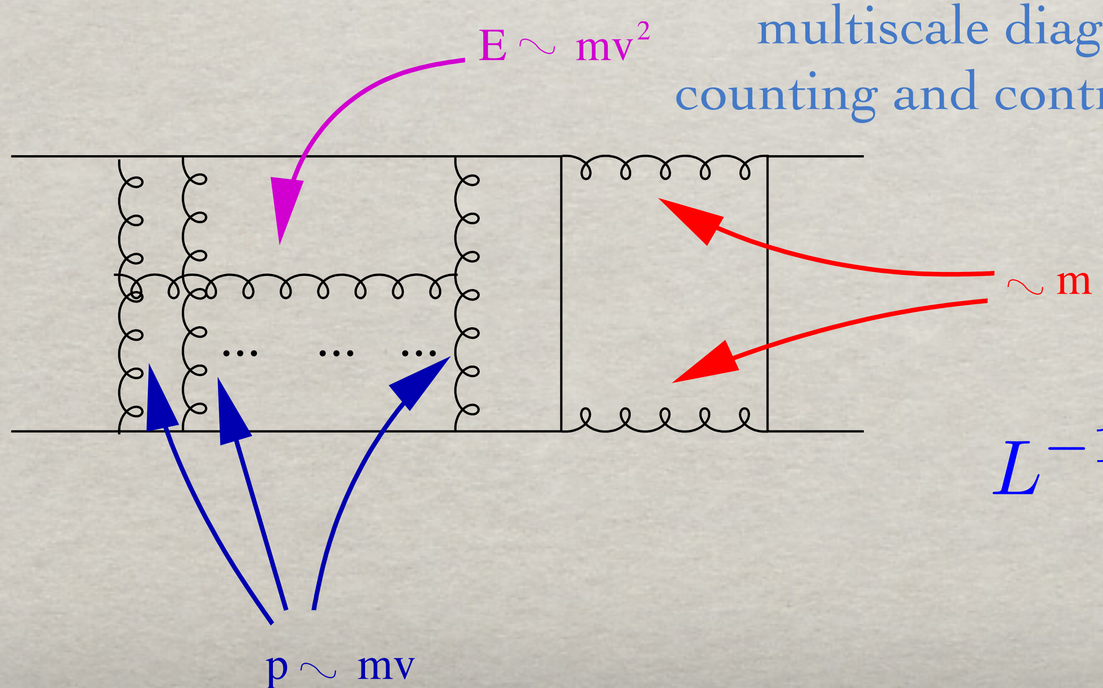

multiscale diagrams have a complicate power counting and contribute to all orders in the coupling

Difficult also for the lattice!

$$L^{-1} \ll \lambda \ll \Lambda \ll a^{-1}$$

QCD theory of Quarkonium: a very hard problem even at T=0

Close to the bound state $\alpha_s \sim v$

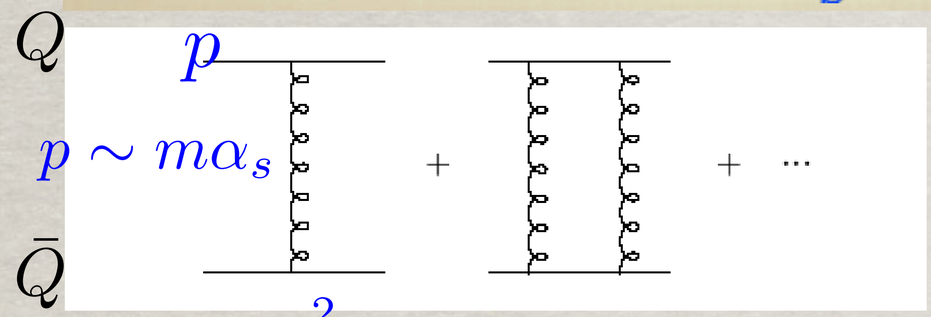

$$\frac{g^2}{p^2}\left(1+\frac{m\alpha_s}{p}\right)$$

$$\sim \frac{1}{E-\left(\frac{p^2}{m}+V\right)}$$

- From $\left(\frac{p^2}{m}+V\right)\phi = E\phi \rightarrow p \sim mv$ and $E = \frac{p^2}{m}+V \sim mv^2$.

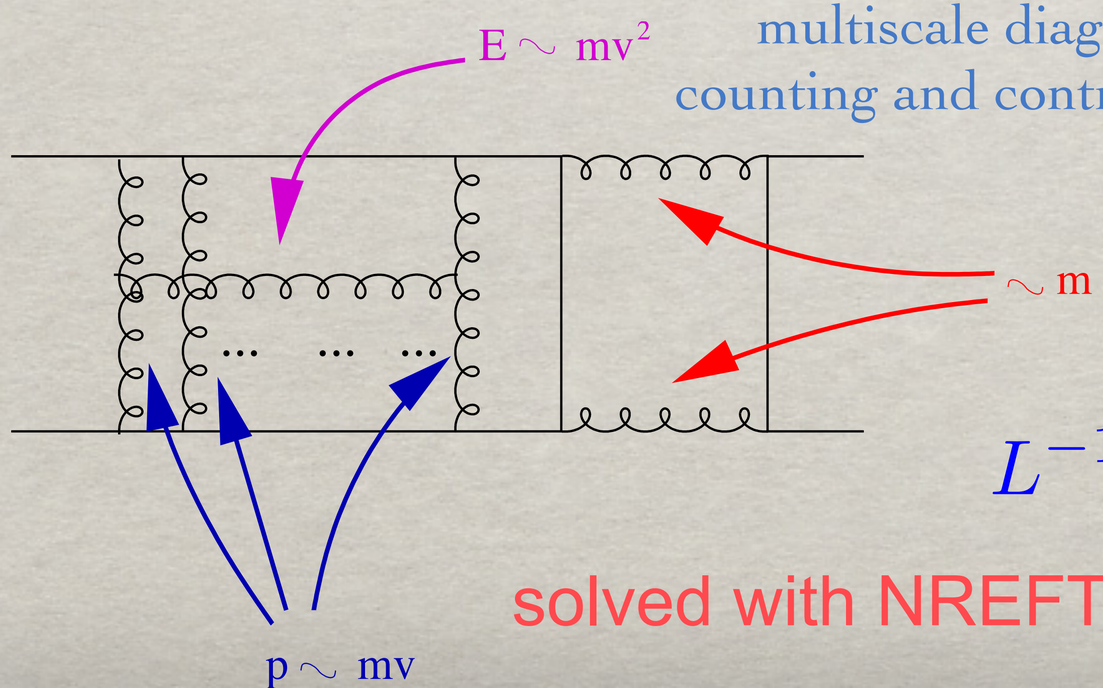

multiscale diagrams have a complicate power counting and contribute to all orders in the coupling

Difficult also for the lattice!

$$L^{-1} \ll \lambda \ll \Lambda \ll a^{-1}$$

solved with NREFT

Quarkonium with NR EFT

Color degrees of freedom
3X3=1+8
singlet and octet QQbar

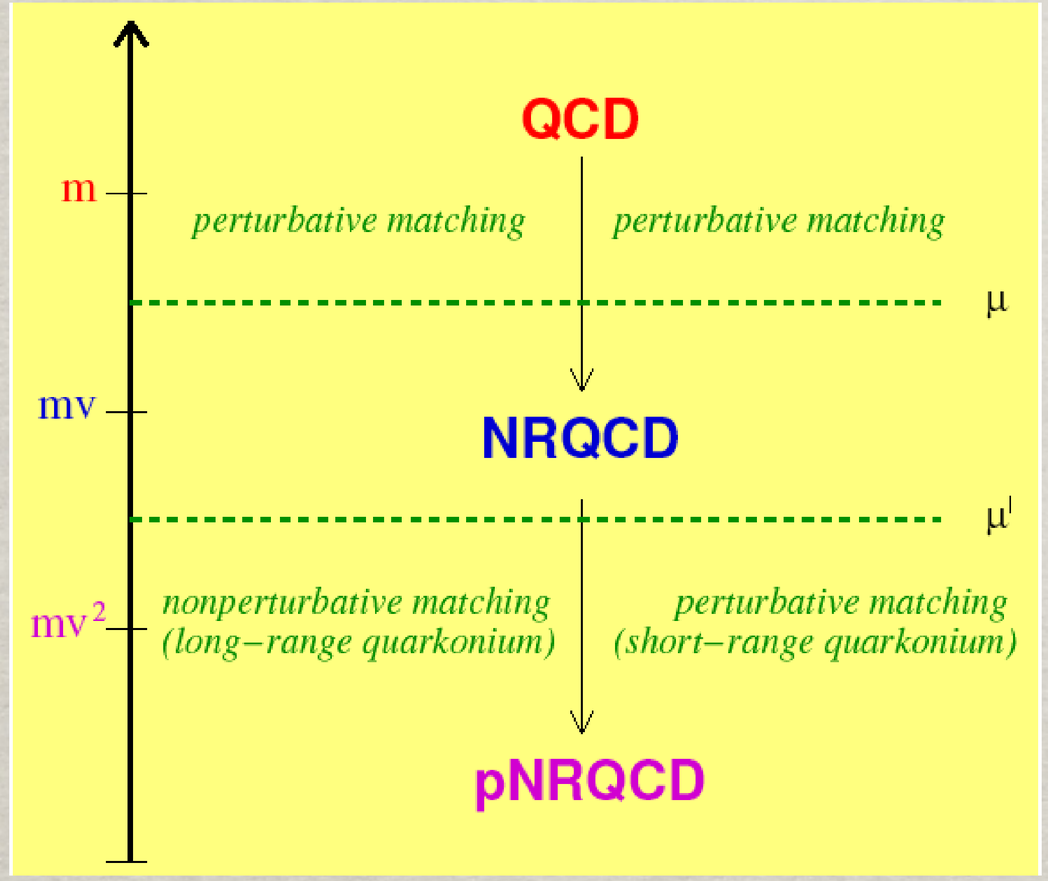

Hard

Soft
(relative
momentum)

Ultrasoft
(binding energy)

Quarkonium with NR EFT

Color degrees of freedom
3X3=1+8
singlet and octet QQbar

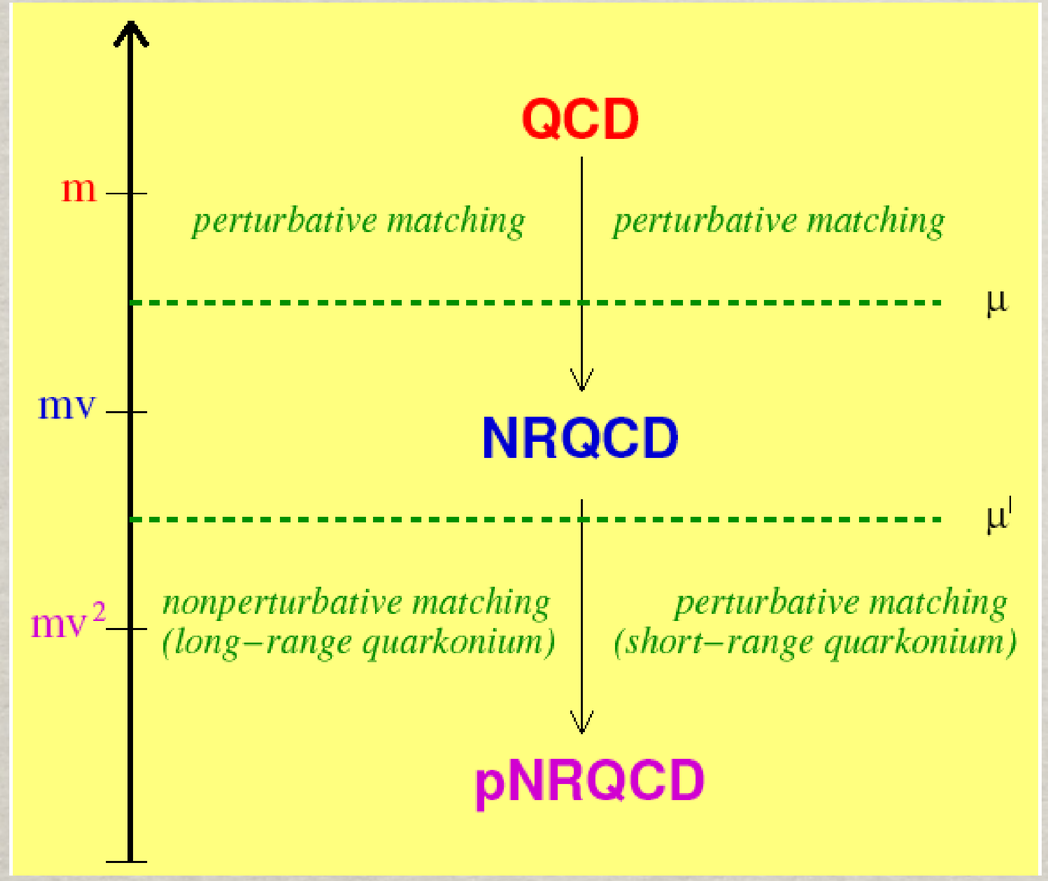

Hard

Soft
(relative
momentum)

Ultrasoft
(binding energy)

$$\mathcal{L}_{\rm EFT} = \sum_n c_n(E_\Lambda/\mu)\frac{O_n(\mu,\lambda)}{E_\Lambda}$$

Quarkonium with NR EFT

Color degrees of freedom
3X3=1+8
singlet and octet QQbar

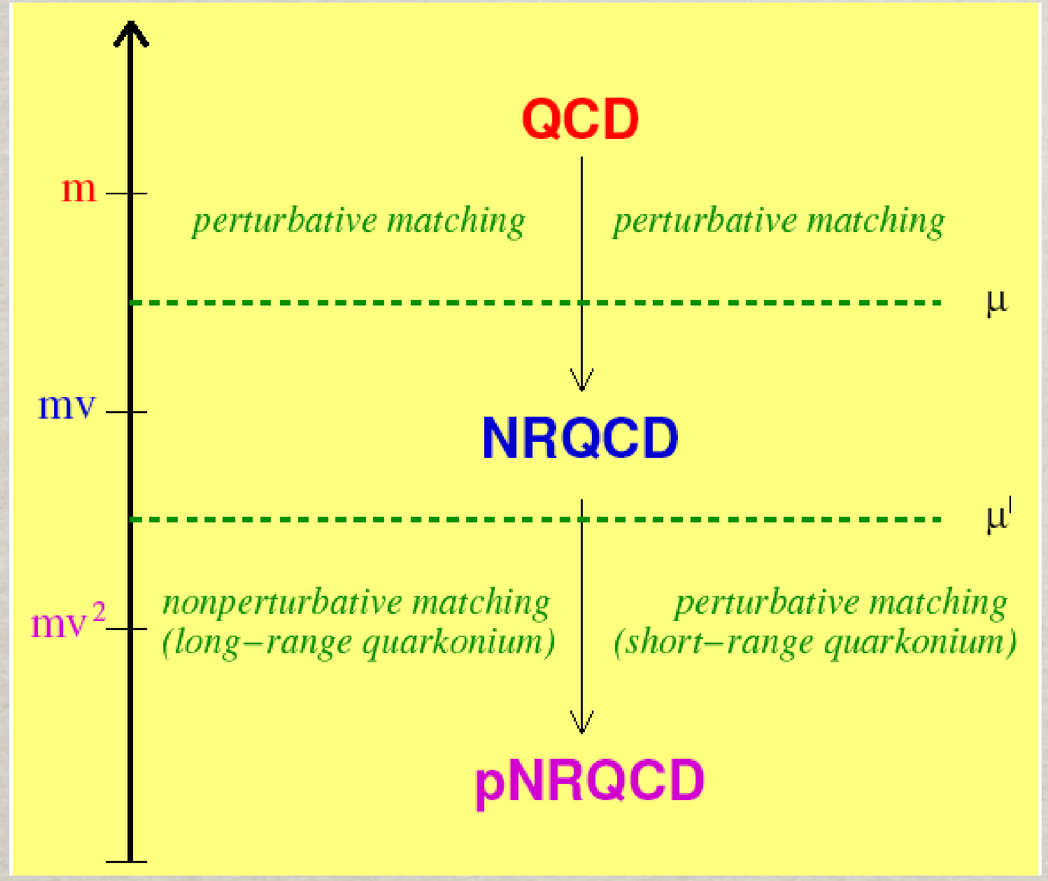

Hard

Soft
(relative
momentum)

Ultrasoft
(binding energy)

$$\mathcal{L}_{\rm EFT} = \sum_n c_n(E_\Lambda/\mu)\frac{O_n(\mu,\lambda)}{E_\Lambda}$$

$$\langle O_n \rangle \sim E_\lambda^n$$

Quarkonium with NR EFT

Color degrees of freedom
3X3=1+8
singlet and octet QQbar

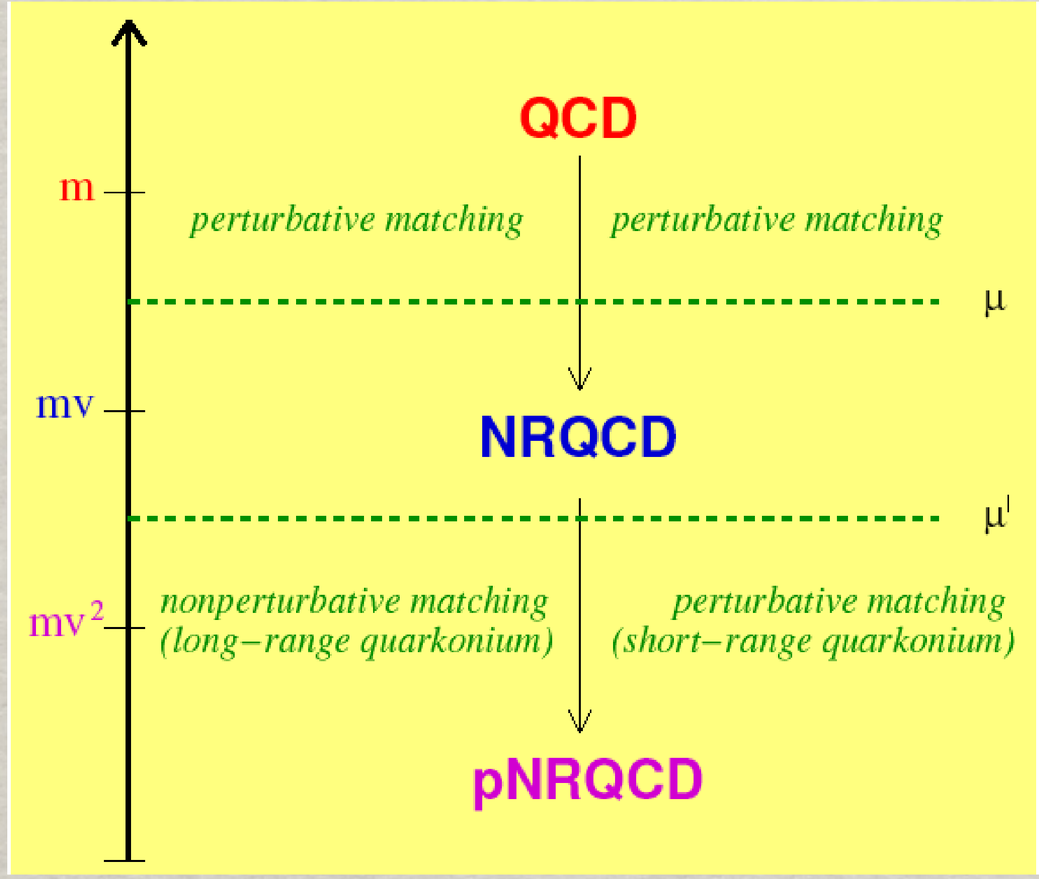

Hard

$$\frac{E_\lambda}{E_\Lambda} = \frac{mv}{m}$$

Soft
(relative
momentum)

Ultrasoft
(binding energy)

$$\mathcal{L}_{\rm EFT} = \sum_n c_n(E_\Lambda/\mu)\frac{O_n(\mu,\lambda)}{E_\Lambda}$$

$$\langle O_n \rangle \sim E_\lambda^n$$

Quarkonium with NR EFT

Color degrees of freedom
3X3=1+8
singlet and octet QQbar

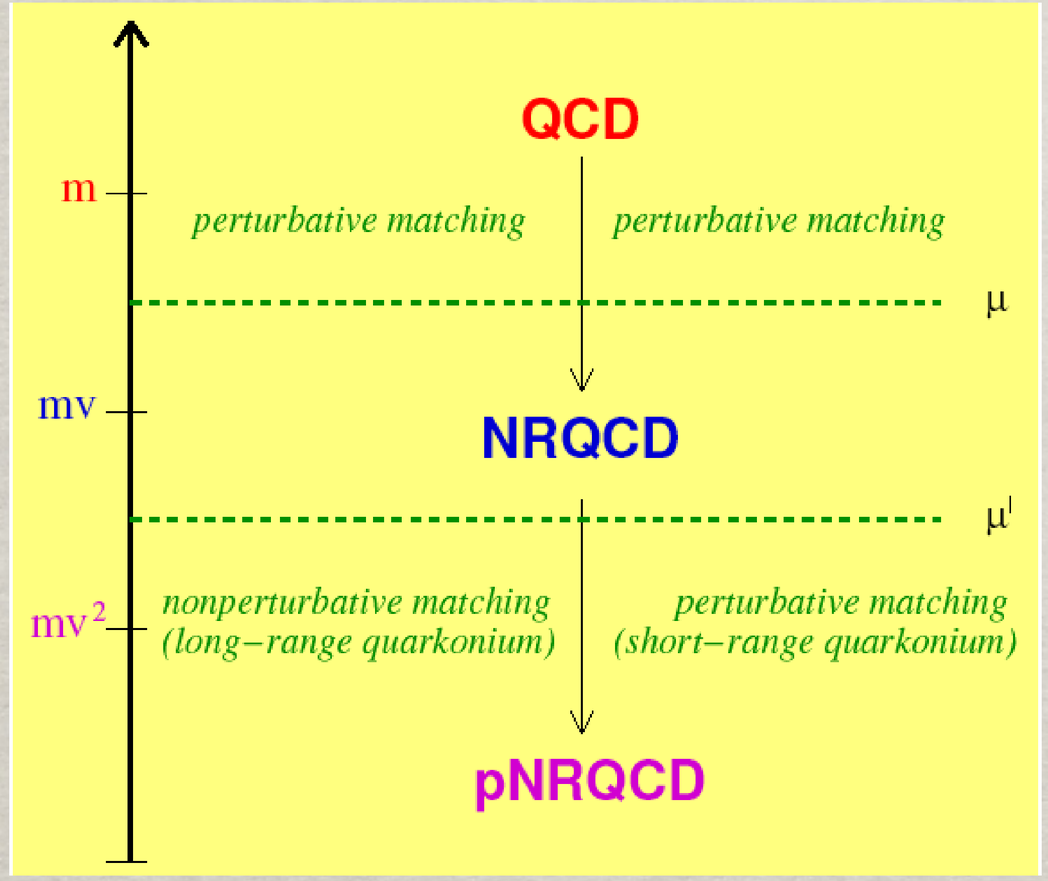

Hard

$$\frac{E_\lambda}{E_\Lambda} = \frac{mv}{m}$$

Soft
(relative
momentum)

$$\frac{E_\lambda}{E_\Lambda} = \frac{mv^2}{mv}$$

Ultrasoft
(binding energy)

$$\mathcal{L}_{\rm EFT} = \sum_n c_n(E_\Lambda/\mu)\frac{O_n(\mu,\lambda)}{E_\Lambda}$$

$$\langle O_n \rangle \sim E_\lambda^n$$

Quarkonium with NR EFT: Non Relativistic QCD (NRQCD)

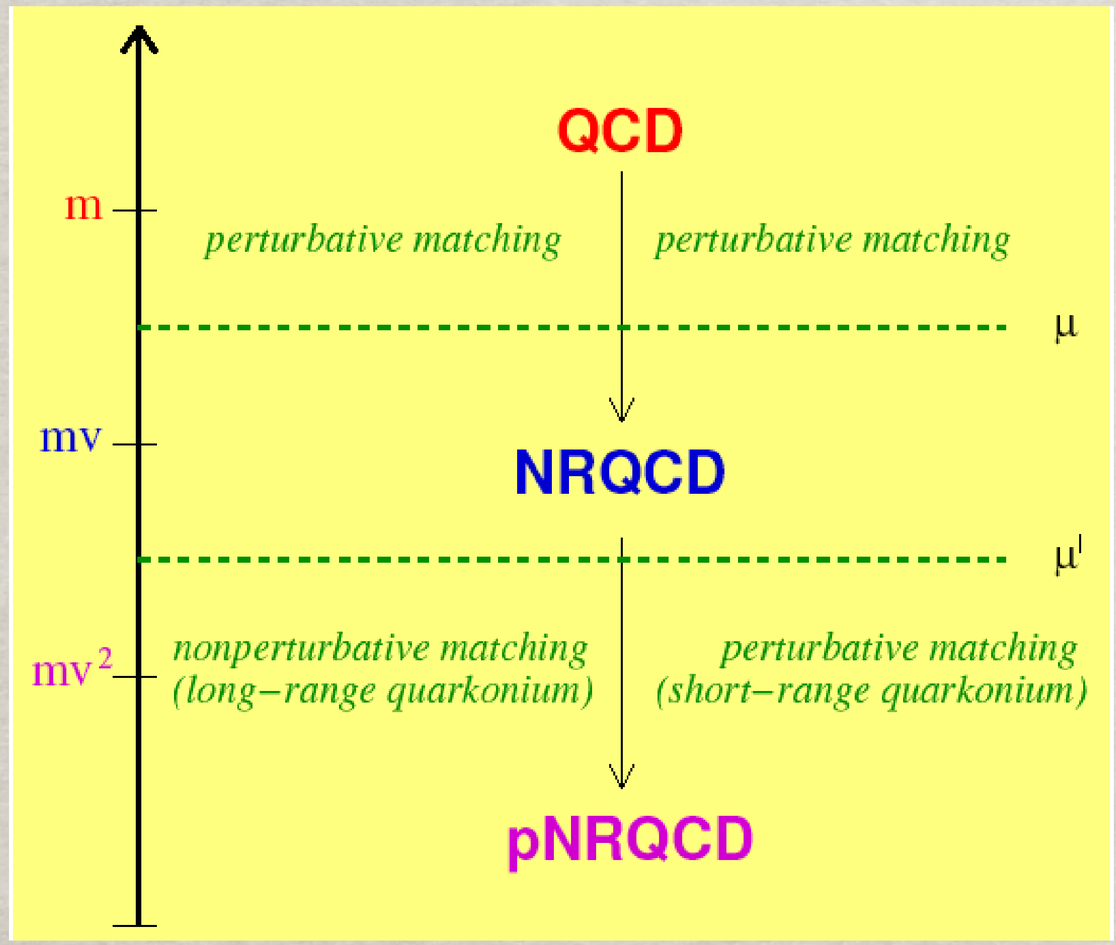

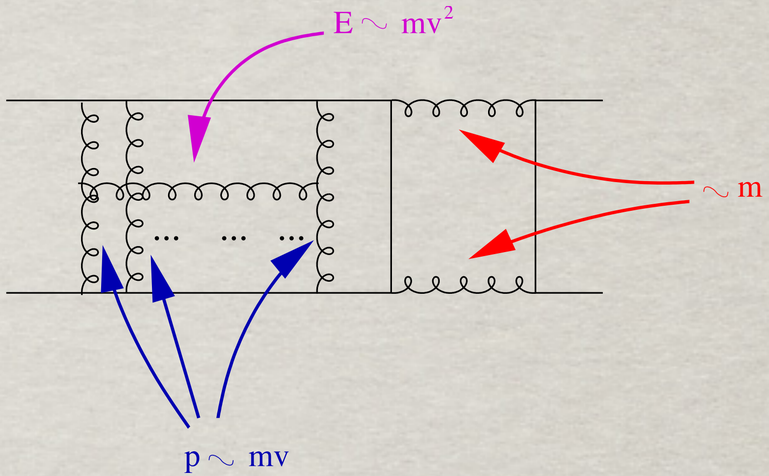

Quarkonium with NR EFT: Non Relativistic QCD (NRQCD)

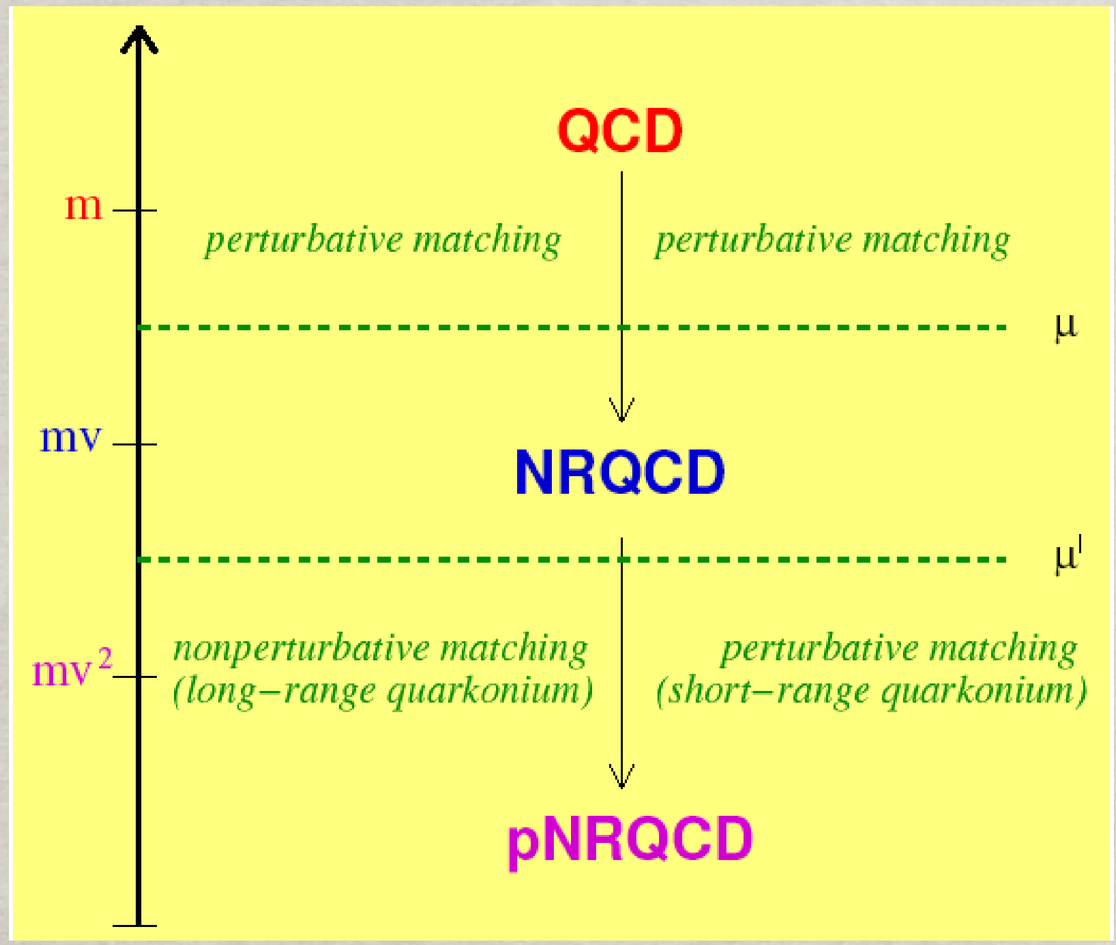

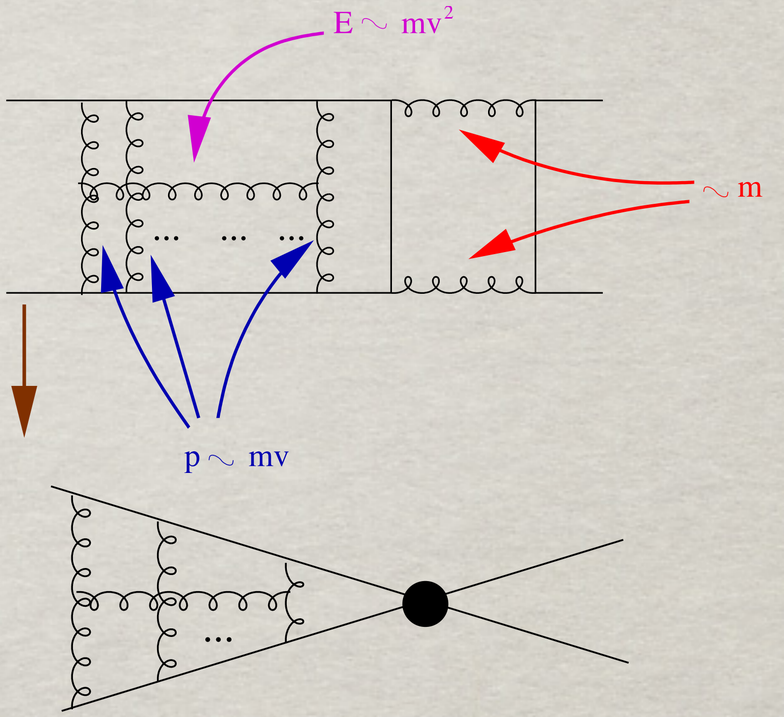

Quarkonium with NR EFT: Non Relativistic QCD (NRQCD)

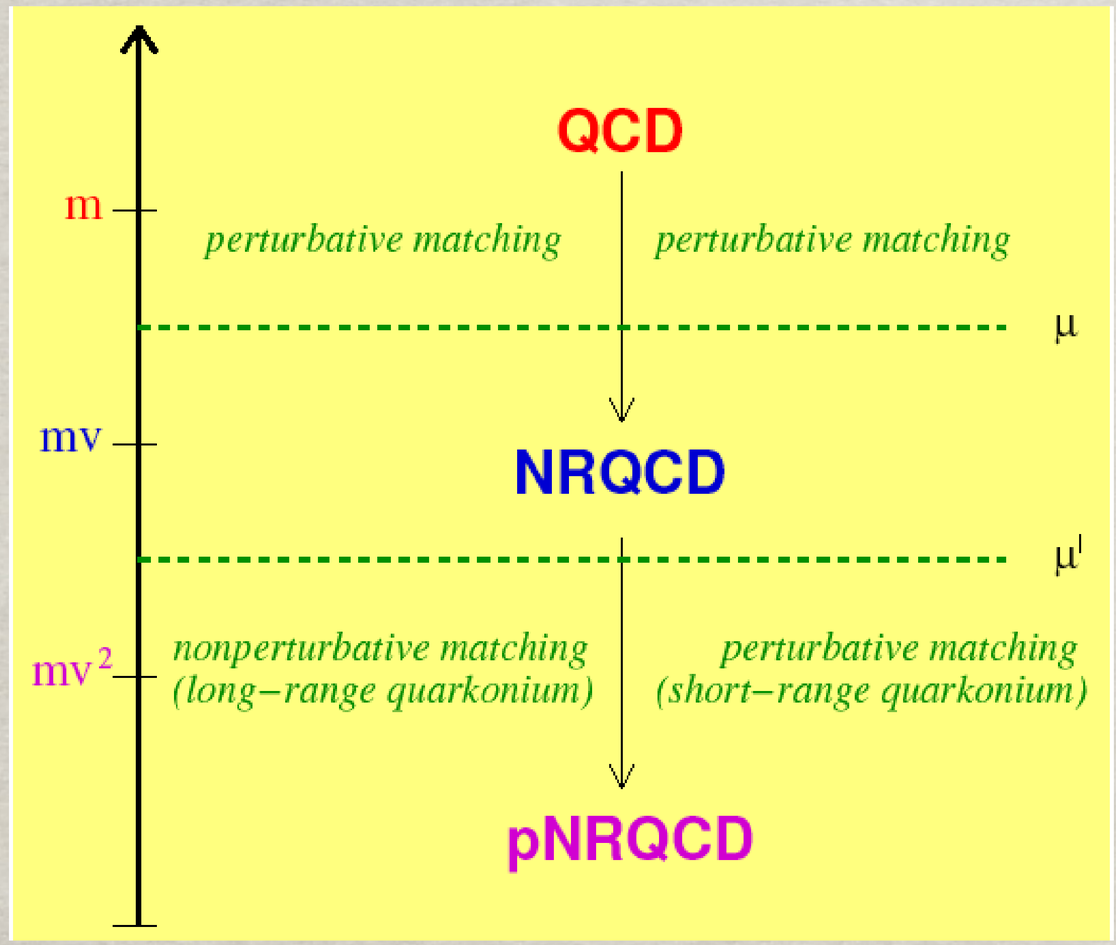

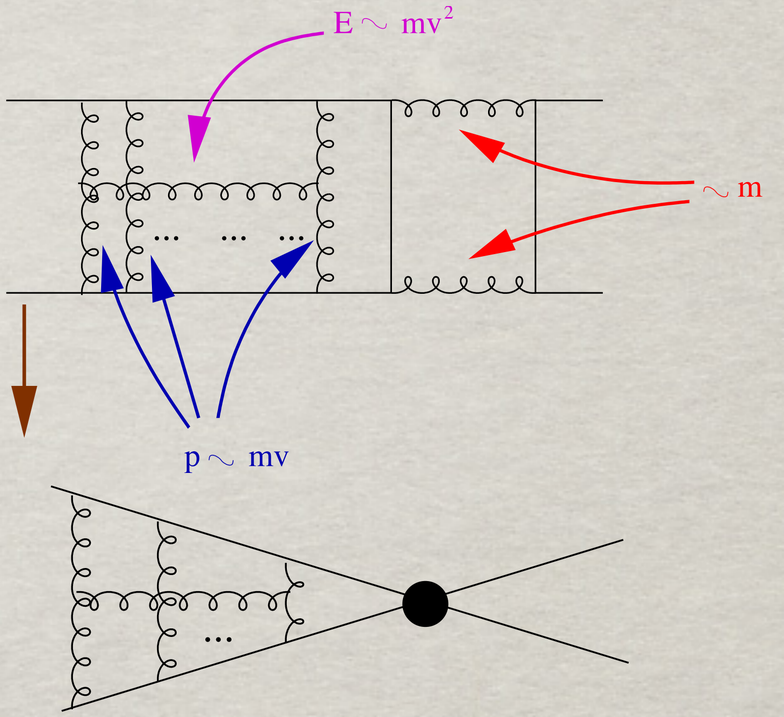

$$\mathcal{L}_{\rm NRQCD} = \sum_n c(\alpha_{\rm s}(m/\mu)) \times \frac{O_n(\mu,\lambda)}{m^n}$$

Quarkonium with NR EFT: potential NonRelativistic QCD (pNRQCD)

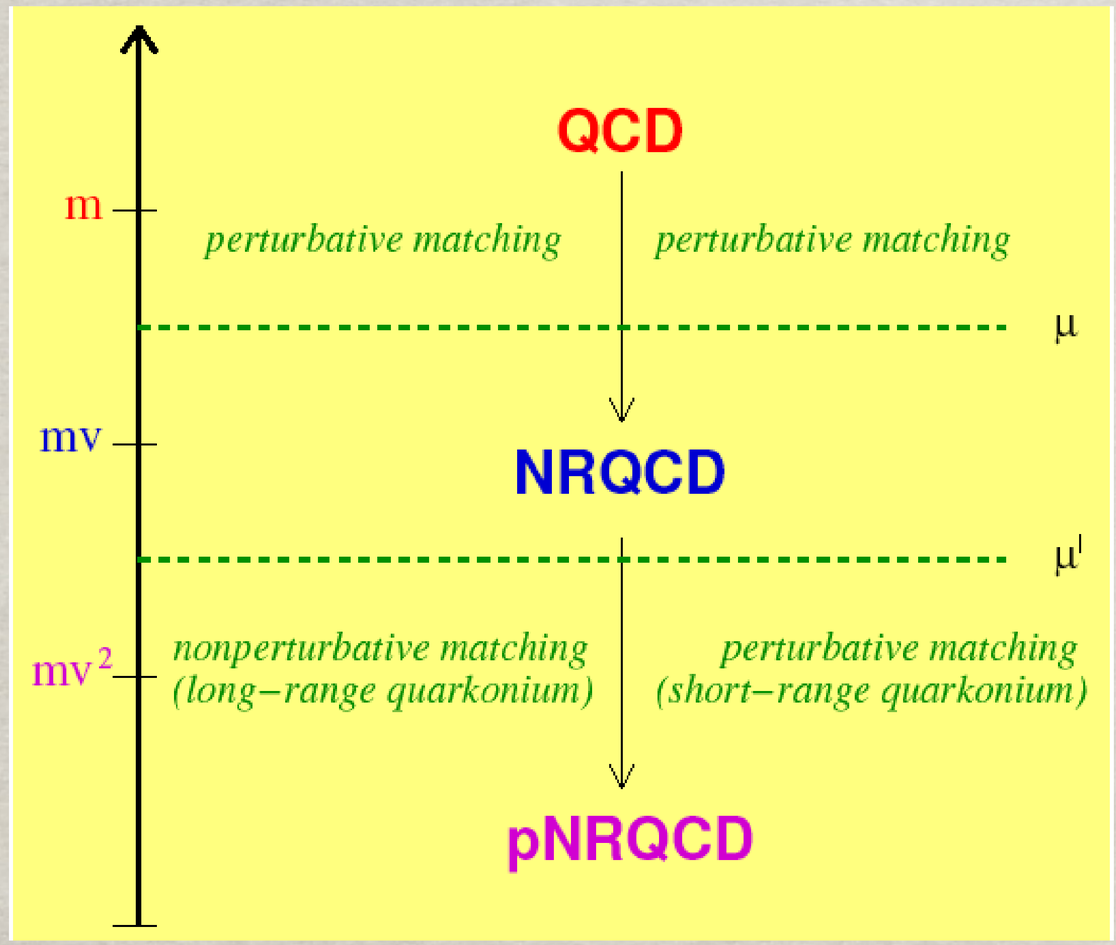

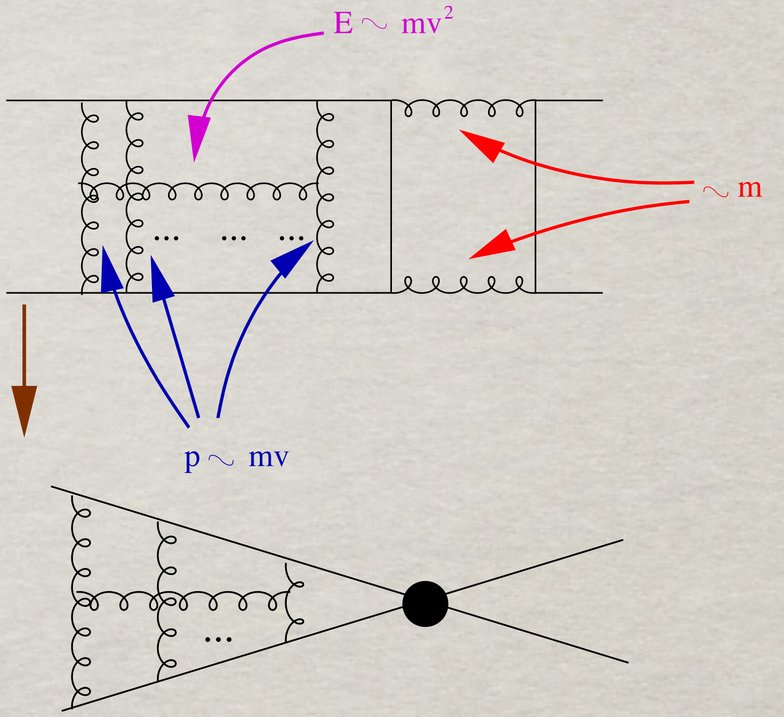

Quarkonium with NR EFT: potential NonRelativistic QCD (pNRQCD)

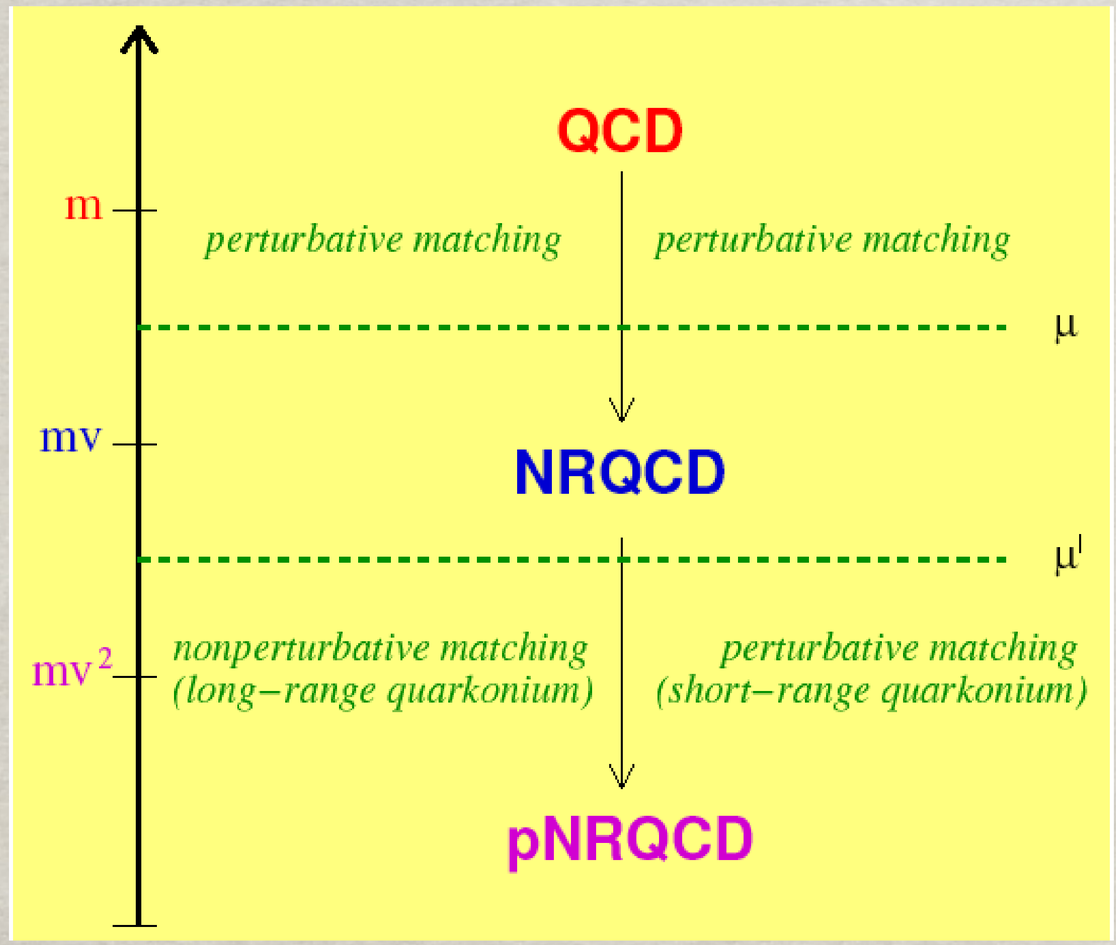

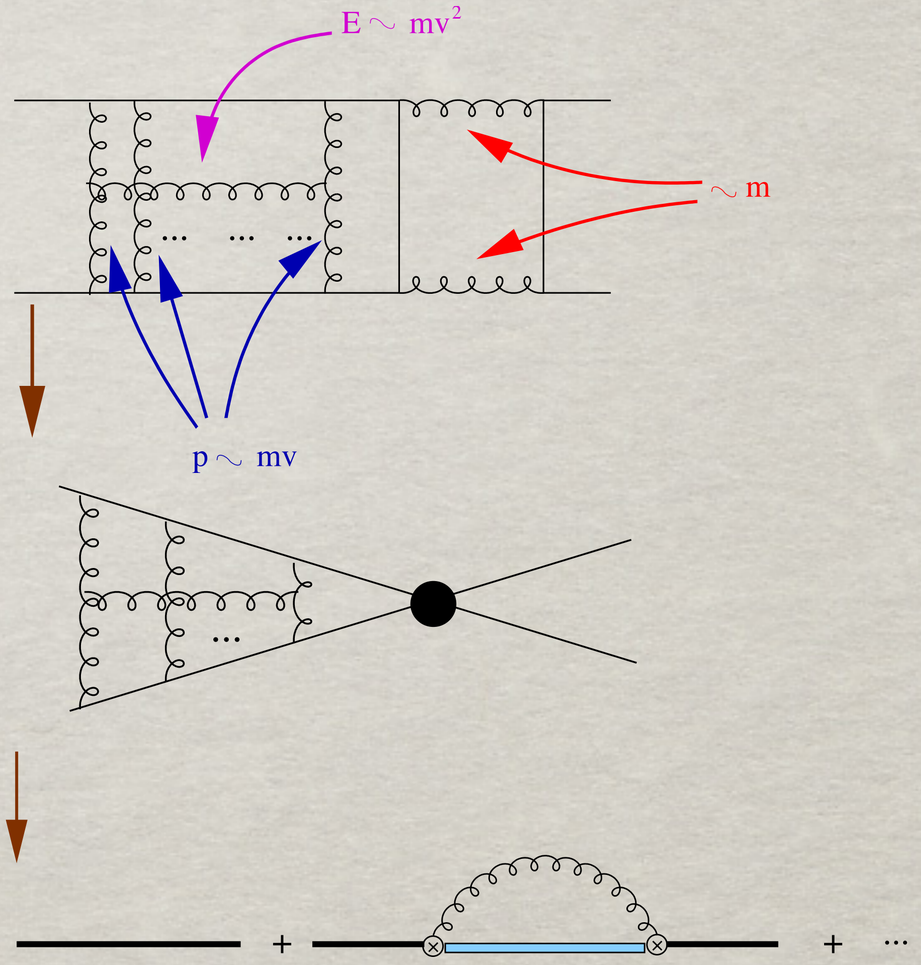

Quarkonium with NR EFT: potential NonRelativistic QCD (pNRQCD)

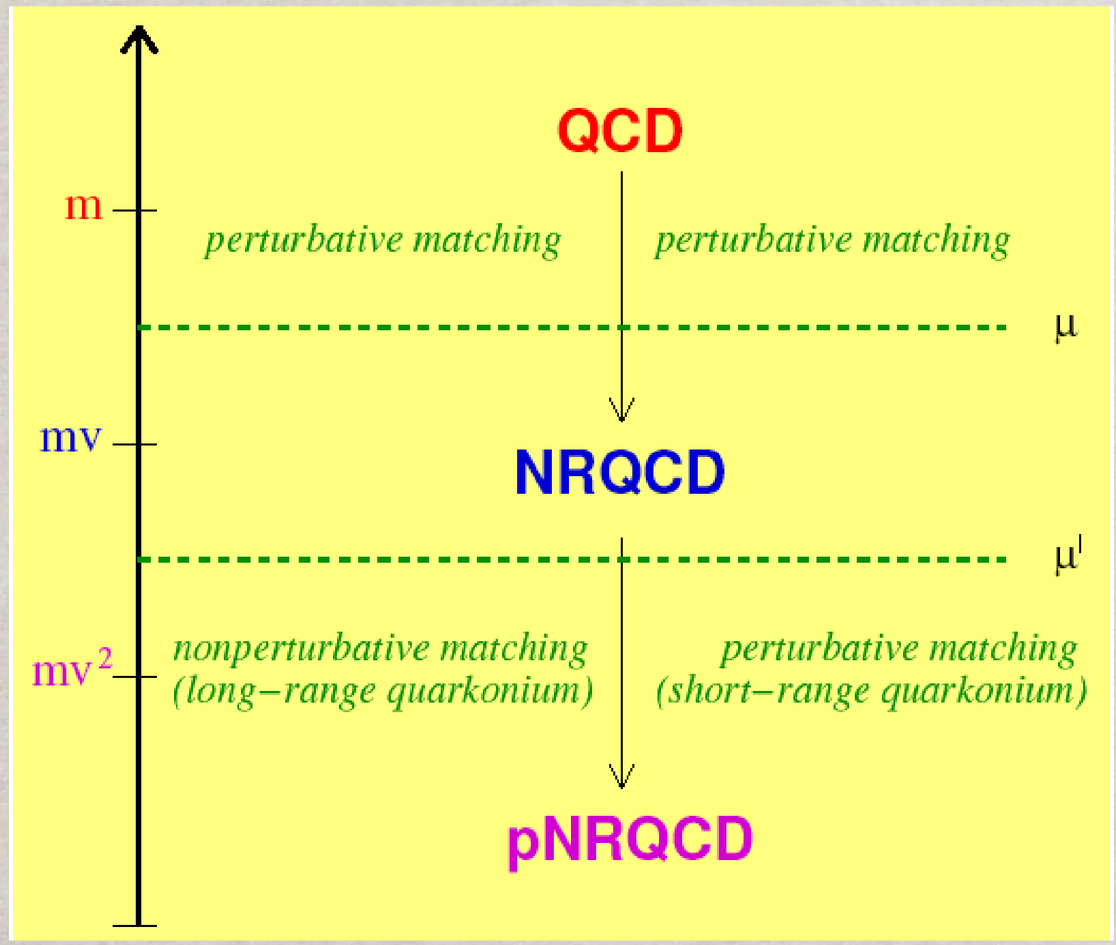

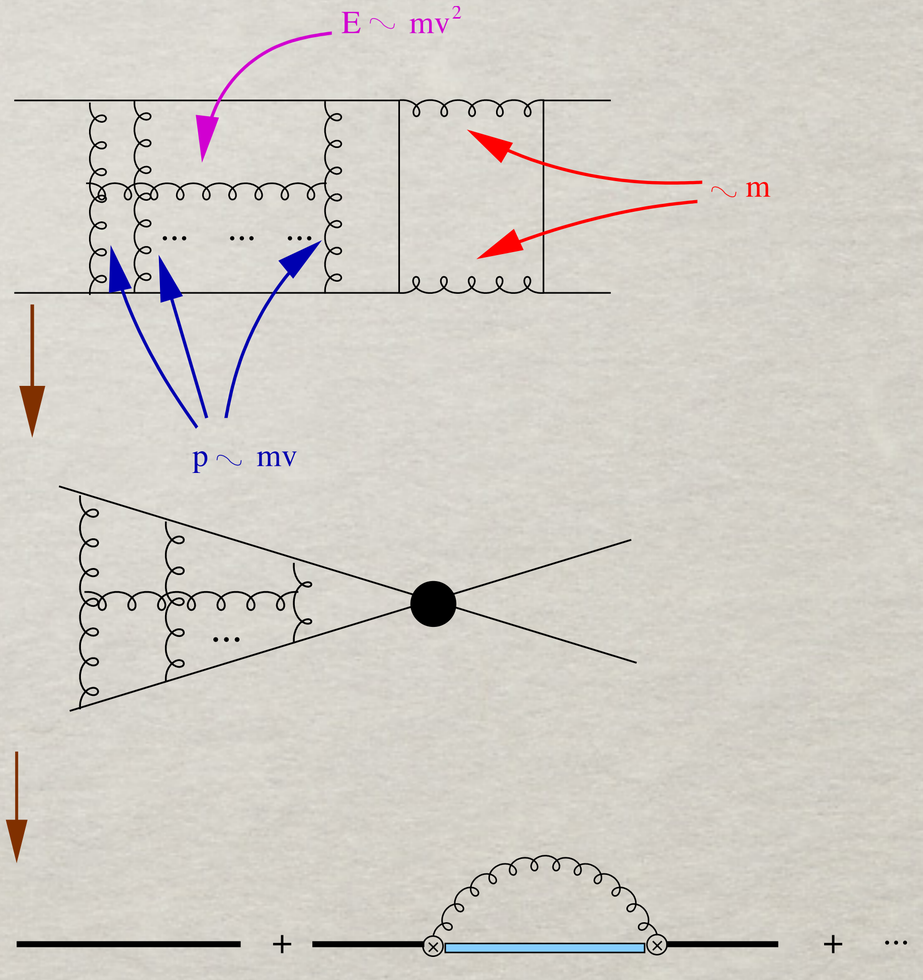

$$\mathcal{L}_{\rm pNRQCD} = \sum_k \sum_n \frac{1}{m^k} c_k(\alpha_{\rm s}(m/\mu)) \times V(r\mu', r\mu) \times O_n(\mu', \lambda)\, r^n$$

Quarkonium with NR EFT: potential NonRelativistic QCD (pNRQCD)

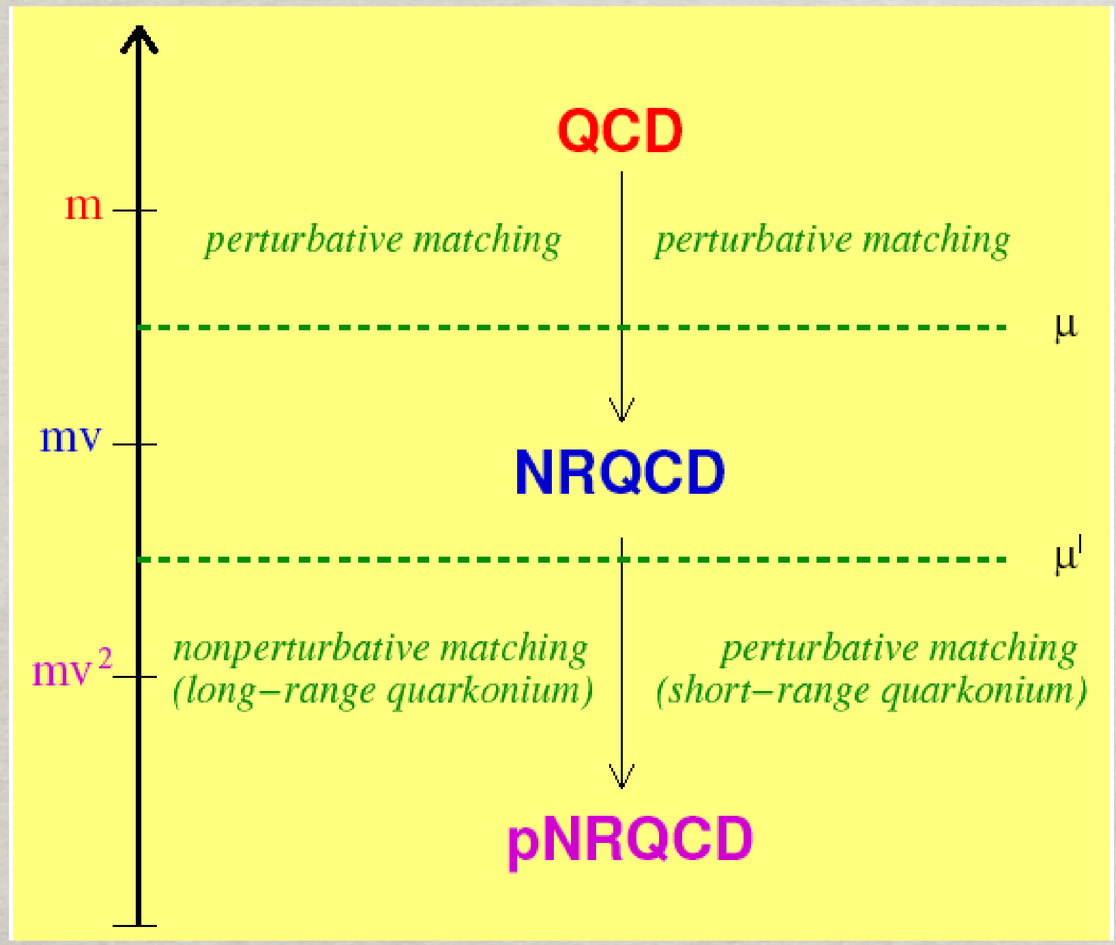

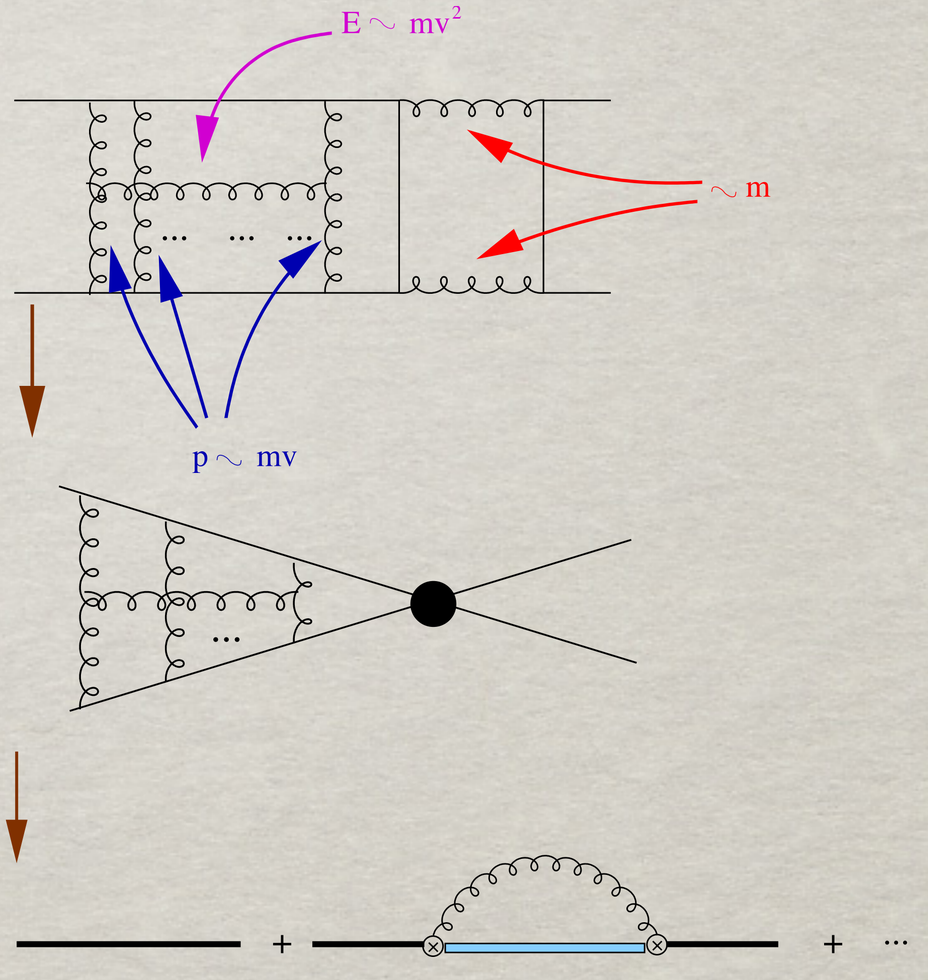

$$\mathcal{L}_{\rm pNRQCD} = \sum_k \sum_n \frac{1}{m^k} c_k(\alpha_{\rm s}(m/\mu)) \times V(r\mu', r\mu) \times O_n(\mu', \lambda)\, r^n$$

Quarkonium with NREFT: pNRQCD

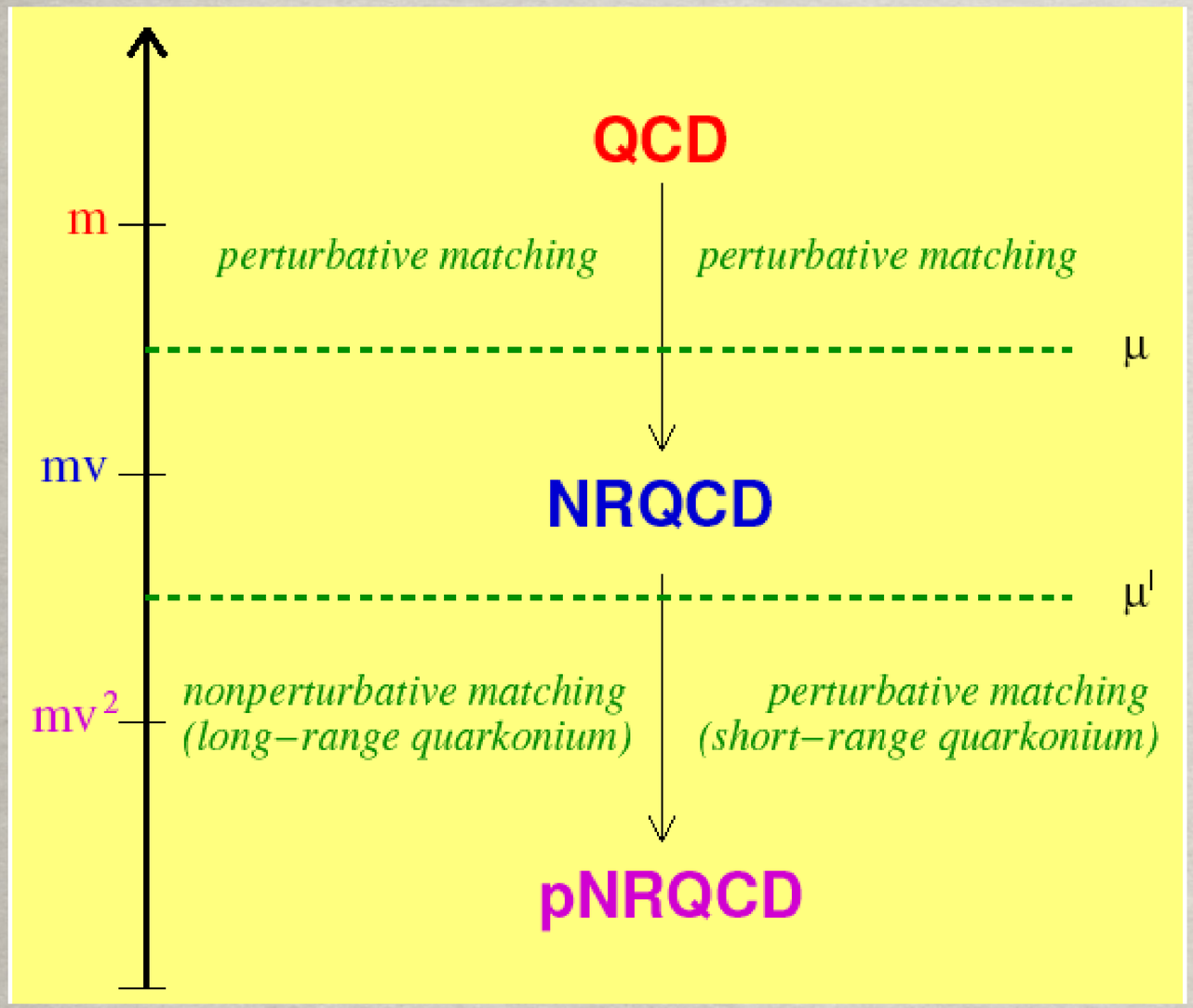

Quarkonium with NREFT: pNRQCD

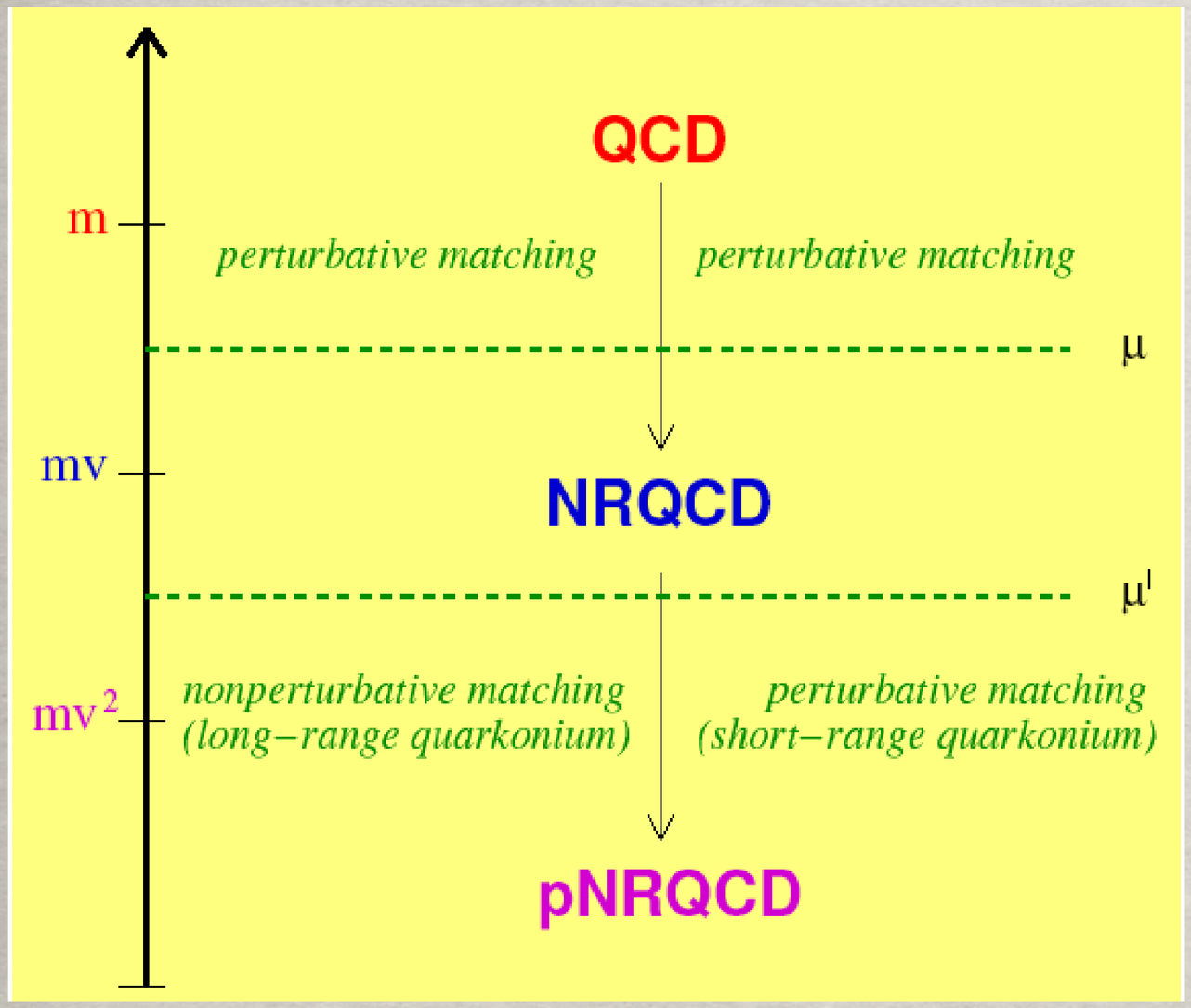

In QCD another scale is relevant $\Lambda_{\rm QCD}$

Quarkonium with NREFT: pNRQCD

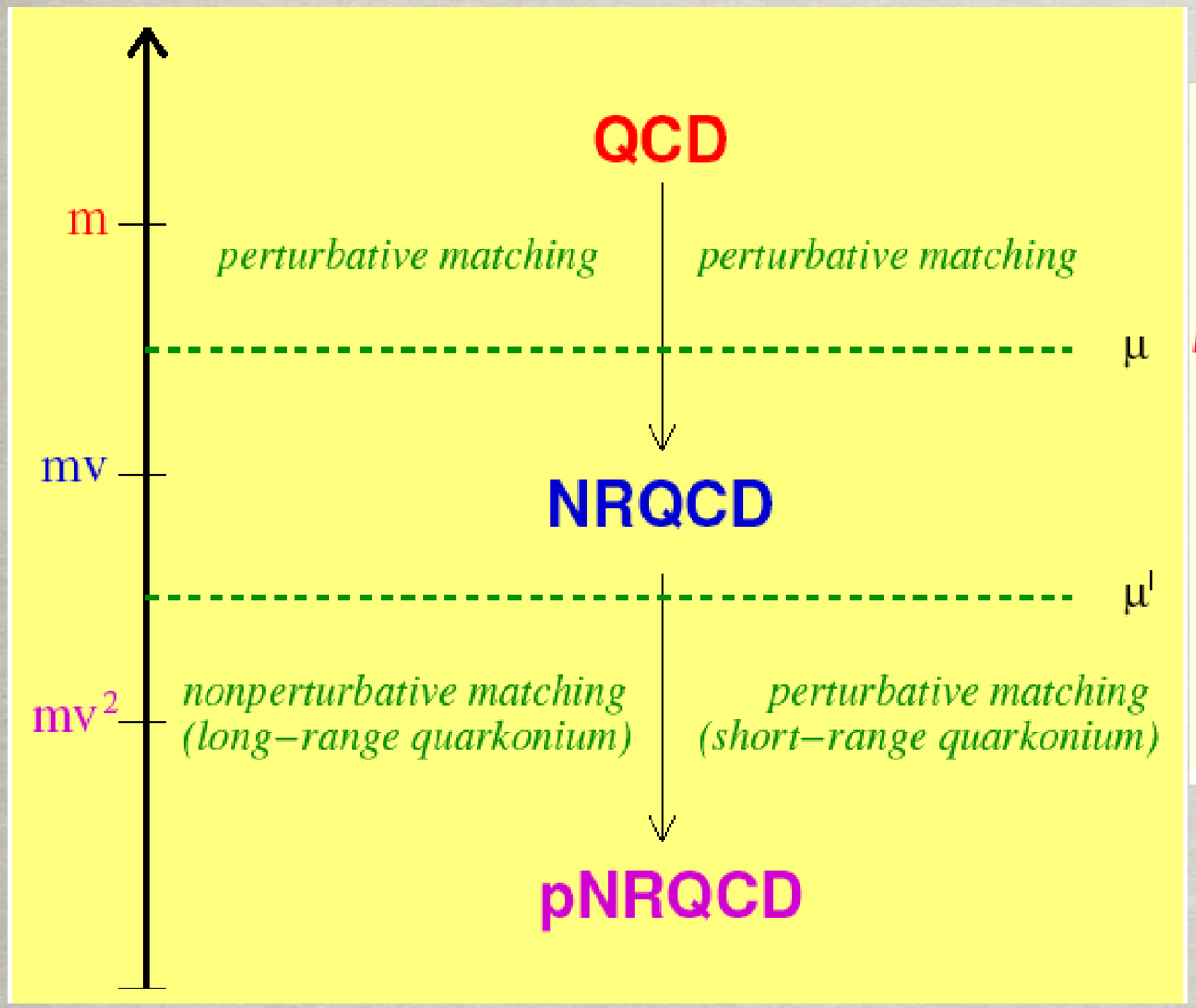

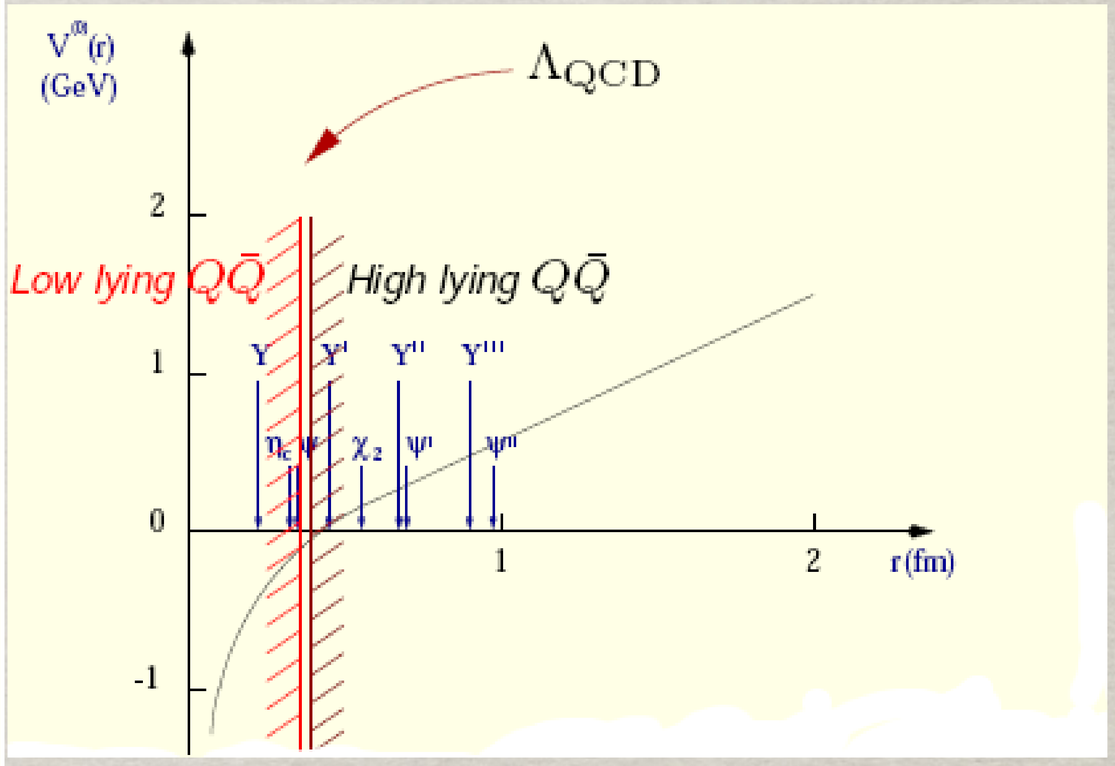

In QCD another scale is relevant $\Lambda_{\rm QCD}$

Quarkonium with NREFT: pNRQCD

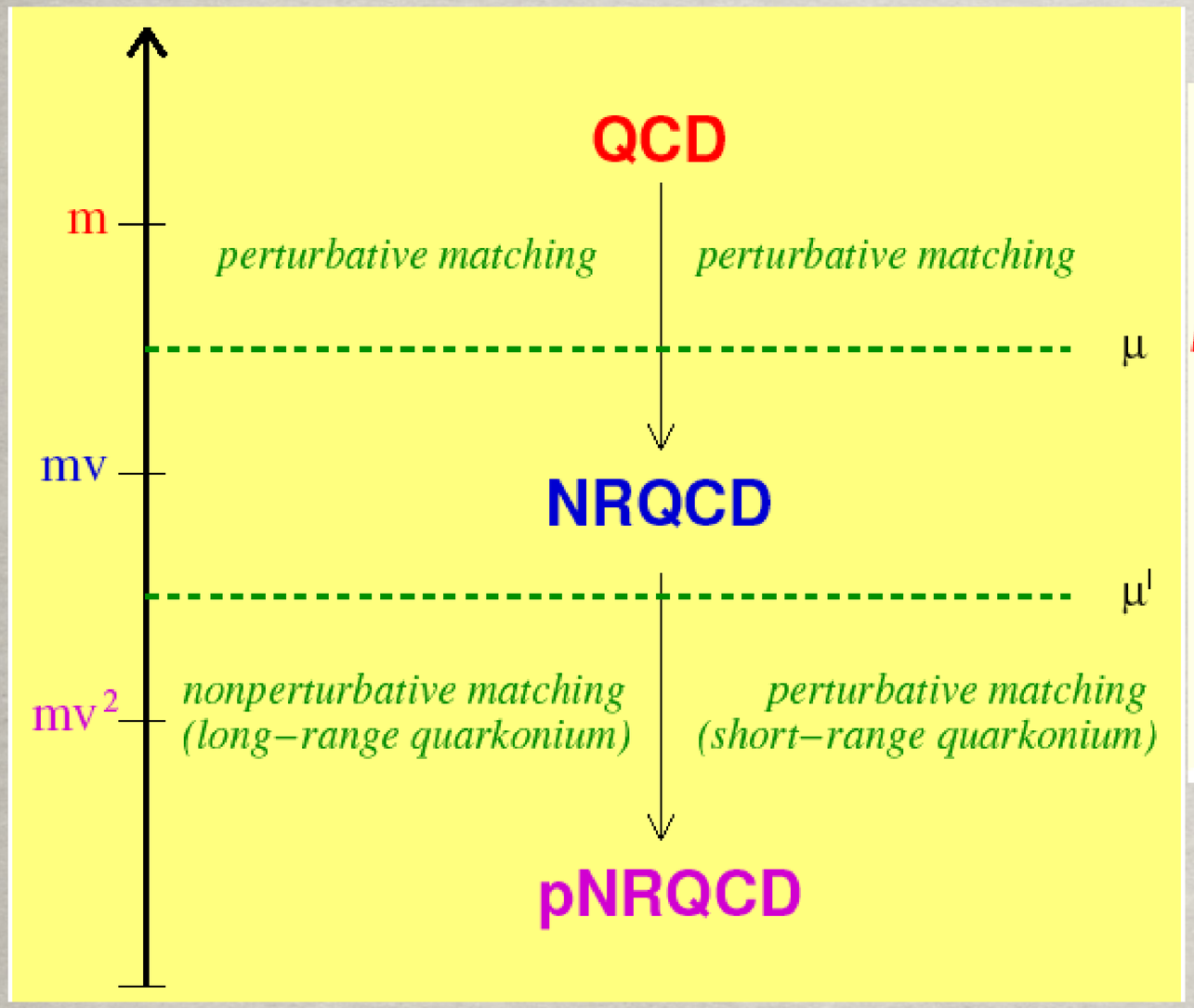

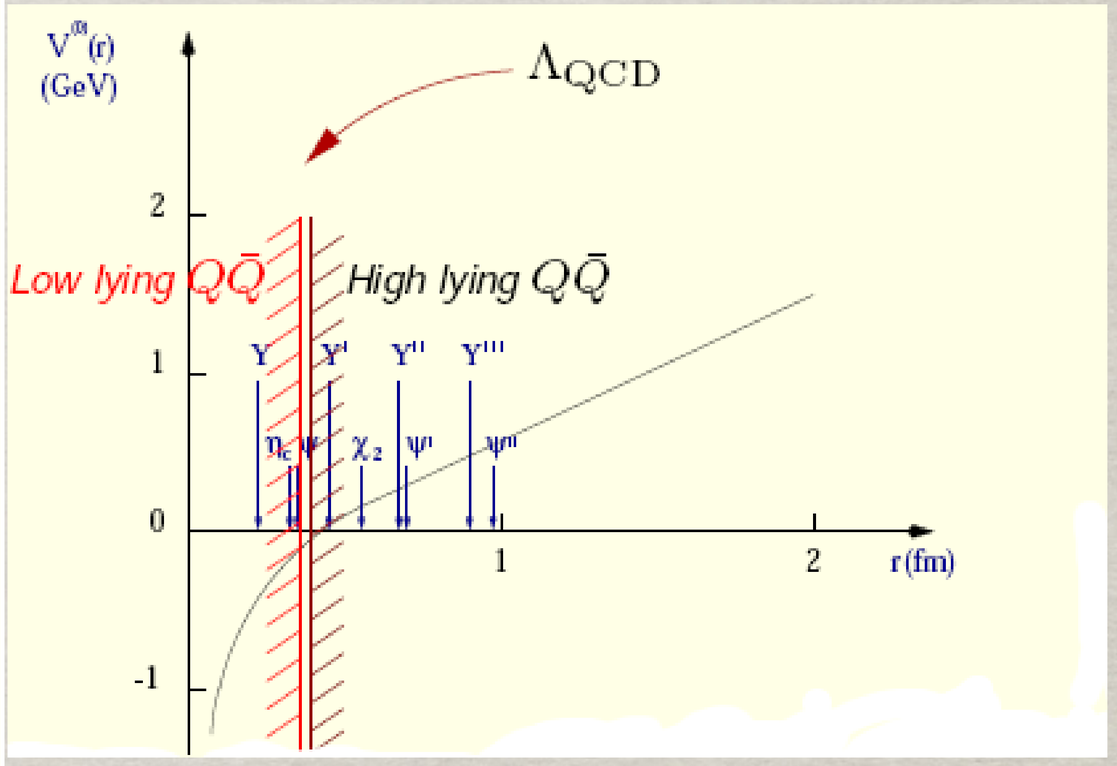

A potential picture arises at the level of pNRQCD:

- the potential is perturbative if $mv \gg \Lambda_{\rm QCD}$
- the potential is non-perturbative if $mv \sim \Lambda_{\rm QCD}$

In QCD another scale is relevant $\Lambda_{\rm QCD}$

Quarkonium with NREFT: pNRQCD

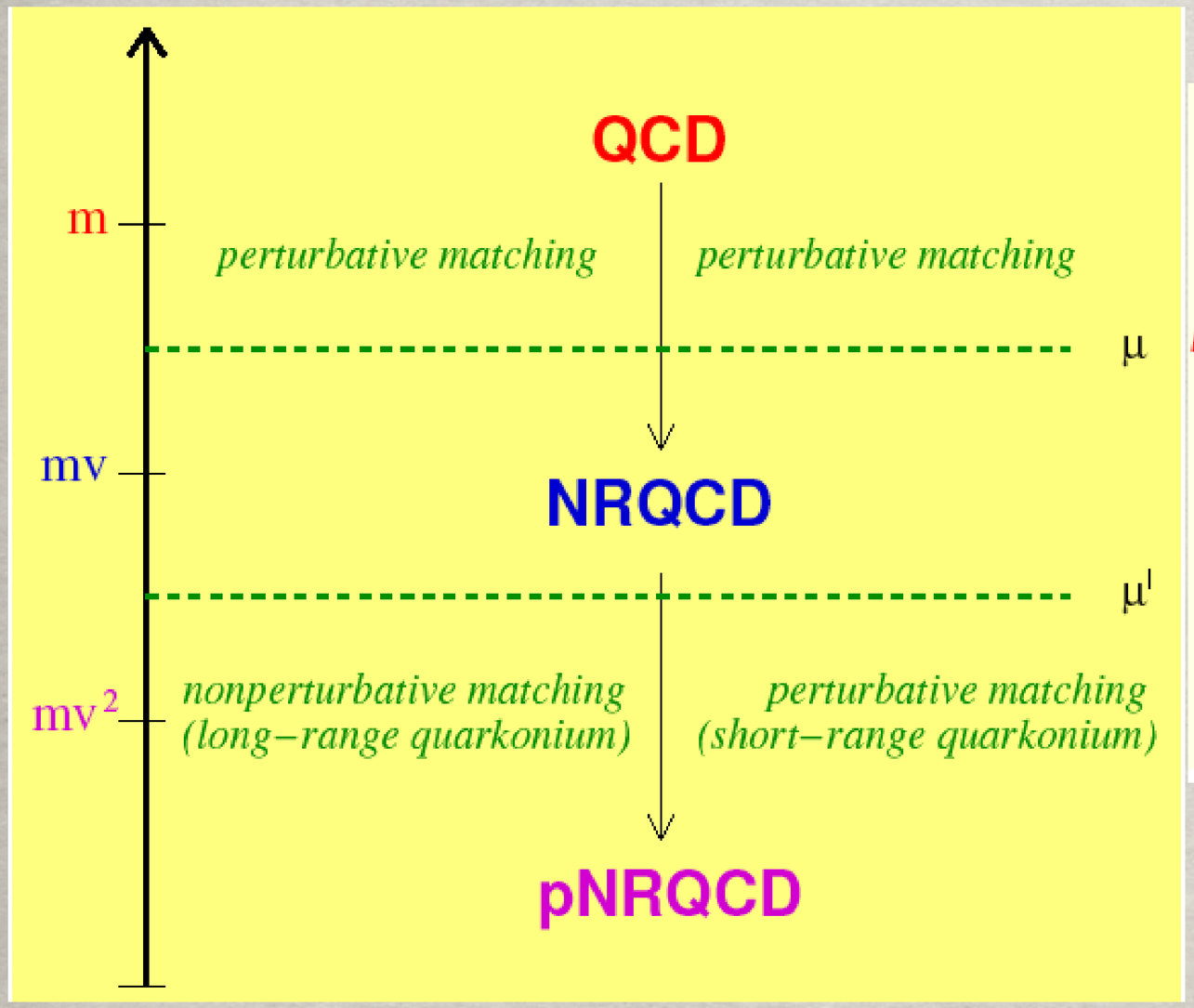

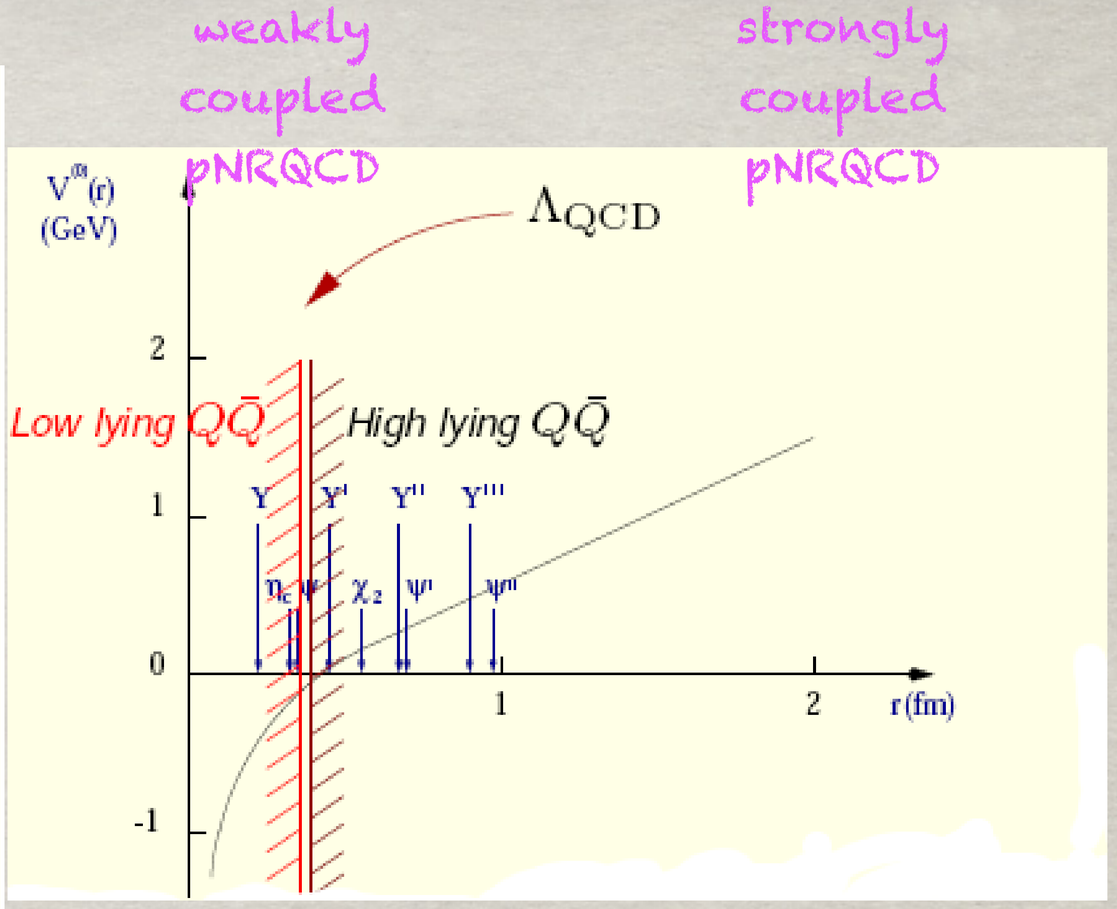

A potential picture arises at the level of pNRQCD:

- the potential is perturbative if $mv \gg \Lambda_{\rm QCD}$
- the potential is non-perturbative if $mv \sim \Lambda_{\rm QCD}$

In QCD another scale is relevant $\Lambda_{\rm QCD}$

Quarkonium with NREFT

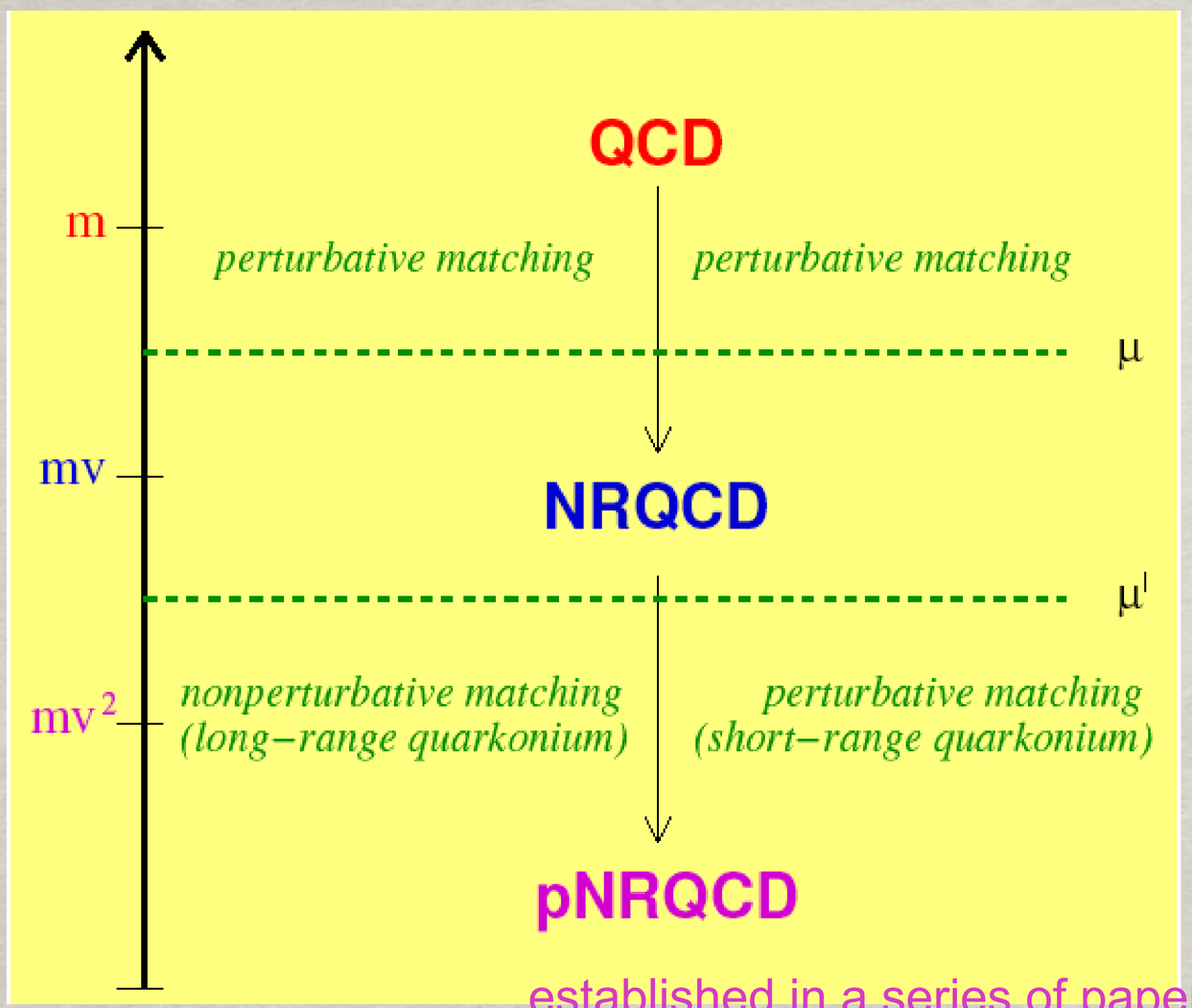

Caswell, Lepage 86,
Lepage, Thacker 88
Bodwin, Braaten, Lepage 95.....

Pineda, Soto 97, N.B. et al, 99,00,
Luke Manohar 97, Luke Savage 98,
Beneke Smirnov 98, Labelle 98
Labelle 98, Grinstein Rothstein 98
Kniehl, Penin 99, Griesshammer 00,
Manohar Stewart 00, Luke et al 00,
Hoang et al 01, 03->

established in a series of papers:
Pineda, Soto 97, N.B., Pineda, Soto, Vairo 99
N.B. Vairo, et al. 00–022
N.B., Pineda, Soto, Vairo Review of Modern Physis 77(2005) 1423

pNRQCD addresses the bound state dynamics

$$\mathcal{L}_{\mathrm{pNREFT}} = \int d^3r \phi^\dagger (i\partial_0 - \frac{\mathbf{p}^2}{m} - V)\phi + \Delta\mathcal{L}$$

pNRQCD addresses the bound state dynamics

$$\mathcal{L}_{\rm pNREFT} = \int d^3r \phi^\dagger (i\partial_0 - \frac{\mathbf{p}^2}{m} - V)\phi + \Delta\mathcal{L}$$

- It is obtained by integrating out hard and soft gluons with p or E scaling like m, mv.
- The d.o.f. are $Q\bar{Q}$ pairs (sometimes cast in color singlet S and color octet O) and ultrasoft modes (e.g. light quarks, low-energy gluons):
  $\phi = S$
- The Lagrangian is organized as an expansion in $1/m$ and r.
- The form of $\Delta\mathcal{L}$ and of the ultrasoft modes depends on the low energy dynamics.

pNRQCD addresses the bound state dynamics

$$\mathcal{L}_{\rm pNREFT} = \int d^3 r \phi^\dagger (i\partial_0 - \frac{\mathbf{p}^2}{m} - V)\phi + \Delta\mathcal{L}$$

- It is obtained by integrating out hard and soft gluons with p or E scaling like m, mv.
- The d.o.f. are $Q\bar{Q}$ pairs (sometimes cast in color singlet S and color octet O) and ultrasoft modes (e.g. light quarks, low-energy gluons): $\phi = S$
- The Lagrangian is organized as an expansion in $1/m$ and r.
- The form of $\Delta\mathcal{L}$ and of the ultrasoft modes depends on the low energy dynamics.

In QCD another scale is relevant $\Lambda_{\rm QCD}$

- The leading picture is Schoedinger eq.,the potentials appear once all scales above the energy have been been integrated out
- non potential effects appear as correction to the leading picture and are nonperturbative
- Any prediction of pNRQCD is a prediction of QCD at the given order of expansion
- Effects at the nonperturbative scale are carried by gauge invariant purely glue dependent correlators to be calculated on the lattice or in QCD vacuum models

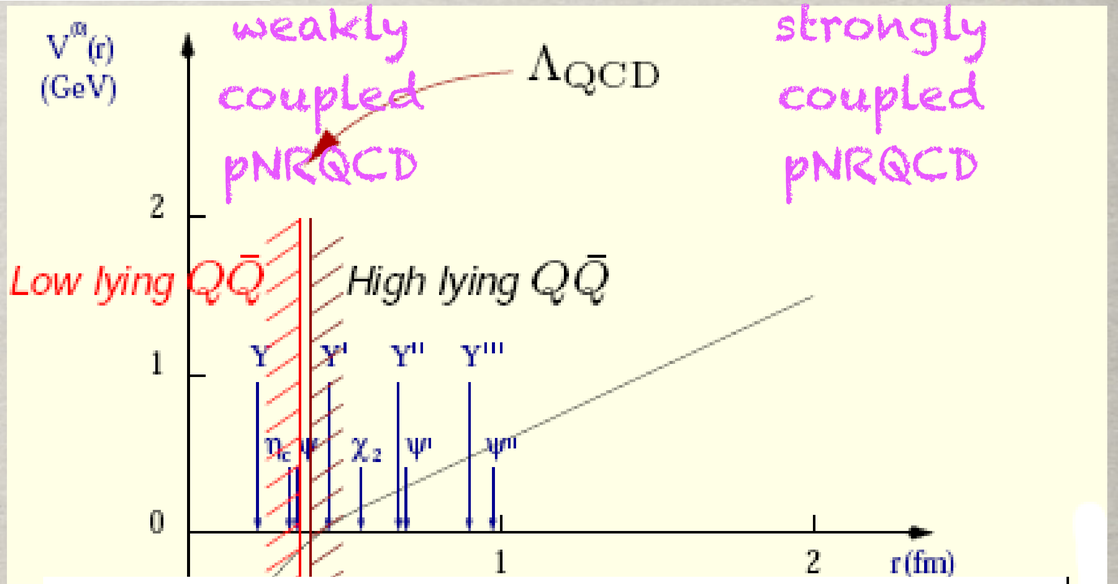

A potential picture arises at the level of pNRQCD:

- the potential is perturbative if $mv \gg \Lambda_{\rm QCD}$
- the potential is non-perturbative if $mv \sim \Lambda_{\rm QCD}$

Weakly coupled pNRQCD

- Pineda Soto NP PS 64 (1998) 428
  Brambilla Pineda Soto Vairo NPB 566 (2000) 275

- If $mv \gg \Lambda_{\rm QCD}$, the matching is perturbative

  Non-analytic behaviour in $r \to$ matching coefficients V

The gauge fields are multipole expanded:

$$A(R,r,t) = A(R,t) + \mathbf{r}\cdot\boldsymbol{\nabla} A(R,t) + \dots$$

$\mathbf{R}$ = center of mass

$\mathbf{r} = Q\bar{Q}$ distance

$$\mathcal{L}^{\rm pNRQCD} = \int d^3r\, {\rm Tr}\,\{S^\dagger(i\partial_0 - \frac{\mathbf{p}^2}{m} - V_S + \cdots)S + O^\dagger(iD_0 - \frac{\mathbf{p}^2}{m} - V_O + \cdots)O + \quad \text{LO in r}$$

$$+V_A(S^\dagger \mathbf{r}\cdot g\mathbf{E} O + O^\dagger \mathbf{r}\cdot g\mathbf{E} S) + \frac{V_B}{2}(O^\dagger \mathbf{r}\cdot g\mathbf{E} O + O^\dagger O \mathbf{r}\cdot g\mathbf{E})\} + \dots \quad \text{NLO in r}$$

$$-\frac{1}{4}F^a_{\mu\nu}F^{\mu\nu\,a} + \sum_{i=1}^{n_f}\bar{q}_i\, i\not{D} q_i$$

Weakly coupled pNRQCD

- If $mv \gg \Lambda_{\rm QCD}$, the matching is perturbative

  Non-analytic behaviour in $r \to$ matching coefficients V

Pineda Soto NP PS 64 (1998) 428

Brambilla Pineda Soto Vairo NPB 566 (2000) 275

The gauge fields are multipole expanded:

$$A(R,r,t) = A(R,t) + \mathbf{r}\cdot\boldsymbol{\nabla} A(R,t) + \dots$$

$\mathbf{R}$ = center of mass

$\mathbf{r}$ = $Q\bar{Q}$ distance

$$\mathcal{L}^{\rm pNRQCD} = \int d^3r\, {\rm Tr}\,\{S^\dagger(i\partial_0 - \frac{\mathbf{p}^2}{m} - V_S + \cdots)S + O^\dagger(iD_0 - \frac{\mathbf{p}^2}{m} - V_O + \cdots)O +$$

$$+V_A(S^\dagger \mathbf{r}\cdot g\mathbf{E} O + O^\dagger \mathbf{r}\cdot g\mathbf{E} S) + \frac{V_B}{2}(O^\dagger \mathbf{r}\cdot g\mathbf{E} O + O^\dagger O \mathbf{r}\cdot g\mathbf{E})\} + \dots$$

LO in r

NLO in r

$$-\frac{1}{4}F^a_{\mu\nu}F^{\mu\nu\,a} + \sum_{i=1}^{n_f}\bar{q}_i\, i\not{D} q_i$$

The matching coefficients are the Coulomb potential

$$V_S(r) = -C_F\frac{\alpha_{\rm s}}{r} + \dots, \qquad V_o(r) = \frac{1}{2N}\frac{\alpha_{\rm s}}{r} + \dots,$$

$$V_A = 1 + \mathcal{O}(\alpha_{\rm s}^2),\ V_B = 1 + \mathcal{O}(\alpha_{\rm s}^2).$$

Feynman rules

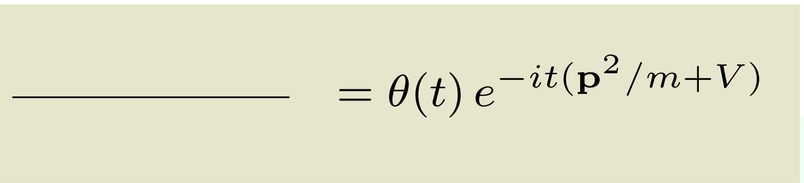

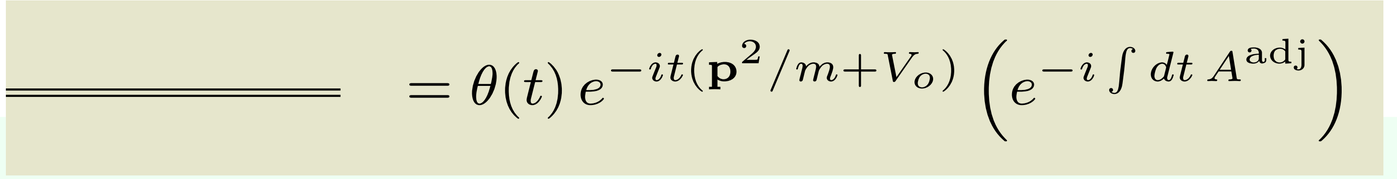

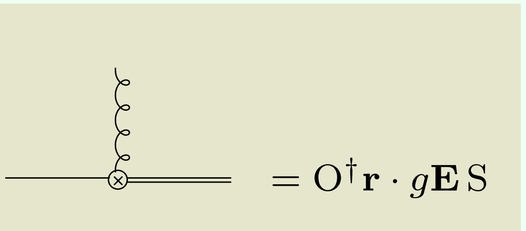

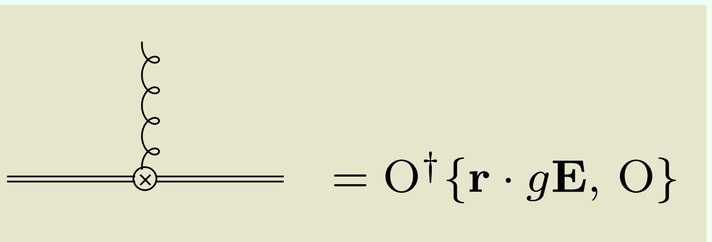

Strongly coupled pNRQCD

$$\mathcal{L} = \mathrm{Tr}\left\{ \mathrm{S}^\dagger \left(i\partial_0 - \frac{\mathbf{p}^2}{m} - V_s \right) \mathrm{S} \right\} + \Delta\mathcal{L}(\mathrm{US\ light\ quarks})$$

static — spin dependent — velocity dependent

$$V = V_0 + \frac{1}{m} V_1 + \frac{1}{m^2}(V_{SD} + V_{VD})$$

$$V^{(1)} = -\frac{1}{2}\int_0^\infty dt\, t \left\langle \right\rangle$$

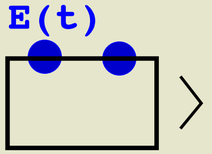

$$V_{\mathrm{SD}}^{(2)} = -\frac{r^k}{r^2} c_F\, \epsilon^{kij}\, i \int_0^\infty dt\, t \left\langle \right\rangle \mathbf{L}_1 \cdot \mathbf{S}_2 + (1 \leftrightarrow 2)\ |V_{LS}^{(2)}$$

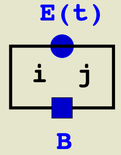

$$-\frac{r^k}{r^2}\left(c_F\, \epsilon^{kij}\, i \int_0^\infty dt\, t \left\langle \right\rangle - \frac{2c_F - 1}{2} \nabla^k V^{(0)} \right) \mathbf{L}_1 \cdot \mathbf{S}_1 + (1 \leftrightarrow 2)\ |V_{LS}^{(1)}$$

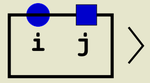

$$-c_F^2 \hat{r}_i \hat{r}_j i \int_0^\infty dt \left(\left\langle \right\rangle - \frac{\delta_{ij}}{3} \left\langle \right\rangle \right) \left(\mathbf{S}_1 \cdot \mathbf{S_2} - 3(\mathbf{S}_1 \cdot \hat{\mathbf{r}})(\mathbf{S_2} \cdot \hat{\mathbf{r}}) \right) |V_T$$

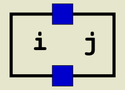

$$+\left(\frac{2}{3} c_F^2 i \int_0^\infty dt \left\langle \right\rangle - 4\left(d_{sv} + \frac{4}{3} d_{vv} \right) \delta^{(3)}(\mathbf{r}) \right) \mathbf{S}_1 \cdot \mathbf{S_2}\ |V_S +$$

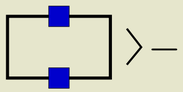

$c_F = 1 + \alpha_{\mathrm{s}}/\pi(13/6 + 3/2 \ln m/\mu) + ...)$, $d_{sv,vv} = O(\alpha_{\mathrm{s}}^2)$ from NRQCD.

- Pineda Vairo PRD 63 (2001) 054007
- Brambilla Pineda Soto Vairo PRD 63 (2001) 014023

Strongly coupled pNRQCD

$$\mathcal{L} = \mathrm{Tr}\left\{ \mathrm{S}^\dagger \left(i\partial_0 - \frac{\mathbf{p}^2}{m} - V_s \right) \mathrm{S} \right\} + \Delta\mathcal{L}(\mathrm{US\ light\ quarks})$$

static — spin dependent — velocity dependent

$$V = V_0 + \frac{1}{m} V_1 + \frac{1}{m^2}(V_{SD} + V_{VD})$$

$$V^{(1)} = -\frac{1}{2}\int_0^\infty dt\, t \left\langle \right\rangle$$

E(t)

$$V_{\mathrm{SD}}^{(2)} = -\frac{r^k}{r^2} c_F\, \epsilon^{kij}\, i \int_0^\infty dt\, t \langle \; \mathrm{i} \quad \mathrm{j} \; \rangle \; \mathbf{L}_1 \cdot \mathbf{S}_2 + (1 \leftrightarrow 2) \; |V_{LS}^{(2)}$$

E(t), i, j, B

$$-\frac{r^k}{r^2}\left(c_F\, \epsilon^{kij}\, i \int_0^\infty dt\, t \, \langle \; \mathrm{i} \quad \mathrm{j} \; \rangle - \frac{2c_F - 1}{2} \nabla^k V^{(0)} \right) \mathbf{L}_1 \cdot \mathbf{S}_1 + (1 \leftrightarrow 2) \; |V_{LS}^{(1)}$$

$$-c_F^2 \hat{r}_i \hat{r}_j i \int_0^\infty dt \left(\langle \; \mathrm{i} \quad \mathrm{j} \; \rangle - \frac{\delta_{ij}}{3} \left\langle \right\rangle \right) \left(\mathbf{S}_1 \cdot \mathbf{S_2} - 3(\mathbf{S}_1 \cdot \hat{\mathbf{r}})(\mathbf{S_2} \cdot \hat{\mathbf{r}}) \right) |V_T$$

$$+\left(\frac{2}{3} c_F^2 i \int_0^\infty dt \langle \; \rangle - 4\left(d_{sv} + \frac{4}{3} d_{vv} \right) \delta^{(3)}(\mathbf{r}) \right) \mathbf{S}_1 \cdot \mathbf{S_2} \; |V_S -$$

$c_F = 1 + \alpha_{\mathrm{s}}/\pi(13/6 + 3/2 \ln m/\mu) + ...)$, $d_{sv,vv} = O(\alpha_{\mathrm{s}}^2)$ from NRQCD.

- Pineda Vairo PRD 63 (2001) 054007
- Brambilla Pineda Soto Vairo PRD 63 (2001) 014023

- the potentials contain the contribution of the scale m inherited from NRQCD matching coefficients—> they cancel any QM divergences, good UV behaviour
- the nonperturbative part is factorized and depends only on the glue —> only one lattice calculation to get the dynamics and the observables instead of an ab initio calculation of multiple Green functions

Low energy (nonperturbative) factorized effects depend on the size of the physical system

The EFT factorizes the low energy nonperturbative part.
Depending on the physical system:

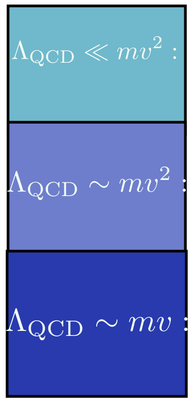

local condensates

$\langle F^2(0)\rangle$ $\Upsilon(1S)$, ...

non local condensates

$\Lambda_{\rm QCD} \sim t$ $\langle F(t)F(0)\rangle$ annihilations, short range $c\bar{c}$, $b\bar{b}$, gluelumps, ...

$\Lambda_{\rm QCD} \sim loop$ $\langle e^{ig\oint dx A(x)}\rangle$ long range $c\bar{c}$, $b\bar{b}$, hybrids, glueballs, ...

Wilson loops

The more extended the physical object, the more we probe the non-perturbative vacuum.

Low energy (nonperturbative) factorized effects depend on the size of the physical system

The EFT factorizes the low energy nonperturbative part.
Depending on the physical system:

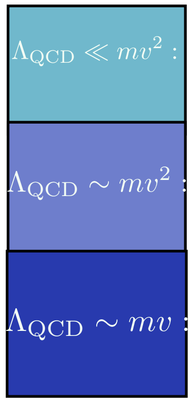

local condensates

$\Lambda_{\rm QCD} \ll mv^2$: $\langle F^2(0)\rangle$ $\Upsilon(1S)$, ...

non local condensates

$\Lambda_{\rm QCD} \sim t$ — $\Lambda_{\rm QCD} \sim mv^2$: $\langle F(t)F(0)\rangle$ annihilations, short range $c\bar{c}$, $b\bar{b}$, gluelumps, ...

$\Lambda_{\rm QCD} \sim loop$ — $\Lambda_{\rm QCD} \sim mv$: $\langle e^{ig\oint dx A(x)}\rangle$ long range $c\bar{c}$, $b\bar{b}$, hybrids, glueballs, ...

Wilson loops

The more extended the physical object, the more we probe the non-perturbative vacuum.

GAIN:

Inside the EFT:Model independent predictions, power counting

Lattice Calculation of only few nonperturbative objects, universal and depending only on the glue—> at variance with the state dependent calculation of each single observable with the full dynamics!

Inside the EFT: flexible phenomenological applications, understanding of the underlying degrees of freedom and dynamics

Low energy (nonperturbative) factorized effects depend on the size of the physical system

The EFT factorizes the low energy nonperturbative part.
Depending on the physical system:

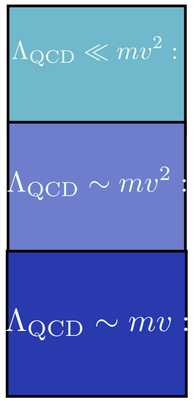

local condensates

$\Lambda_{\rm QCD} \ll mv^2$: $\langle F^2(0)\rangle$ $\Upsilon(1S)$, ...

non local condensates

$\Lambda_{\rm QCD} \sim t$ $\Lambda_{\rm QCD} \sim mv^2$: $\langle F(t)F(0)\rangle$ annihilations, short range $c\bar{c}$, $b\bar{b}$, gluelumps, ...

$\Lambda_{\rm QCD} \sim loop$ $\Lambda_{\rm QCD} \sim mv$: $\langle e^{ig\oint dx A(x)}\rangle$ long range $c\bar{c}$, $b\bar{b}$, hybrids, glueballs, ...

Wilson loops

The more extended the physical object, the more we probe the non-perturbative vacuum.

GAIN:

Inside the EFT:Model independent predictions, power counting

Lattice Calculation of only few nonperturbative objects, universal and depending only on the glue—> at variance with the state dependent calculation of each single observable with the full dynamics!

Inside the EFT: flexible phenomenological applications, understanding of the underlying degrees of freedom and dynamics

CHALLENGE:

Need techniques to reduce noise and improve convergence to continuum for calculation of chromelectric and chomomagnetic fields—> Gradient flow

one leitmotiv of this talk is to expose the glue dependent objects that are needed to be calculated on the lattice

Lattice input needed for the quarkonium at T=0, in medium, exotics

Below strong decay threshold

Weakly coupled pNRQCD: enables precise and systematic high order calculations on bound state allowing the extraction of precise determinations of standard model parameters like the quark masses and alpha_s from quarkonium

Strongly coupled pNRQCD: factorizes low energy nonperturbative contributions in terms of generalised gauge invariant Wilson loops depending only on the glue to be calculated on the lattice on in QCD vacuum model-> study of confinement, spectrum, decay, production

in hot medium

pNRQCD at finite temperature : defines the quark-antiquark potential at finite temperature; with open quantum systems allows to describe the nonequilibrium evolution of quarkonium inside the quark gluon plasma in heavy ion collisions —> may be relevant for the description of X Y Z in heavy ion collisions

at or above the strong decay threshold

BOEFT : allows to address in the same framework: hybrids, tetraquarks, molecules and pentaquark: XYZ states

Lattice input needed for the quarkonium at T=0, in medium, exotics

Below strong decay threshold

Weakly coupled pNRQCD: enables precise and systematic high order calculations on bound state

We need lattice calculation of local and time nonlocal correlators

Strongly coupled pNRQCD:

We need some lattice calculations of generalised Wilson loops,
correlators of electric fields
—> lattice could calculate the LDME of quarkonium production!

in hot medium

pNRQCD at finite temp

we need the lattice calculation of transport coefficients like:

$$\kappa = \frac{g^2}{18}\,\mathrm{Re}\int_{-\infty}^{+\infty} ds\,\langle\,\mathrm{T}\,E^{a,i}(s,\mathbf{0})\,\phi^{ab}(s,0)\,E^{b,i}(0,\mathbf{0})\rangle$$

input for nonequilibrium studies!

at or above the strong decay threshold

BOEFT :

We need lattice calculation of static energies, gluelump masses, correlators, generalised wilson loops

Quarkonium in a hot medium:the finite T potential in equilibrium

the change of paradigm from the screening to the imaginary part of the potential

Quarkonium in a hot medium:the finite T potential in equilibrium

the change of paradigm from the screening to the imaginary part of the potential

up to few years ago phenonological potentials were used the free energies from the lattice or the internal energy

pNRQCD at finite T defines what is the potential

Free energy vs potential

- Either phenomenological potentials have been used so far or the free energy calculated on the lattice.
- The free energy is not the static potential: the average free energy ($\sim \langle \mathrm{Tr}\, L^\dagger(r) \mathrm{Tr}\, L(0) \rangle$) is an overlap of singlet and octet quark-antiquark states, what is called the singlet ($\sim \langle \mathrm{Tr}\, L^\dagger(r)\, L(0) \rangle$) and the octet ($\sim \langle \mathrm{Tr}\, L^\dagger(r) \mathrm{Tr}\, L(0) \rangle - 1/3\, \langle \mathrm{Tr}\, L^\dagger(r)\, L(0) \rangle$) free energy are gauge dependent;

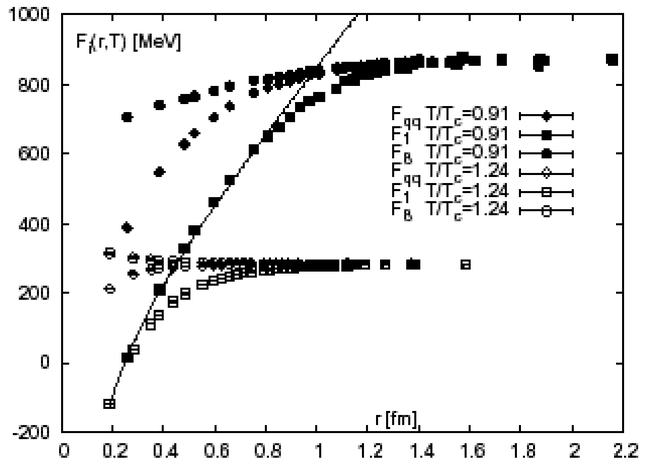

Kaczmarek Zantow PRD 71 (2005) 11451(

pNRQCD at finite T: the static potential

in pNRQCD the potential has a clear definition: it a matching coefficient and comes from the integration of all scales from mv up to (and not included) the energy mv^2

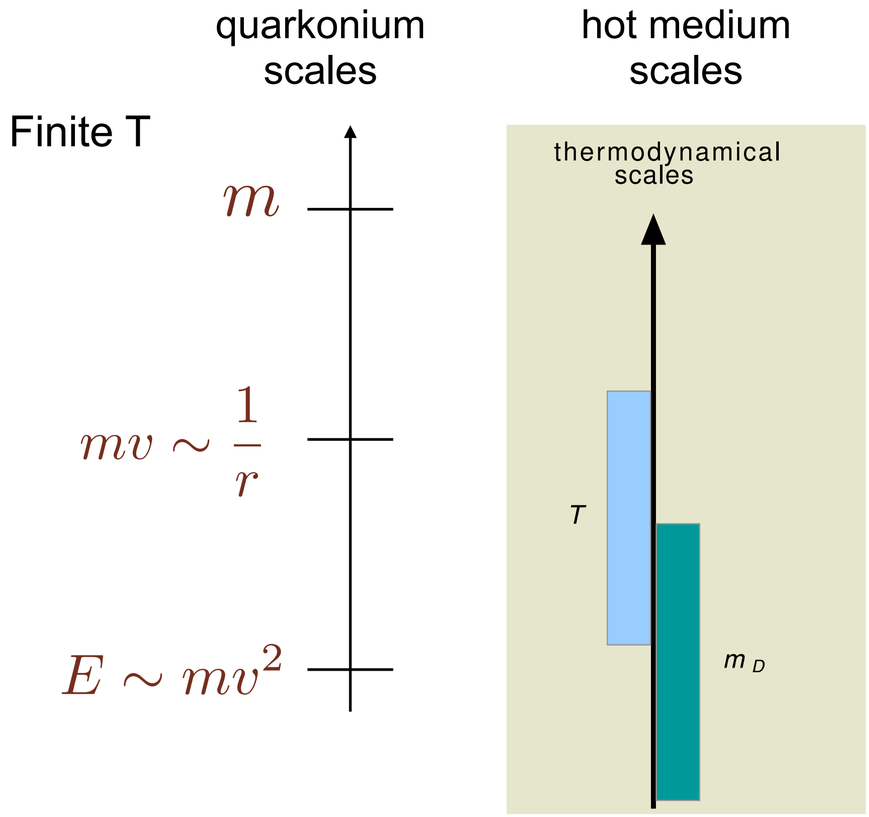

$$m \gg \Lambda_{QCD}$$

pNRQCD at finite T: the static potential

in pNRQCD the potential has a clear definition: it a matching coefficient and comes from the integration of all scales from mv up to (and not included) the energy mv^2

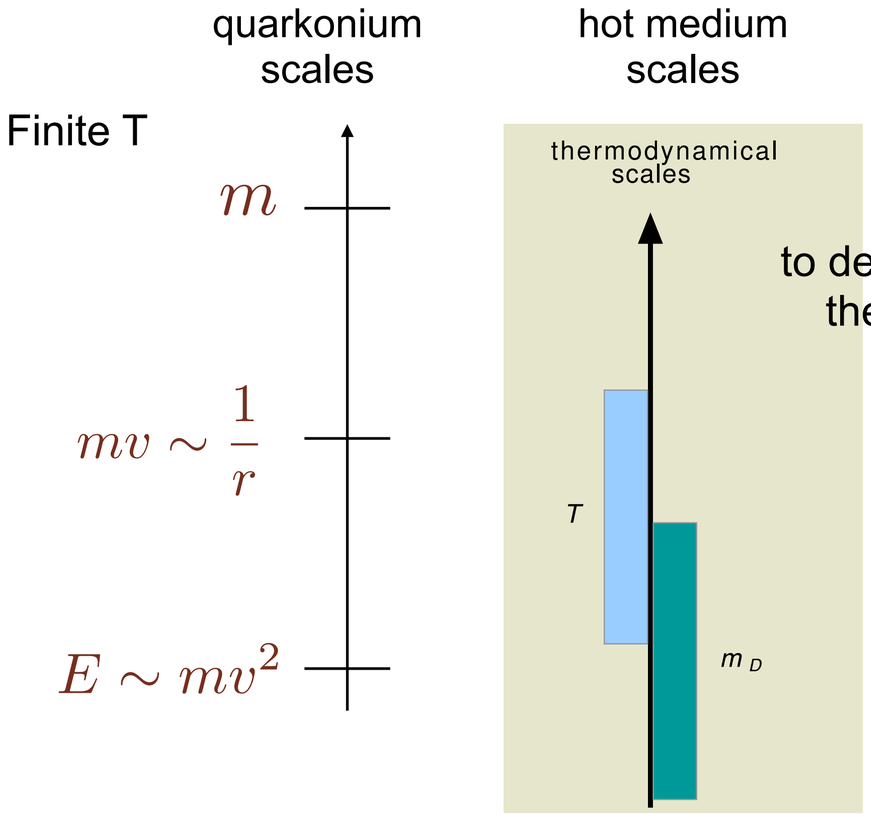

to define the potential we have to integrate out all the scales bigger than E including T and m_d

if T is of order E or less will give contribution to the energy and not to the potential

$$m \gg \Lambda_{QCD}$$

Notice:

The potential V(r,T) dictates through the Schroedinger equation the real time evolution of the QQbar in the medium

The finite T potential: how to obtain it

in pNRQCD the potential has a clear definition: it a matching coefficient and comes from the integration of all scales from mv up to (and not included) the energy mv^2

Finite T

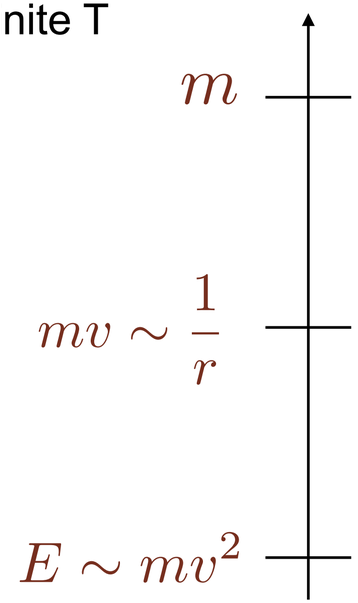

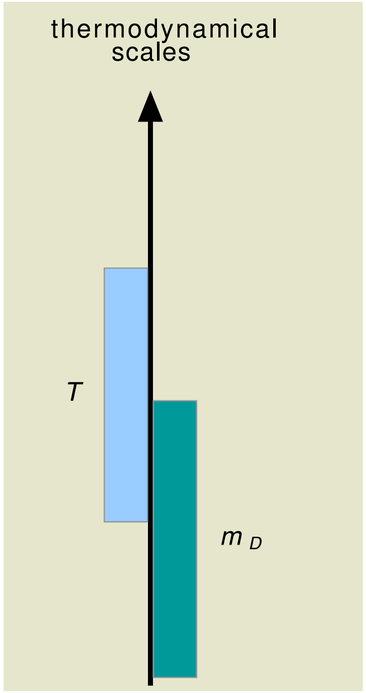

$$m \gg \Lambda_{QCD}$$

We assume that bound states exist for

- $T \ll m$
- $1/r \sim mv \gtrsim m_D$

We neglect smaller thermodynamical scales.

Inside these constraints we consider all the possible scales hierarchies

we work in the weak coupling regime

- $v \sim \alpha_s \ll 1$; valid for tightly bound states
- $T \gg gT \sim m_D$.

The thermal part of the potential has a real and an imaginary part

$\mathrm{Re}V_S(r,T)$

$\mathrm{Im}V_S(r,T)$

thermal width of $Q\bar{Q}$

New effect, specific of QCD
dominates for E/m_D>>1

Known from QED
dominates for m_D/E>>1

Singlet-to-octet

N.B Ghiglieri, Petreczky, Vairo 2008

Landau damping

Laine Philipssen Romatsche Tassler al 07,
Escobedo Soto 07

The thermal part of the potential has a real and an imaginary part

$\mathrm{Re}V_S(r,T)$

$\mathrm{Im}V_S(r,T)$

thermal width of $Q\bar{Q}$

New effect, specific of QCD
dominates for E/m_D>>1

Known from QED
dominates for m_D/E>>1

Singlet-to-octet

N.B Ghiglieri, Petreczky, Vairo 2008

(gluo dissociation)

N. B. Escobedo, Ghiglieri , Vairo 2011

Landau damping

Laine Philipssen Romatsche Tassler al 07,
Escobedo Soto 07

(inelastic parton scattering)

N. B. Escobedo, Ghiglieri , Vairo 2013

The singlet static potential and the static energy

you always have a real and an imaginary part

- Temperature effects can be other than screening

$T > 1/r$ and $1/r \sim m_D \sim gT$

exponential screening but $\mathrm{Im}V \gg \mathrm{Re}V$

$T > 1/r$ and $1/r > m_D \sim gT$ or $\frac{1}{r} \gg T \gg E$

no exponential screening but power-like T corrections

$T < E_{bin}$

no corrections to the potential, corrections to the energy

for the detailed form of the potentials in each regime see:

N.B Ghiglieri, Petreczky, Vairo Phys.Rev. D78 (2008) 014017

The singlet static potential and the static energy

you always have a real and an imaginary part

- Temperature effects can be other than screening

$T > 1/r$ and $1/r \sim m_D \sim gT$

exponential screening but $\mathrm{Im}V \gg \mathrm{Re}V$

$T > 1/r$ and $1/r > m_D \sim gT$ or $\frac{1}{r} \gg T \gg E$

no exponential screening but power-like T corrections

$T < E_{bin}$

no corrections to the potential, corrections to the energy

for the detailed form of the potentials in each regime see: N.B Ghiglieri, Petreczky, Vairo Phys.Rev. D78 (2008) 014017

imaginary parts in the potential have subsequently been found also for a strongly coupled plasma on the lattice (A. Rothkopf et al, Petreczky, Weber..) and in strings calculations

Change in the paradigm of dissociation

- The imaginary part is bigger than the real part before the screening exp{-m_D r} sets in

->the imaginary part is responsible for QQbar dissociation

$$T \gg 1/r \gg m_D \gg V$$

- Quarkonium dissociates at a temperature such that $\mathrm{Im}\, V_s(r) \sim \mathrm{Re}\, V_s(r) \sim \alpha_s/r$: $E_{\mathrm{binding}} \sim \Gamma$

$$\pi T_{\mathrm{dissociation}} \sim m g^{4/3}$$

- The interaction is screened when $\langle 1/r \rangle \sim m_D$, hence

$$\pi T_{\mathrm{screening}} \sim m g \gg \pi T_{\mathrm{dissociation}}$$

- Escobedo Soto arXiv:0804.0691
  Laine arXiv:0810.1112

Change in the paradigm of dissociation

- The imaginary part is bigger than the real part before the screening exp{-m_D r} sets in

->the imaginary part is responsible for QQbar dissociation

$$T \gg 1/r \gg m_D \gg V$$

- Quarkonium dissociates at a temperature such that $\mathrm{Im}\, V_s(r) \sim \mathrm{Re}\, V_s(r) \sim \alpha_s/r$: $E_{\mathrm{binding}} \sim \Gamma$

$$\pi T_{\mathrm{dissociation}} \sim m g^{4/3}$$

- The interaction is screened when $\langle 1/r \rangle \sim m_D$, hence

$$\pi T_{\mathrm{screening}} \sim m g \gg \pi T_{\mathrm{dissociation}}$$

- Escobedo Soto arXiv:0804.0691
  Laine arXiv:0810.1112

the EFT offers a systematic framework to do the calculations of the energy and width in a hot medium

Change in the paradigm of dissociation

- The imaginary part is bigger than the real part before the screening exp{-m_D r} sets in

->the imaginary part is responsible for QQbar dissociation

$$T \gg 1/r \gg m_D \gg V$$

- Quarkonium dissociates at a temperature such that $\mathrm{Im}\, V_s(r) \sim \mathrm{Re}\, V_s(r) \sim \alpha_s/r$:

$$\pi T_{\rm dissociation} \sim m g^{4/3}$$

$E_{\rm binding} \sim \Gamma$

- Escobedo Soto arXiv:0804.0691
  Laine arXiv:0810.1112

- The interaction is screened when $\langle 1/r \rangle \sim m_D$, hence

$$\pi T_{\rm screening} \sim m g \gg \pi T_{\rm dissociation}$$

the EFT offers a systematic framework to do the calculations of the energy and width in a hot medium

The bottomonium ground state , which is a weakly coupled non-relativistic bound state: $mv \sim m\alpha_{\rm s}$, $mv^2 \sim m\alpha_{\rm s}^2 \gtrsim \Lambda_{\rm QCD}$, produced in the QCD medium of heavy-ion collisions at the LHC may possibly realize the hierarchy

$$m \approx 5\ \text{GeV} \ > m\alpha_{\rm s} \approx 1.5\ \text{GeV} \ > \pi T \approx 1\ \text{GeV} \ > m\alpha_{\rm s}^2 \approx 0.5\ \text{GeV} \ \gtrsim m_D, \Lambda_{\rm QCD}$$

T_dissociation in the $\Upsilon(1S)$ case is about 450 MeV.

bottomonium 1S below the melting temperature T_d

The complete mass and width up to $\mathcal{O}(m\alpha_s^5)$

$$\delta E_{1S}^{(\mathrm{thermal})} = \frac{34\pi}{27}\alpha_s^2\,T^2 a_0 + \frac{7225}{324}\frac{E_1\alpha_s^3}{\pi}\left[\ln\left(\frac{2\pi T}{E_1}\right)^2 - 2\gamma_E\right] + \frac{128 E_1\alpha_s^3}{81\pi}L_{1,0} - 3a_0^2\left\{\left[\frac{6}{\pi}\zeta(3)+\frac{4\pi}{3}\right]\alpha_s\,T\,m_D^2 - \frac{8}{3}\zeta(3)\,\alpha_s^2\,T^3\right\}$$

$$\Gamma_{1S}^{(\mathrm{thermal})} = \frac{1156}{81}\alpha_s^3 T + \frac{7225}{162}E_1\alpha_s^3 + \frac{32}{9}\alpha_s\,T m_D^2\,a_0^2\,I_{1,0} - \left[\frac{4}{3}\alpha_s T m_D^2\left(\ln\frac{E_1^2}{T^2} + 2\gamma_E - 3 - \ln 4 - 2\frac{\zeta'(2)}{\zeta(2)}\right) + \frac{32\pi}{3}\ln 2\,\alpha_s^2\,T^3\right]a_0^2$$

where $E_1 = -\frac{4m\alpha_s^2}{9}$, $a_0 = \frac{3}{2m\alpha_s}$ and $L_{1,0}$ (similar $I_{1,0}$) is the Bethe logarithm.

- Brambilla Escobedo Ghiglieri Soto Vairo JHEP 1009 (2010) 038

first systematic calculation of the thermal contributions to quarkonium mass and width

Consistent with lattice calculations of spectral functions

- Aarts Allton Kim Lombardo Oktay Ryan Sinclair Skullerud JHEP 1111 (2011) 103

the EFT calculation gives a framework to define the potential, calculate it and systematically calculate energy levels and widths but calculations have been made in (resummed) perturbation theory

the EFT calculation gives a framework to define the potential, calculate it and systematically calculate energy levels and widths but calculations have been made in (resummed) perturbation theory

For large g one has to evaluate the Wilson loop with lattice QCD at finite T and extract a real and an imaginary part

the EFT calculation gives a framework to define the potential, calculate it and systematically calculate energy levels and widths but calculations have been made in (resummed) perturbation theory

For large g one has to evaluate the Wilson loop with lattice QCD at finite T and extract a real and an imaginary part

Complex Heavy-Quark Potential at Finite Temperature from Lattice QCD PRL 108 (2012) A. Rothkopf, T. Hatsuda, S. Sasaki

the first paper observing an imaginary part: **We confirm the existence of an imaginary part above the critical temperature Tc, which grows as a function of r and underscores the importance of collisions with the gluonic environment for the melting of heavy quarkonia in the quark-gluon-plasma.**

In this case EFT has inspired Lattice QCD

more precise lattice calculations are ongoing but the extraction of the imaginary part is challenging

Bala et al. 2110.11659, 2112.00664 Hoying et al 2110.00565

Bala and S. Datta 1909.10549

To describe quarkonium in QGP we should account for: screening, dissociation effects (singlet to octet, inelastic parton scattering), recombination effects

To describe quarkonium in QGP we should account for: screening, dissociation effects (singlet to octet, inelastic parton scattering), recombination effects

—->The non equilibrium evolution of quarkonium in the QGP

Using pNRQCD and Open Quantum Systems (OQS) we could use bottomonium as a probe of a strongly coupled QGP (T \sim gT) and obtain master equations for the singlet and octet matrix density evolution

The equations are quantum, nonabelian and conserve the number of heavy quarks

Quarkonium in the fireball

- After the heavy-ion collisions, heavy quark-antiquarks propagate freely up to 0.6 fm.
- From 0.6 fm to the freeze-out time t_F they propagate in the medium.
- We assume the medium infinite, homogeneous and isotropic.
- We assume the heavy quarks comoving with the medium.
- We assume the medium to be locally in thermal equilibrium,

  i.e., the temperature T of the medium changes (slowly) with time:

Quarkonium in the fireball

- After the heavy-ion collisions, heavy quark-antiquarks propagate freely up to 0.6 fm.
- From 0.6 fm to the freeze-out time t_F they propagate in the medium.
- We assume the medium infinite, homogeneous and isotropic.
- We assume the heavy quarks comoving with the medium.
- We assume the medium to be locally in thermal equilibrium,

  i.e., the temperature T of the medium changes (slowly) with time:

Quarkonium as a small radius probe: bottomonium

Hierarchy of scales:

$$m \gg 1/r \sim m\alpha_s \gg T \sim gT \gg E$$

Coulombic bound state:

quark-antiquark color singlet Hamiltonian $$h_s = \frac{\mathbf{p}^2}{m} - \frac{4}{3}\frac{\alpha_s}{r}$$

quark-antiquark color octet Hamiltonian $$h_o = \frac{\mathbf{p}^2}{m} + \frac{1}{6}\frac{\alpha_s}{r}$$

The octet potential describes an unbound quark-antiquark pair.

Quarkonium in the fireball

- After the heavy-ion collisions, heavy quark-antiquarks propagate freely up to 0.6 fm.
- From 0.6 fm to the freeze-out time t_F they propagate in the medium.
- We assume the medium infinite, homogeneous and isotropic.
- We assume the heavy quarks comoving with the medium.
- We assume the medium to be locally in thermal equilibrium,

  i.e., the temperature T of the medium changes (slowly) with time:

Open Quantum system

- Subsystem: heavy quarks/quarkonium
- Environment: quark gluon plasma

N.B., J. Soto, M. Escobedo, A. Vairo 2016, 2018 (1612.07248, 1711.04515)

Quarkonium as a small radius probe: bottomonium

Hierarchy of scales:

$$m \gg 1/r \sim m\alpha_s \gg T \sim gT \gg E$$

Coulombic bound state:

quark-antiquark color singlet Hamiltonian $\quad h_s = \dfrac{\mathbf{p}^2}{m} - \dfrac{4}{3}\dfrac{\alpha_s}{r}$

quark-antiquark color octet Hamiltonian $\quad h_o = \dfrac{\mathbf{p}^2}{m} + \dfrac{1}{6}\dfrac{\alpha_s}{r}$

The octet potential describes an unbound quark-antiquark pair.

We may define a density matrix in pNRQCD for the heavy quark-antiquark pair in a singlet and octet configuration:

$$\begin{aligned}
\langle \mathbf{r}', \mathbf{R}' | \rho_s(t'; t) | \mathbf{r}, \mathbf{R} \rangle &\equiv \mathrm{Tr}\{\rho_{\mathrm{full}}(t_0)\, S^\dagger(t, \mathbf{r}, \mathbf{R}) S(t', \mathbf{r}', \mathbf{R}')\} \\
\langle \mathbf{r}', \mathbf{R}' | \rho_o(t'; t) | \mathbf{r}, \mathbf{R} \rangle \frac{\delta^{ab}}{8} &\equiv \mathrm{Tr}\{\rho_{\mathrm{full}}(t_0)\, O^{a\dagger}(t, \mathbf{r}, \mathbf{R}) O^b(t', \mathbf{r}', \mathbf{R}')\}
\end{aligned}$$

Quarkonium in the fireball

- After the heavy-ion collisions, heavy quark-antiquarks propagate freely up to 0.6 fm.
- From 0.6 fm to the freeze-out time t_F they propagate in the medium.
- We assume the medium infinite, homogeneous and isotropic.
- We assume the heavy quarks comoving with the medium.
- We assume the medium to be locally in thermal equilibrium,

  i.e., the temperature T of the medium changes (slowly) with time:

Quarkonium as a small radius probe: bottomonium

Hierarchy of scales:

$$m \gg 1/r \sim m\alpha_s \gg T \sim gT \gg E$$

Coulombic bound state:

quark-antiquark color singlet Hamiltonian $\quad h_s = \dfrac{\mathbf{p}^2}{m} - \dfrac{4}{3}\dfrac{\alpha_s}{r}$

quark-antiquark color octet Hamiltonian $\quad h_o = \dfrac{\mathbf{p}^2}{m} + \dfrac{1}{6}\dfrac{\alpha_s}{r}$

The octet potential describes an unbound quark-antiquark pair.

Open Quantum system

- Subsystem: heavy quarks/quarkonium
- Environment: quark gluon plasma

N.B., J. Soto, M. Escobedo, A. Vairo 2016, 2018 (1612.07248, 1711.04515)

We may define a density matrix in pNRQCD for the heavy quark-antiquark pair in a singlet and octet configuration:

$$\begin{aligned}
\langle \mathbf{r}', \mathbf{R}' | \rho_s(t'; t) | \mathbf{r}, \mathbf{R} \rangle &\equiv \mathrm{Tr}\{\rho_{\mathrm{full}}(t_0)\, S^\dagger(t, \mathbf{r}, \mathbf{R}) S(t', \mathbf{r}', \mathbf{R}')\} \\
\langle \mathbf{r}', \mathbf{R}' | \rho_o(t'; t) | \mathbf{r}, \mathbf{R} \rangle \frac{\delta^{ab}}{8} &\equiv \mathrm{Tr}\{\rho_{\mathrm{full}}(t_0)\, O^{a\dagger}(t, \mathbf{r}, \mathbf{R}) O^b(t', \mathbf{r}', \mathbf{R}')\}
\end{aligned}$$

The system is in non-equilibrium because through interaction with the environment (quark gluon plasma) singlet and octet quark-antiquark states continuously transform in each other although the number of heavy quarks is conserved: $\mathrm{Tr}\{\rho_s\} + \mathrm{Tr}\{\rho_o\} = 1$.

Closed time path formalism

In the closed-time path formalism we can represent the density matrices as 12 propagators on a closed time path:

$$\begin{aligned} \langle \mathbf{r}', \mathbf{R}' | \rho_s(t'; t) | \mathbf{r}, \mathbf{R} \rangle &= \langle S_1(t', \mathbf{r}', \mathbf{R}') S_2^\dagger(t, \mathbf{r}, \mathbf{R}) \rangle \\ \langle \mathbf{r}', \mathbf{R}' | \rho_o(t'; t) | \mathbf{r}, \mathbf{R} \rangle \frac{\delta^{ab}}{8} &= \langle O_1^b(t', \mathbf{r}', \mathbf{R}') O_2^{a\dagger}(t, \mathbf{r}, \mathbf{R}) \rangle \end{aligned}$$

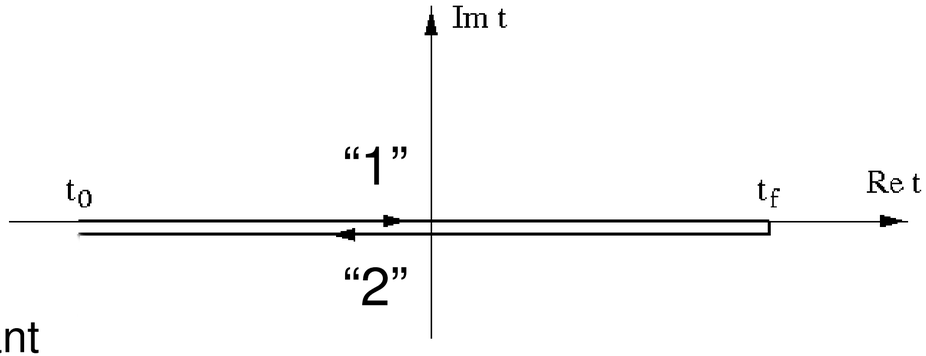

Differently from the thermal equilibrium case 12 propagators are relevant (in thermal equilibrium they are exponentially suppressed).

12 propagators are not time ordered, while 11 and 22 operators select the forward time direction $\propto \theta(t - t')$, $\theta(t' - t)$.

The evolution depends on the density at initial time: non Markovian evolution.

Closed time path formalism

In the closed-time path formalism we can represent the density matrices as 12 propagators on a closed time path:

$$\begin{aligned} \langle \mathbf{r}', \mathbf{R}' | \rho_s(t'; t) | \mathbf{r}, \mathbf{R} \rangle &= \langle S_1(t', \mathbf{r}', \mathbf{R}') S_2^\dagger(t, \mathbf{r}, \mathbf{R}) \rangle \\ \langle \mathbf{r}', \mathbf{R}' | \rho_o(t'; t) | \mathbf{r}, \mathbf{R} \rangle \frac{\delta^{ab}}{8} &= \langle O_1^b(t', \mathbf{r}', \mathbf{R}') O_2^{a\dagger}(t, \mathbf{r}, \mathbf{R}) \rangle \end{aligned}$$

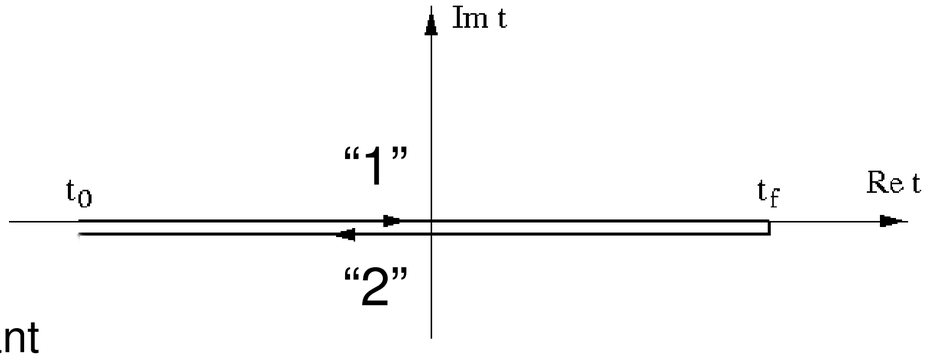

Differently from the thermal equilibrium case 12 propagators are relevant (in thermal equilibrium they are exponentially suppressed).

12 propagators are not time ordered, while 11 and 22 operators select the forward time direction $\propto \theta(t - t'), \theta(t' - t)$.

Expansions

- The density of heavy quarks is much smaller than the one of light quarks: we expand at first order in the heavy quark-antiquark density.
- We consider T much smaller than the Bohr radius of the quarkonium: we expand up to order r^2 in the multipole expansion.

The evolution depends on the density at initial time: non Markovian evolution.

LO and NLO evolution

For $t > t_0$, the LO singlet density matrix is

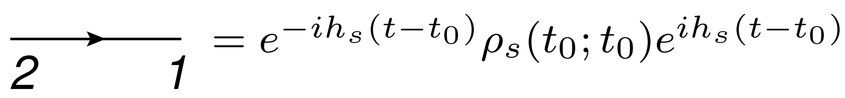

$$= e^{-ih_s(t-t_0)} \rho_s(t_0;t_0) e^{ih_s(t-t_0)}$$

($h_{s,o}$ = singlet/octet pNRQCD Hamiltonian $= V_{s,o}$ in the static limit)

LO and NLO evolution

For $t > t_0$, the LO singlet density matrix is

$$= e^{-ih_s(t-t_0)}\rho_s(t_0;t_0)e^{ih_s(t-t_0)}$$

($h_{s,o}$ = singlet/octet pNRQCD Hamiltonian $= V_{s,o}$ in the static limit)

and the NLO (in the multipole expansion) corrections are at first order in the density

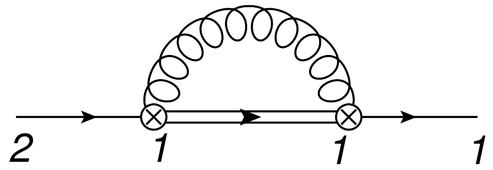

$$= -\int_{t_0}^{t} dt_1\, e^{-ih_s(t-t_1)}\, \Sigma_s(t_1)\, e^{-ih_s(t_1-t_0)}\, \rho_s(t_0;t_0)\, e^{ih_s(t-t_0)}$$

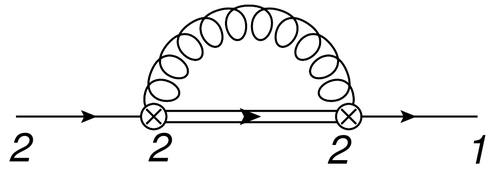

$$= -\int_{t_0}^{t} dt_1\, e^{-ih_s(t-t_0)}\, \rho_s(t_0;t_0)\, e^{ih_s(t_1-t_0)}\, \Sigma_s^\dagger(t_1)\, e^{ih_s(t-t_1)}$$

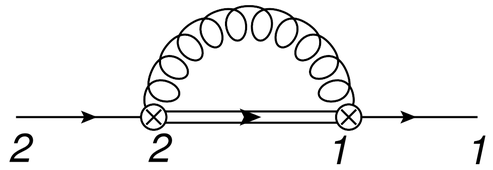

$$= \int_{t_0}^{t} dt_1\, e^{-ih_s(t-t_1)}\, \Xi_{so}(\rho_o(t_0;t_0),t_1)\, e^{ih_s(t-t_1)}$$

and similar for the octet

$$\Sigma_s(t) = \frac{g^2}{2N_c}\int_{t_0}^{t} dt_2\, r^i\, e^{-ih_o(t-t_2)}\, r^j\, e^{ih_s(t-t_2)}\, \langle E^{a,i}(t,\mathbf{0}) E^{a,j}(t_2,\mathbf{0})\rangle$$

$$\Xi_{so}(\rho_o(t_0;t_0),t) = \frac{g^2}{2N_c(N_c^2-1)}\int_{t_0}^{t} dt_2 \Big[r^i\, e^{-ih_o(t-t_0)}\, \rho_o(t_0;t_0)\, e^{ih_o(t_2-t_0)} \times r^j\, e^{ih_s(t-t_2)}\, \langle E^{a,j}(t_2,\mathbf{0}) E^{a,i}(t,\mathbf{0})\rangle + \text{H.c.}\Big]$$

A Wilson line in the adjoint representation is understood in the chromoelectric correlators.

and similar for the octet

contains everything :
screening, singlet to octet, all effects

$$\Sigma_s(t) = \frac{g^2}{2N_c}\int_{t_0}^{t} dt_2\, r^i\, e^{-ih_o(t-t_2)}\, r^j\, e^{ih_s(t-t_2)}\, \langle E^{a,i}(t,\mathbf{0}) E^{a,j}(t_2,\mathbf{0})\rangle$$

$$\Xi_{so}(\rho_o(t_0;t_0),t) = \frac{g^2}{2N_c(N_c^2-1)}\int_{t_0}^{t} dt_2 \Big[r^i\, e^{-ih_o(t-t_0)}\, \rho_o(t_0;t_0)\, e^{ih_o(t_2-t_0)} \times r^j\, e^{ih_s(t-t_2)}\, \langle E^{a,j}(t_2,\mathbf{0}) E^{a,i}(t,\mathbf{0})\rangle + \text{H.c.}\Big]$$

and similar for the octet

contains everything :
screening, singlet to octet, all effects

A Wilson line in the adjoint representation is understood in the chromoelectric correlators.

Diagrams and resummation

Resumming $(t-t_0)\times$ self-energy contributions à la Schwinger–Dyson ...

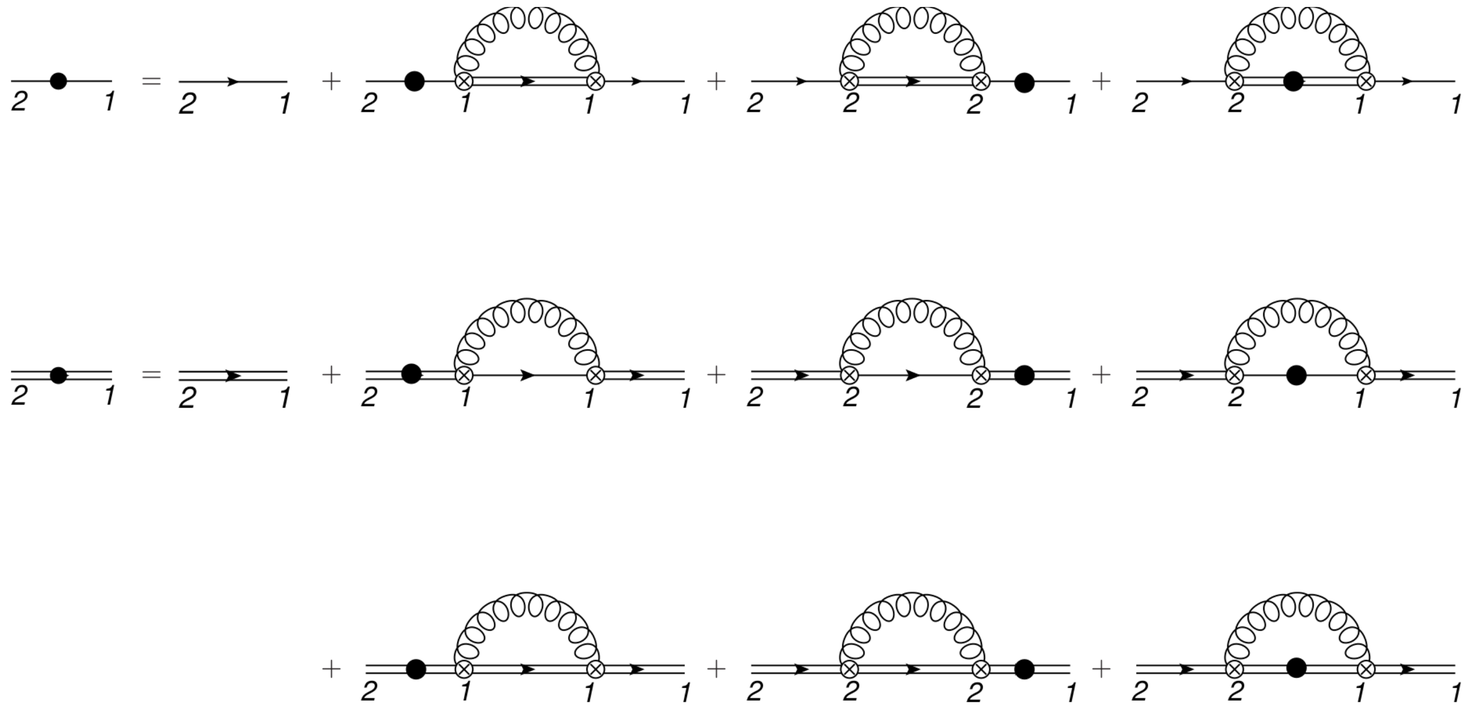

Singlet and octet density matrix evolution equations

... and differentiating over time we obtain the coupled evolution equations:

$$\frac{d\rho_s(t;t)}{dt} = -i[h_s, \rho_s(t;t)] - \Sigma_s(t)\rho_s(t;t) - \rho_s(t;t)\Sigma_s^\dagger(t) + \Xi_{so}(\rho_o(t;t), t)$$

$$\frac{d\rho_o(t;t)}{dt} = -i[h_o, \rho_o(t;t)] - \Sigma_o(t)\rho_o(t;t) - \rho_o(t;t)\Sigma_o^\dagger(t) + \Xi_{os}(\rho_s(t;t), t) + \Xi_{oo}(\rho_o(t;t), t)$$

The evolution equations are Markovian.

Singlet and octet density matrix evolution equations

... and differentiating over time we obtain the coupled evolution equations:

$$\frac{d\rho_s(t;t)}{dt} = -i[h_s,\rho_s(t;t)] - \Sigma_s(t)\rho_s(t;t) - \rho_s(t;t)\Sigma_s^\dagger(t) + \Xi_{so}(\rho_o(t;t),t)$$

$$\frac{d\rho_o(t;t)}{dt} = -i[h_o,\rho_o(t;t)] - \Sigma_o(t)\rho_o(t;t) - \rho_o(t;t)\Sigma_o^\dagger(t) + \Xi_{os}(\rho_s(t;t),t) + \Xi_{oo}(\rho_o(t;t),t)$$

The evolution equations are Markovian.

Interpretation

- The self energies Σ_s and Σ_o provide the in-medium induced mass shifts, $\delta m_{s,o}$, and widths, $\Gamma_{s,o}$, for the color-singlet and color-octet heavy quark-antiquark systems respectively:

$$-i\Sigma_{s,o}(t) + i\Sigma_{s,o}^\dagger(t) = 2\,\mathrm{Re}\left(-i\Sigma_{s,o}(t)\right) = 2\delta m_{s,o}(t)$$

$$\Sigma_{s,o}(t) + \Sigma_{s,o}^\dagger(t) = -2\,\mathrm{Im}\left(-i\Sigma_{s,o}(t)\right) = \Gamma_{s,o}(t)$$

- Ξ_{so} accounts for the production of singlets through the decay of octets, and Ξ_{os} and Ξ_{oo} account for the production of octets through the decays of singlets and octets respectively. There are two octet production mechanisms/octet chromoelectric dipole vertices in the pNRQCD Lagrangian.

Singlet and octet density matrix evolution equations

... and differentiating over time we obtain the coupled evolution equations:

The conservation of the trace of the sum of the densities, i.e., the conservation of the number of heavy quarks, follows from

$$\begin{aligned}
\mathrm{Tr}\left\{\rho_s(t;t)\left(\Sigma_s(t)+\Sigma_s^\dagger(t)\right)\right\} &= \mathrm{Tr}\left\{\Xi_{os}(\rho_s(t;t),t)\right\} \\
\mathrm{Tr}\left\{\rho_o(t;t)\left(\Sigma_o(t)+\Sigma_o^\dagger(t)\right)\right\} &= \mathrm{Tr}\left\{\Xi_{so}(\rho_o(t;t),t)+\Xi_{oo}(\rho_o(t;t),t)\right\}
\end{aligned}$$

s are Markovian.

Interpretation

- The self energies Σ_s and Σ_o provide the in-medium induced mass shifts, $\delta m_{s,o}$, and widths, $\Gamma_{s,o}$, for the color-singlet and color-octet heavy quark-antiquark systems respectively:

$$\begin{aligned}
-i\Sigma_{s,o}(t)+i\Sigma_{s,o}^\dagger(t) &= 2\,\mathrm{Re}\left(-i\Sigma_{s,o}(t)\right)=2\delta m_{s,o}(t) \\
\Sigma_{s,o}(t)+\Sigma_{s,o}^\dagger(t) &= -2\,\mathrm{Im}\left(-i\Sigma_{s,o}(t)\right)=\Gamma_{s,o}(t)
\end{aligned}$$

- Ξ_{so} accounts for the production of singlets through the decay of octets, and Ξ_{os} and Ξ_{oo} account for the production of octets through the decays of singlets and octets respectively. There are two octet production mechanisms/octet chromoelectric dipole vertices in the pNRQCD Lagrangian.

Time scales

Environment correlation time: $\tau_E \sim \dfrac{1}{T}$

System intrinsic time scale: $\tau_S \sim \dfrac{1}{E}$

System relaxation time: $\tau_R \sim \dfrac{1}{\text{self-energy}} \sim \dfrac{1}{\alpha_s a_0^2 \Lambda^3}$

a_0=r

$a_0 =$ Bohr radius, $\Lambda = T, E$

- Because we have assumed $1/a_0 \gg \Lambda$, it follows $\tau_R \gg \tau_S, \tau_E$ which, after resummation, qualifies the system as Markovian.
  - Akamatsu PRD 91 (2015) 056002
- If $T \gg E$ then $\tau_S \gg \tau_E$ which qualifies the motion of the system as quantum Brownian.

Time scales

Environment correlation time: $\tau_E \sim \dfrac{1}{T}$

System intrinsic time scale: $\tau_S \sim \dfrac{1}{E}$

System relaxation time: $\tau_R \sim \dfrac{1}{\text{self-energy}} \sim \dfrac{1}{\alpha_s a_0^2 \Lambda^3}$

a_0=r

a_0 = Bohr radius, $\Lambda = T, E$

- Because we have assumed $1/a_0 \gg \Lambda$, it follows $\tau_R \gg \tau_S, \tau_E$ which, after resummation, qualifies the system as Markovian.
  - Akamatsu PRD 91 (2015) 056002
- If $T \gg E$ then $\tau_S \gg \tau_E$ which qualifies the motion of the system as quantum Brownian.

From the evolution equations to the Linblad equations

Under the Markovian

$$\tau_R \gg \tau_S, \tau_E \quad \text{or} \quad \frac{1}{a_0} \gg E, T$$

and quantum Brownian motion condition

$$\tau_S \gg \tau_E \quad \text{or} \quad T \gg E$$

at least at LO in E/T the evolution equations can be written in the Lindblad form.

nonequilibrium evolution of quarkonium: Linblad equations

If $E \ll T \sim m_D$ the Lindblad equation for a strongly coupled plasma reads

$$\rho = \begin{pmatrix} \rho_s & 0 \\ 0 & \rho_o \end{pmatrix}$$

$$\frac{d\rho}{dt} = -i[H,\rho] + \sum_i (C_i \rho C_i^\dagger - \frac{1}{2}\{C_i^\dagger C_i, \rho\})$$

C collapse operators

$$H = \begin{pmatrix} h_s & 0 \\ 0 & h_o \end{pmatrix} + \frac{r^2}{2}\gamma(t) \begin{pmatrix} 1 & 0 \\ 0 & \frac{7}{16} \end{pmatrix},$$

$$C_i^0 = \sqrt{\frac{\kappa(t)}{8}}\, r^i \begin{pmatrix} 0 & 1 \\ \sqrt{8} & 0 \end{pmatrix}, \qquad C_i^1 = \sqrt{\frac{5\kappa(t)}{16}}\, r^i \begin{pmatrix} 0 & 0 \\ 0 & 1 \end{pmatrix}$$

nonequilibrium evolution of quarkonium: Linblad equations

If $E \ll T \sim m_D$ the Lindblad equation for a strongly coupled plasma reads

$$\rho = \begin{pmatrix} \rho_s & 0 \\ 0 & \rho_o \end{pmatrix}$$

$$\frac{d\rho}{dt} = -i[H,\rho] + \sum_i \left(C_i \rho C_i^\dagger - \frac{1}{2}\{C_i^\dagger C_i, \rho\}\right)$$

C collapse operators

$$H = \begin{pmatrix} h_s & 0 \\ 0 & h_o \end{pmatrix} + \frac{r^2}{2}\,\gamma(t) \begin{pmatrix} 1 & 0 \\ 0 & \frac{7}{16} \end{pmatrix},$$

$$C_i^0 = \sqrt{\frac{\kappa(t)}{8}}\, r^i \begin{pmatrix} 0 & 1 \\ \sqrt{8} & 0 \end{pmatrix}, \qquad C_i^1 = \sqrt{\frac{5\kappa(t)}{16}}\, r^i \begin{pmatrix} 0 & 0 \\ 0 & 1 \end{pmatrix}$$

the sQGP is characterised by two nonperturbative parameters (transport coefficients) kappa and gamma that must be calculated on the lattice

κ is the heavy-quark momentum diffusion coefficient:

$$\kappa = \frac{g^2}{18}\,\mathrm{Re}\int_{-\infty}^{+\infty} ds\,\langle\,\mathrm{T}\,E^{a,i}(s,\mathbf{0})\,\phi^{ab}(s,0)\,E^{b,i}(0,\mathbf{0})\rangle$$

$$\gamma = \frac{g^2}{18}\,\mathrm{Im}\int_{-\infty}^{+\infty} ds\,\langle\,\mathrm{T}\,E^{a,i}(s,\mathbf{0})\,\phi^{ab}(s,0)\,E^{b,i}(0,\mathbf{0})\rangle$$

nonequilibrium evolution of quarkonium: Linblad equations

If $E \ll T \sim m_D$ the Lindblad equation for a strongly coupled plasma reads

$$\rho = \begin{pmatrix} \rho_s & 0 \\ 0 & \rho_o \end{pmatrix}$$

$$\frac{d\rho}{dt} = -i[H,\rho] + \sum_i \left(C_i \rho C_i^\dagger - \frac{1}{2}\{C_i^\dagger C_i, \rho\}\right)$$

C collapse operators

$$H = \begin{pmatrix} h_s & 0 \\ 0 & h_o \end{pmatrix} + \frac{r^2}{2}\,\gamma(t) \begin{pmatrix} 1 & 0 \\ 0 & \frac{7}{16} \end{pmatrix},$$

$$C_i^0 = \sqrt{\frac{\kappa(t)}{8}}\, r^i \begin{pmatrix} 0 & 1 \\ \sqrt{8} & 0 \end{pmatrix}, \qquad C_i^1 = \sqrt{\frac{5\kappa(t)}{16}}\, r^i \begin{pmatrix} 0 & 0 \\ 0 & 1 \end{pmatrix}$$

the sQGP is characterised by two nonperturbative parameters (transport coefficients) kappa and gamma that must be calculated on the lattice

κ is the heavy-quark momentum diffusion coefficient:

$$\kappa = \frac{g^2}{18}\,\mathrm{Re}\int_{-\infty}^{+\infty} ds\,\langle\,\mathrm{T}\,E^{a,i}(s,\mathbf{0})\,\phi^{ab}(s,0)\,E^{b,i}(0,\mathbf{0})\rangle$$

$$\gamma = \frac{g^2}{18}\,\mathrm{Im}\int_{-\infty}^{+\infty} ds\,\langle\,\mathrm{T}\,E^{a,i}(s,\mathbf{0})\,\phi^{ab}(s,0)\,E^{b,i}(0,\mathbf{0})\rangle$$

the EFT allows to use lattice QCD equilibrium calculation to study the non equilibrium evolution! EFT is intermediate layer to non equilibrium

Our evolution equations depend
on two transport coefficients kappa and gamma that inside
pNRQCD acquire a field theoretical definition
as gauge invariant correlators of chromoelectric fields

Our evolution equations depend
on two transport coefficients kappa and gamma that inside
pNRQCD acquire a field theoretical definition
as gauge invariant correlators of chromoelectric fields

How to calculate these nonperturbative
transport coefficients?

use lattice QCD

The heavy quark diffusion coefficient

D in real space, related to κ in momentum space

Langevin dynamics of the heavy quark in the med

$$\frac{dp_i}{dt} = -\eta_D p_i + \xi_i(t)$$

$$\eta_D = \frac{\kappa}{2MT}$$

$$\langle \xi(t)\xi(t') \rangle = \kappa\delta(t-t')$$

$$D = \frac{2T^2}{\kappa}$$

$$< x^2(t) >= 6Dt$$

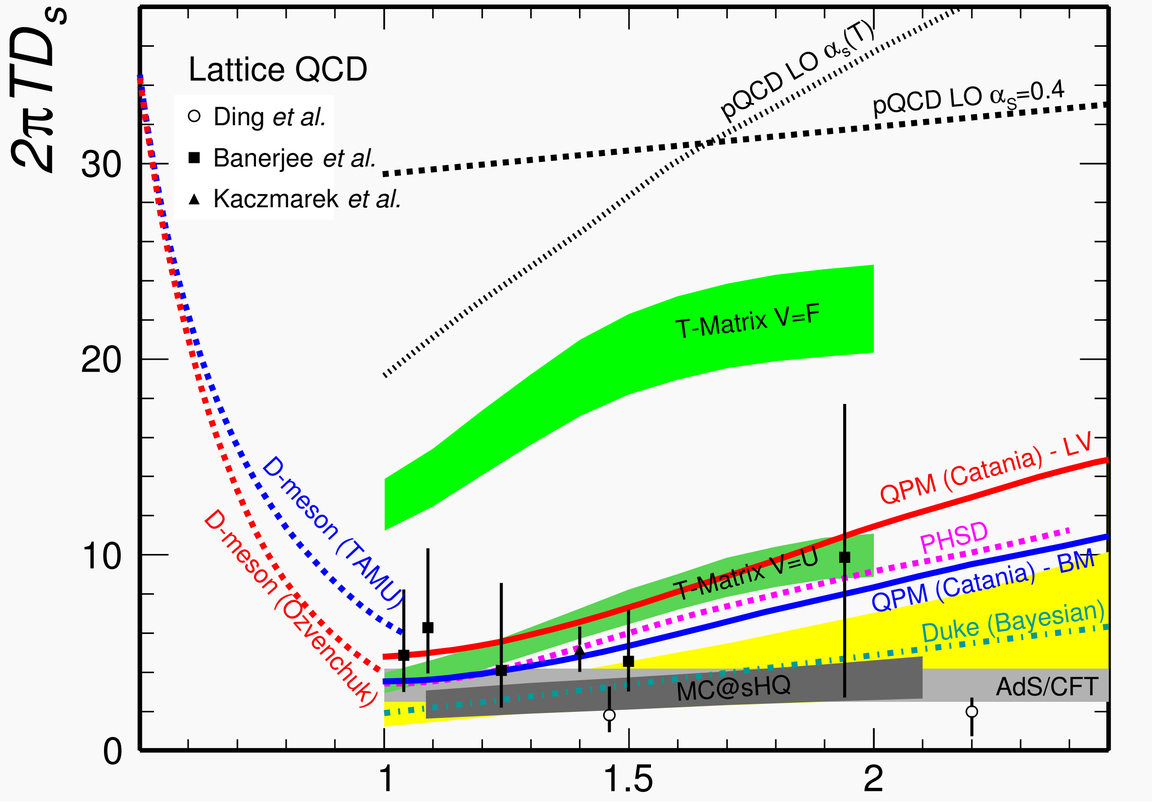

Figure from: X. Dong CIPANP (2018)

The heavy quark diffusion coefficient

D in real space, related to κ in momentum space

Langevin dynamics of the heavy quark in the med

$$\frac{dp_i}{dt} = -\eta_D p_i + \xi_i(t)$$

$$\eta_D = \frac{\kappa}{2MT}$$

$$\langle \xi(t)\xi(t') \rangle = \kappa \delta(t - t')$$

$$< x^2(t) >= 6Dt$$

$$D = \frac{2T^2}{\kappa}$$

in the limit in which the mass M of the heavy quark is the biggest scale one can integrate it out non relativistic effective field theory and from the current current correlator obtain

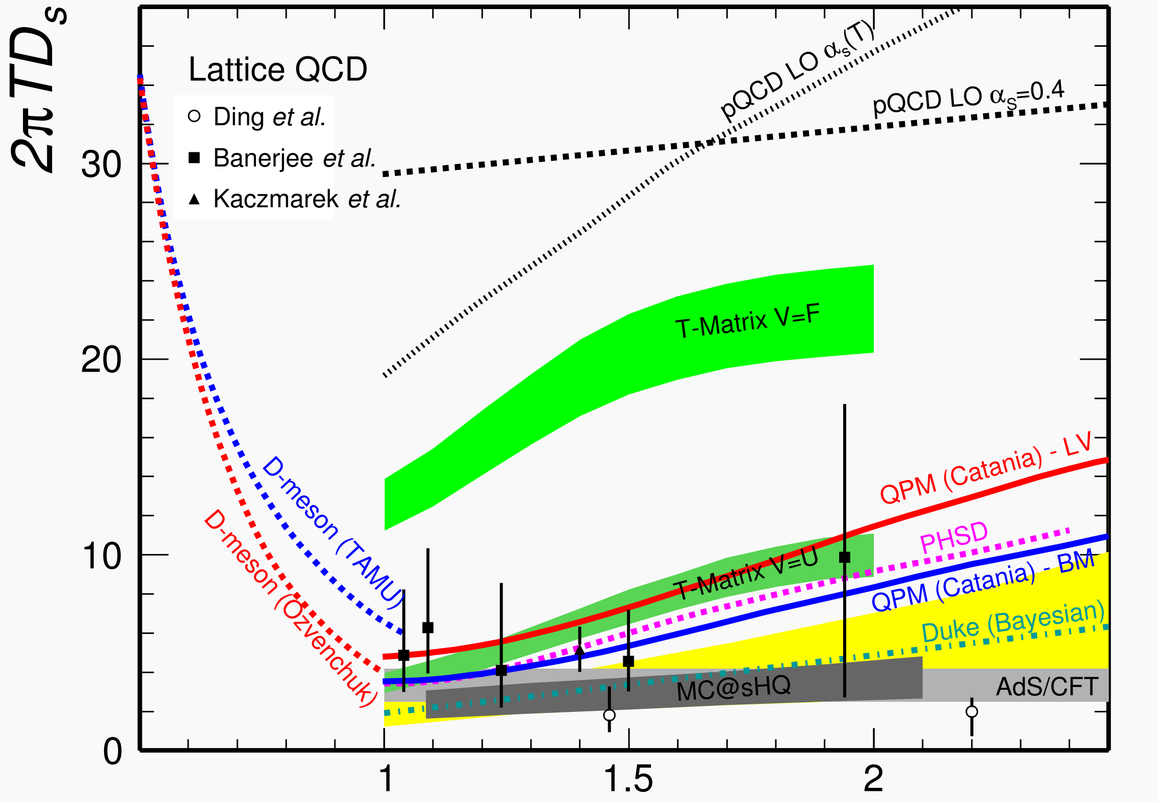

X. Dong CIPANP (2018)

$$\kappa = \frac{g^2}{18} \, \mathrm{Re} \int_{-\infty}^{+\infty} ds \, \langle \, \mathrm{T} \, E^{a,i}(s, \mathbf{0}) \, \phi^{ab}(s, 0) \, E^{b,i}(0, \mathbf{0}) \rangle$$

[4] Casalderrey-Solana, Teaney: Phys. Rev. D 74 (2006) 085012

which is the same transport coefficient kappa that we found studying the non equilibrium evolution of quarkonium in the QGP!

1903.08063

this object was already studied on quenched lattice

Meyer NJP13 (2011),

Ding *et.al.*JPG38 (2011),

Banarjee *et.al.* PRD85 (2012),

Francis *et.al.* PRD92 (2015)

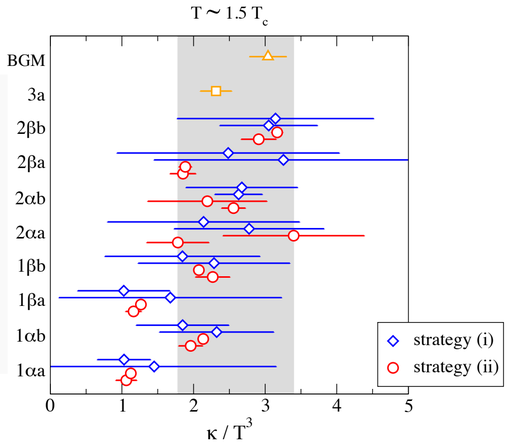

this object was already studied on quenched lattice

Meyer NJP13 (2011),

Ding *et.al.*JPG38 (2011),

Banarjee *et.al.* PRD85 (2012),

Francis *et.al.* PRD92 (2015)

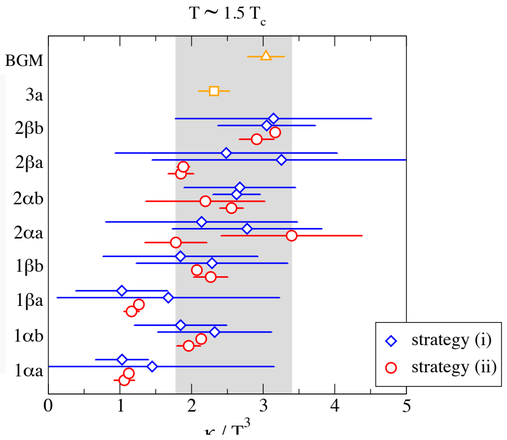

in TUMQCD we studied kappa on quenched latticed with the multilevel algorithm

in a window of T never attempted before

-> we get the T dependence of kappa

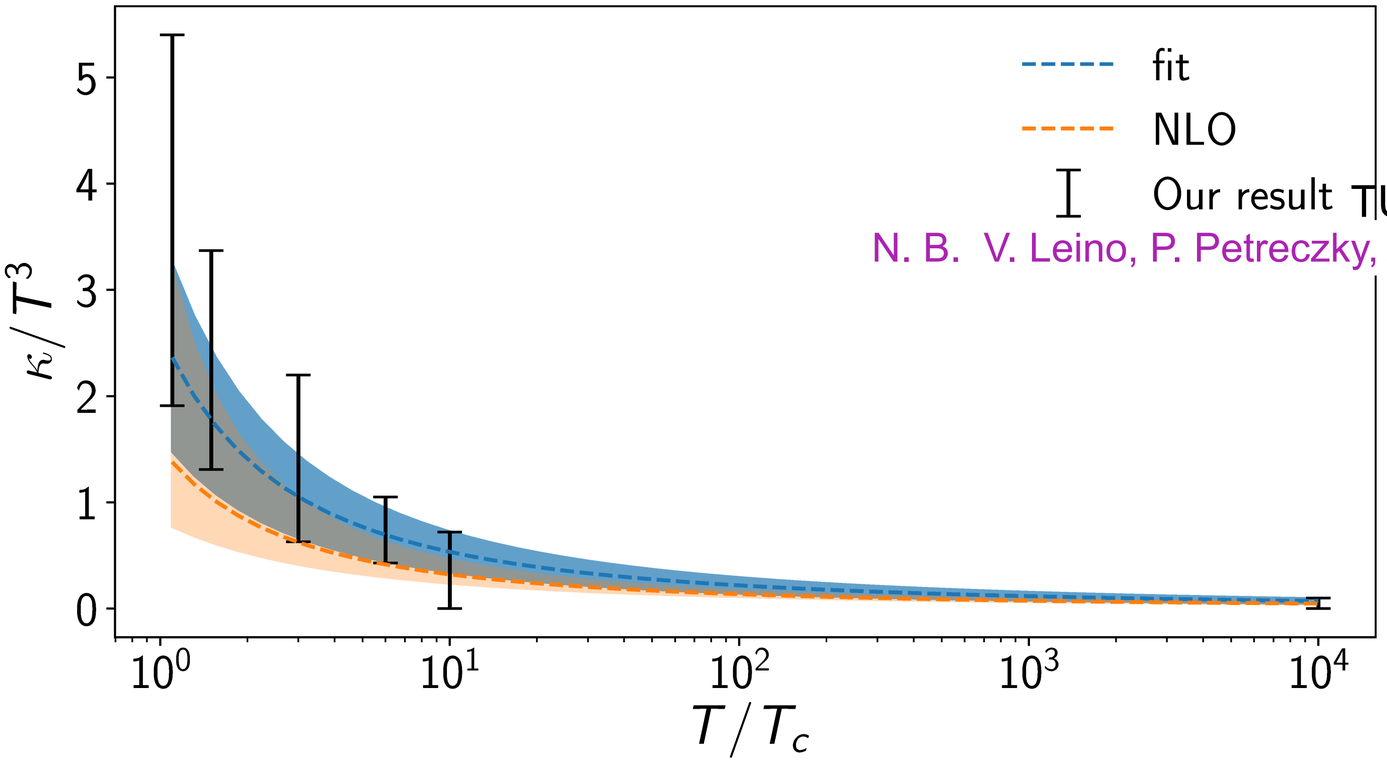

$$1.91 < \frac{\kappa}{T^3} < 5.4 \text{ for } T = 1.1\,T_c\,,$$

$$1.31 < \frac{\kappa}{T^3} < 3.64 \text{ for } T = 1.5\,T_c\,,$$

$$0.63 < \frac{\kappa}{T^3} < 2.20 \text{ for } T = 3\,T_c\,,$$

$$0.43 < \frac{\kappa}{T^3} < 1.05 \text{ for } T = 6\,T_c\,,$$

$$0 < \frac{\kappa}{T^3} < 0.72 \text{ for } T = 10\,T_c\,,$$

$$0 < \frac{\kappa}{T^3} < 0.10 \text{ for } T = 10^4\,T_c\,,$$

within the errors the lattice results are compatible with the next-to-leading order perturbative results

this object was already studied on quenched lattice

Meyer NJP13 (2011),

Ding *et.al.*JPG38 (2011),

Banarjee *et.al.* PRD85 (2012),

Francis *et.al.* PRD92 (2015)

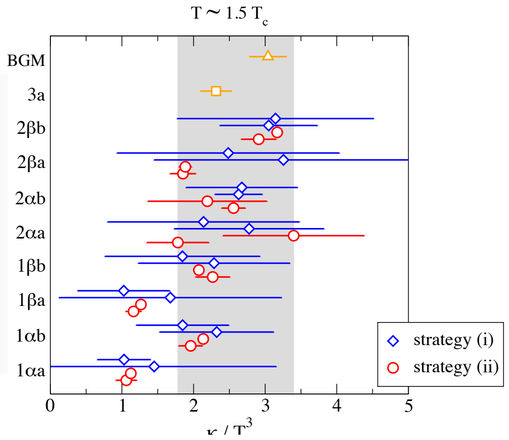

in TUMQCD we studied kappa on quenched latticed with the multilevel algorithm

in a window of T never attempted before

-> we get the T dependence of kappa

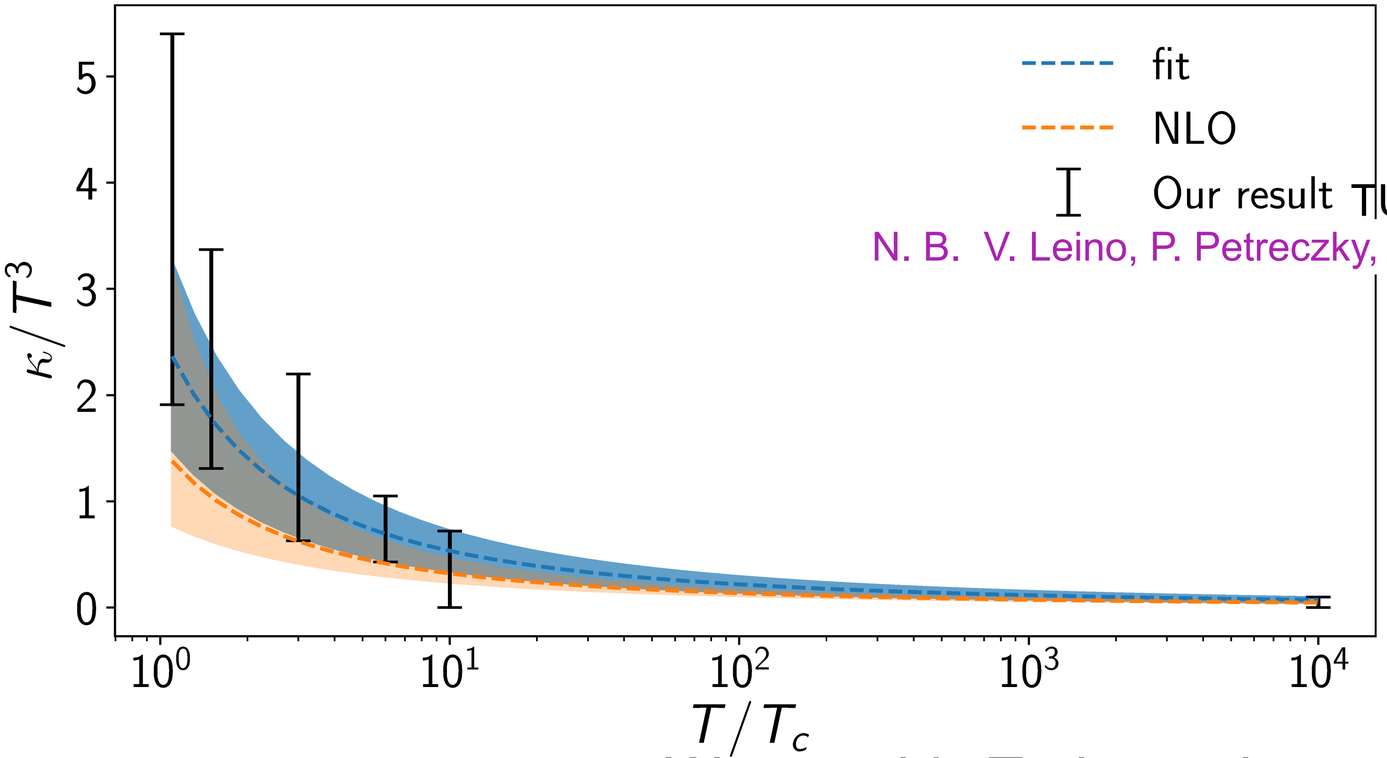

$$1.91 < \frac{\kappa}{T^3} < 5.4 \text{ for } T = 1.1\,T_c\,,$$

$$1.31 < \frac{\kappa}{T^3} < 3.64 \text{ for } T = 1.5\,T_c\,,$$

$$0.63 < \frac{\kappa}{T^3} < 2.20 \text{ for } T = 3\,T_c\,,$$

$$0.43 < \frac{\kappa}{T^3} < 1.05 \text{ for } T = 6\,T_c\,,$$

$$0 < \frac{\kappa}{T^3} < 0.72 \text{ for } T = 10\,T_c\,,$$

$$0 < \frac{\kappa}{T^3} < 0.10 \text{ for } T = 10^4\,T_c\,,$$

We use this T dependence of kappa in our Linblad equation

within the errors the lattice results are compatible with the next-to-leading order perturbative results

Use the EFT to relate kappa (and gamma) to observables: quarkonium thermal mass shift and thermal widths

N.B., M. Escobedo, A. Vairo, P. vander Griend Phys.Rev. D100 (2019) no.5, 054025

kappa is related to the thermal decay width of quarkonium

in the hierarchy $\frac{1}{r} \gg T \gg E$ pNRQCD predicts for 1S states

$$\Gamma(1S) = -2\langle \mathrm{Im}\,(-i\Sigma_s)\rangle = 3 < r^2 > \kappa$$

Use the EFT to relate kappa (and gamma) to observables: quarkonium thermal mass shift and thermal widths

N.B., M. Escobedo, A. Vairo, P. vander Griend Phys.Rev. D100 (2019) no.5, 054025

kappa is related to the thermal decay width of quarkonium

in the hierarchy $\frac{1}{r} \gg T \gg E$ pNRQCD predicts for 1S states

$$\Gamma(1S) = -2\langle \mathrm{Im}\,(-i\Sigma_s)\rangle = 3 < r^2 > \kappa$$

gamma is related to the thermal mass shift of quarkonium pNRQCD predicts for 1S states

$$\delta M(1S) = \langle \mathrm{Re}\,(-i\Sigma_s)\rangle = \frac{3}{2} < r^2 > \gamma$$

Use the EFT to relate kappa (and gamma) to observables: quarkonium thermal mass shift and thermal widths

N.B., M. Escobedo, A. Vairo, P. vander Griend Phys.Rev. D100 (2019) no.5, 054025

kappa is related to the thermal decay width of quarkonium

in the hierarchy $\frac{1}{r} \gg T \gg E$ pNRQCD predicts for 1S states

$$\Gamma(1S) = -2\langle \mathrm{Im}\,(-i\Sigma_s)\rangle = 3 < r^2 > \kappa$$

gamma is related to the thermal mass shift of quarkonium pNRQCD predicts for 1S states

$$\delta M(1S) = \langle \mathrm{Re}\,(-i\Sigma_s)\rangle = \frac{3}{2} < r^2 > \gamma$$

Therefore we can use unquenched lattice data on quarkonium thermal mass shift and widths to get unquenched determination of these transport coefficients

Use lattice data from Aarts, Allton, Kim, Lombardo, Oktay, Ryan, Sinclair and Skullerud (2011) and Kim, Petreczky and Rothkopf (2018). Unquenched.

and the new data from R. Larsen, S. Meinel, S. Mukherjee, P. Petreczy 2019, 2020

Unquenched determinations of kappa and gamma

N.B., M. Escobedo, A. Vairo, P. vander Griend
Phys.Rev. D100 (2019) no.5, 054025

Extraction of kappa from unquenched lattice data for the thermal width of the Y(1S) (black lines) in comparison to a quenched lattice determination (brown) , determinations from the D meson v2 from Alice and Star data (green), model compilation from 1903.07709) (red) and the perturbative calculation (truncated g^5) (blue)

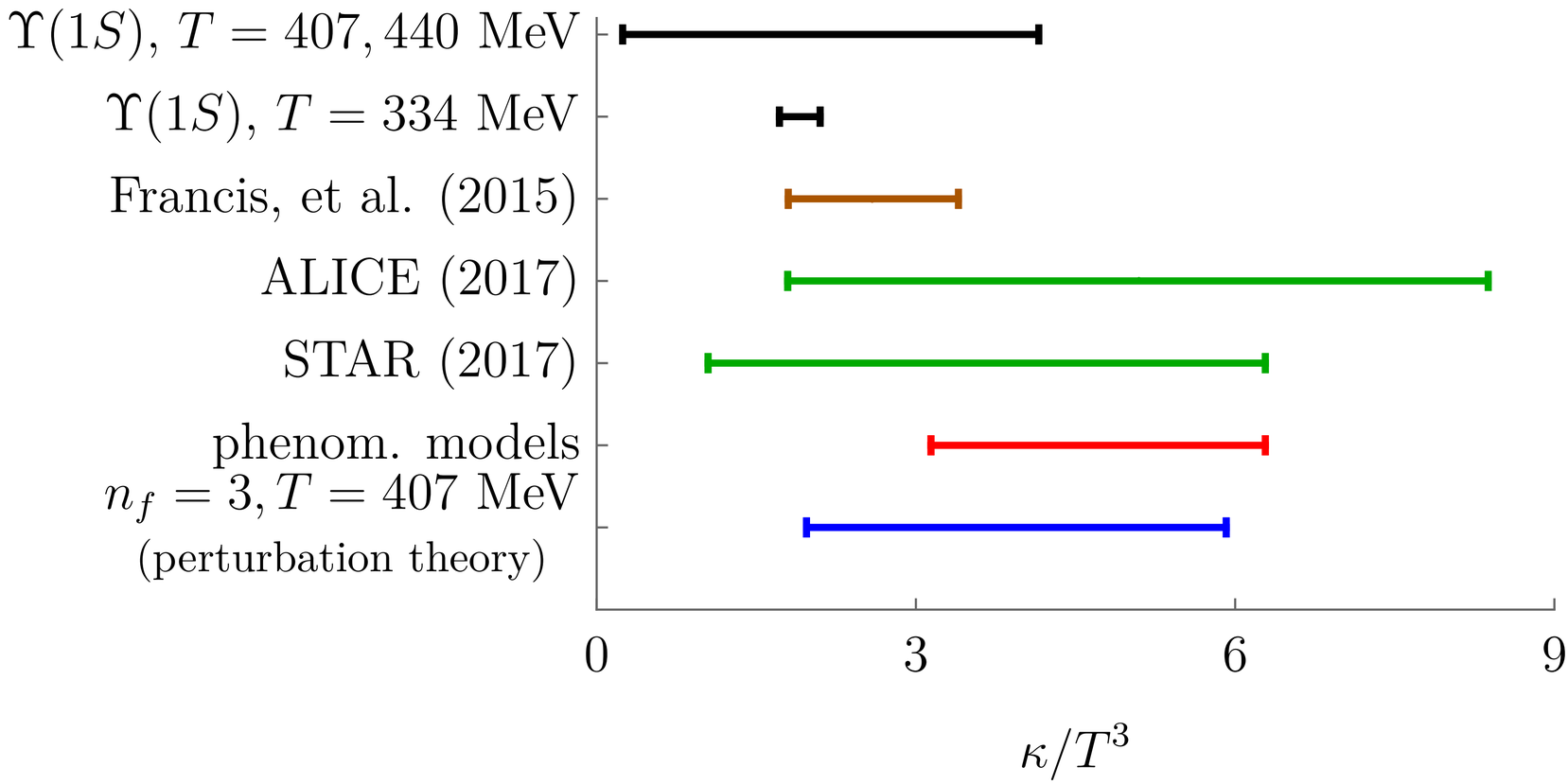

Unquenched determinations of kappa and gamma

N.B., M. Escobedo, A. Vairo, P. vander Griend
Phys.Rev. D100 (2019) no.5, 054025

Extraction of kappa from unquenched lattice data for the thermal width of the Y(1S) (black lines) in comparison to a quenched lattice determination (brown) , determinations from the D meson v2 from Alice and Star data (green), model compilation from 1903.07709) (red) and the perturbative calculation (truncated g^5) (blue)

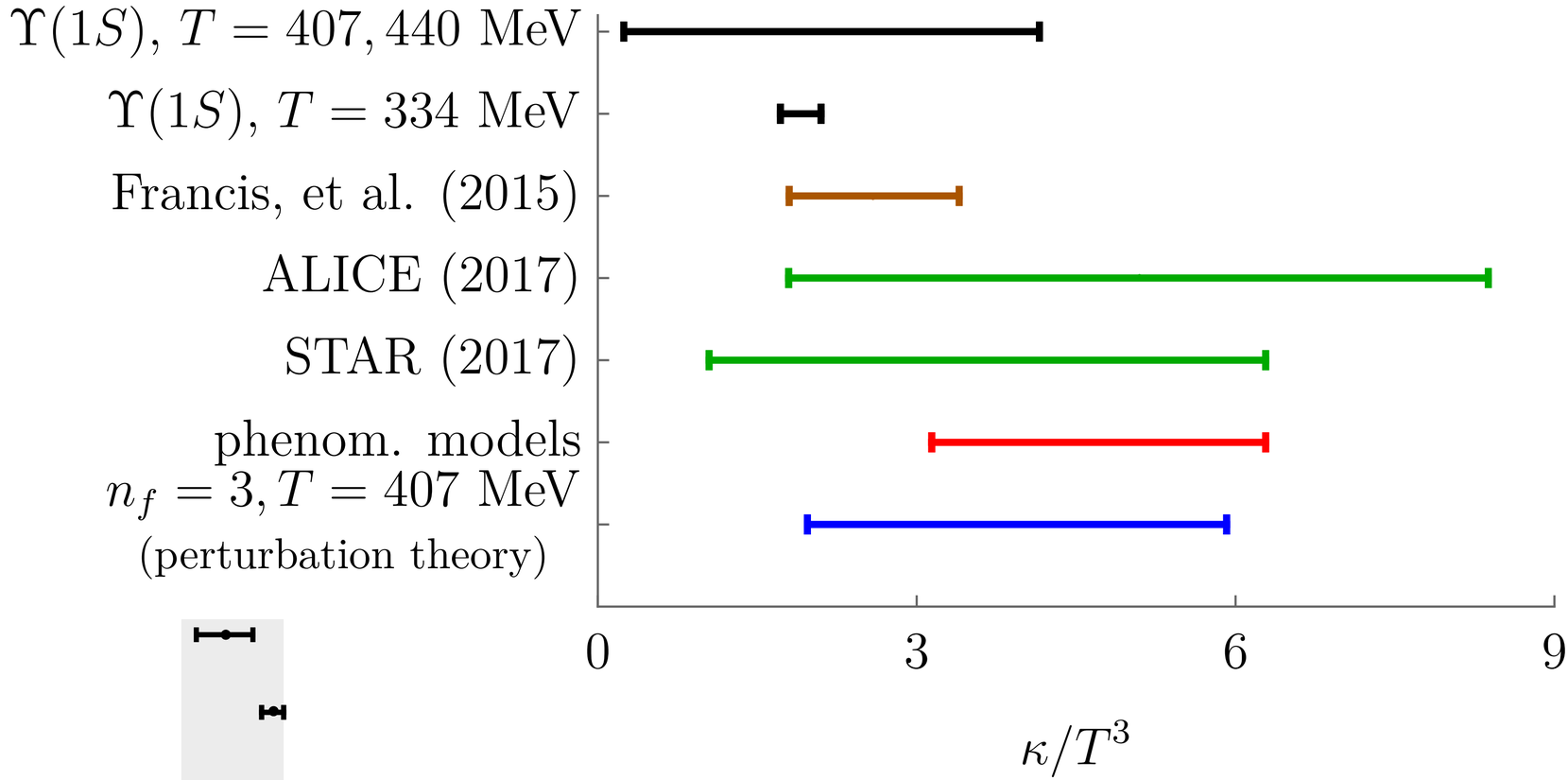

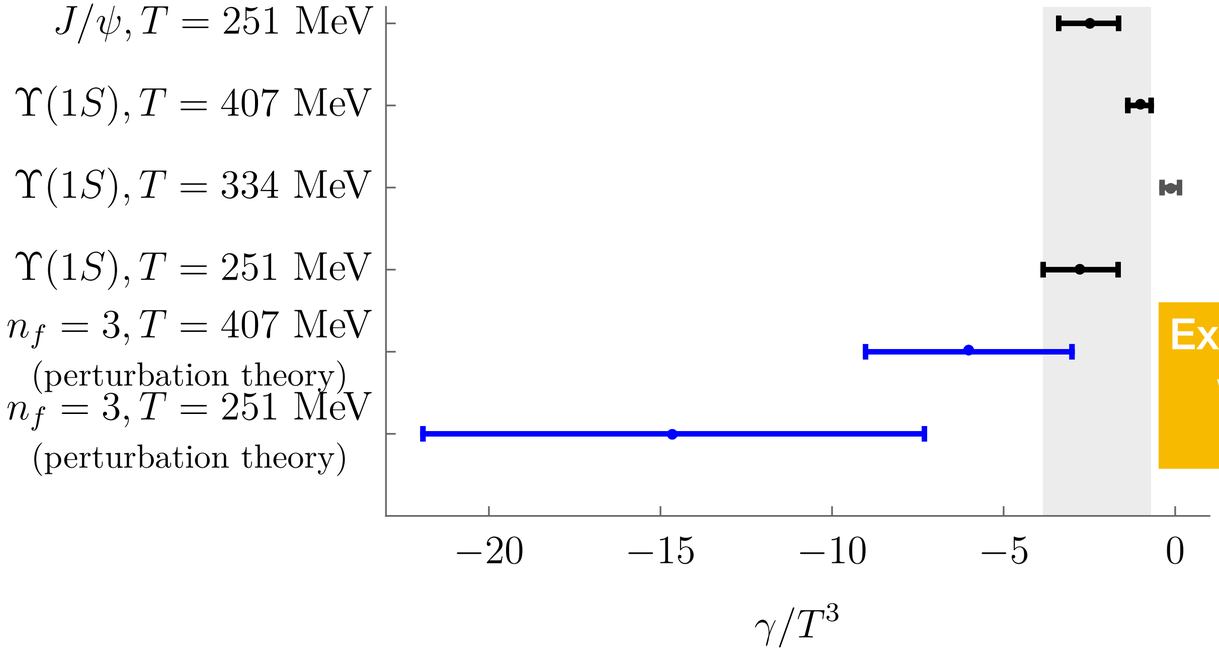

Extraction of gamma from unquenched lattice data for the thermal width of the Y(1S) and J/psi (black lines)n comparison to NLO order perturbation theory at two different T

Solving the Linblad equation : a pretty challenging task

Thanks to the collaboration with Mike Strickland we developed a very efficient (embarassingly parallel) program based on the quantum trajectory algorithm (Qtraj) and we coupled this to the hydrodynamical evolution of the QGP using a 3+1D dissipative relativistic hydrodynamics code that makes use of the quasiparticle anisotropic hydrodynamics (aHydroQP) framework. The code uses a realistic equation of state fit to lattice QCD measurements and is tuned to soft hadronic data collected in 5.02 TeV collisions using smooth optical Glauber initial conditions.

N.B. Escobedo , Strickland, Vairo, Vander Griend, Weber, 2012.01240

- 2107.06222

nonequilibrium evolution of quarkonium in medium: nuclear modification factor R_AA

We compute the nuclear modification factor R_{AA}:

$$R_{AA}(nS) = \frac{\langle n, \mathbf{q}|\rho_s(t_F; t_F)|n, \mathbf{q}\rangle}{\langle n, \mathbf{q}|\rho_s(0; 0)|n, \mathbf{q}\rangle}$$

calculation with no free parameters, results depends on kappa function of T (calculated on the lattice) and gamma (extracted from the lattice)

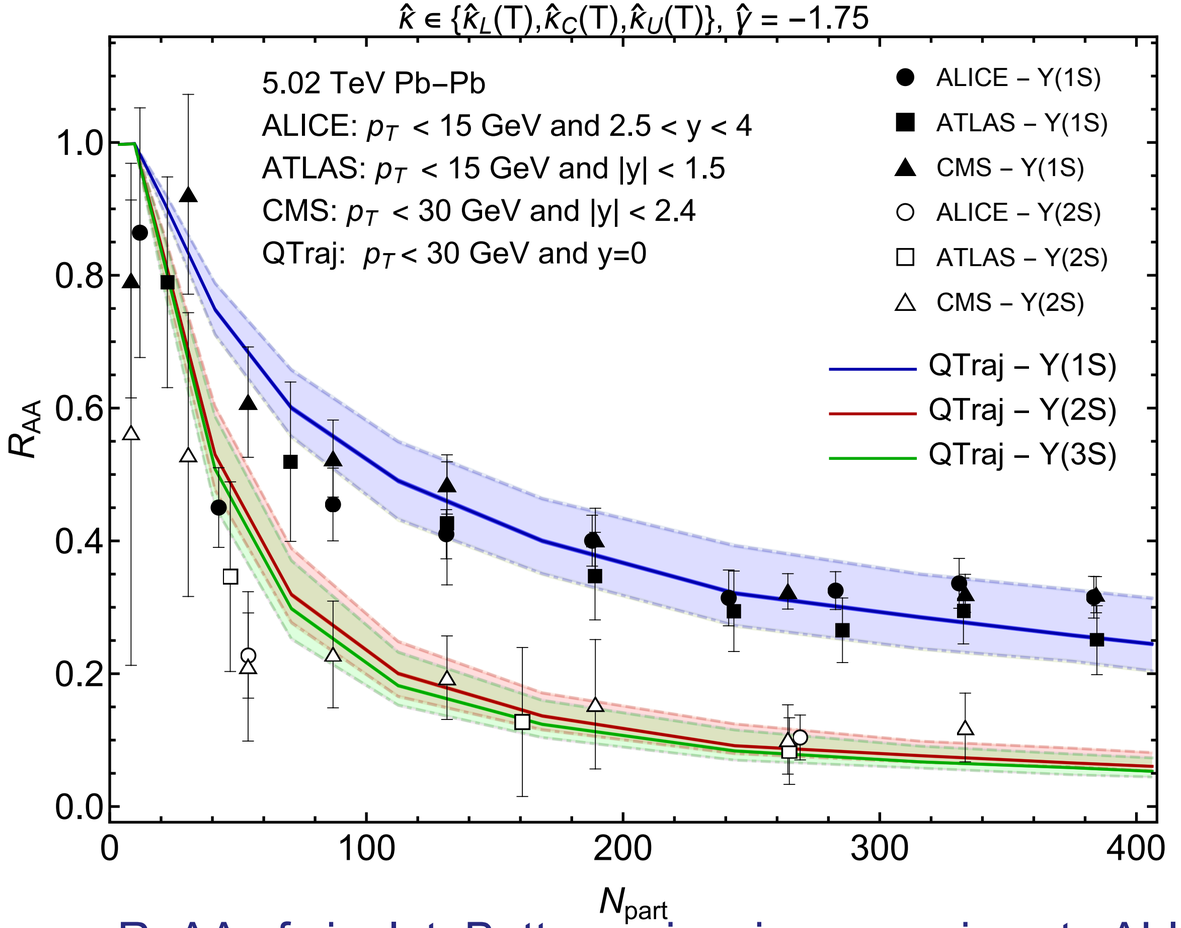

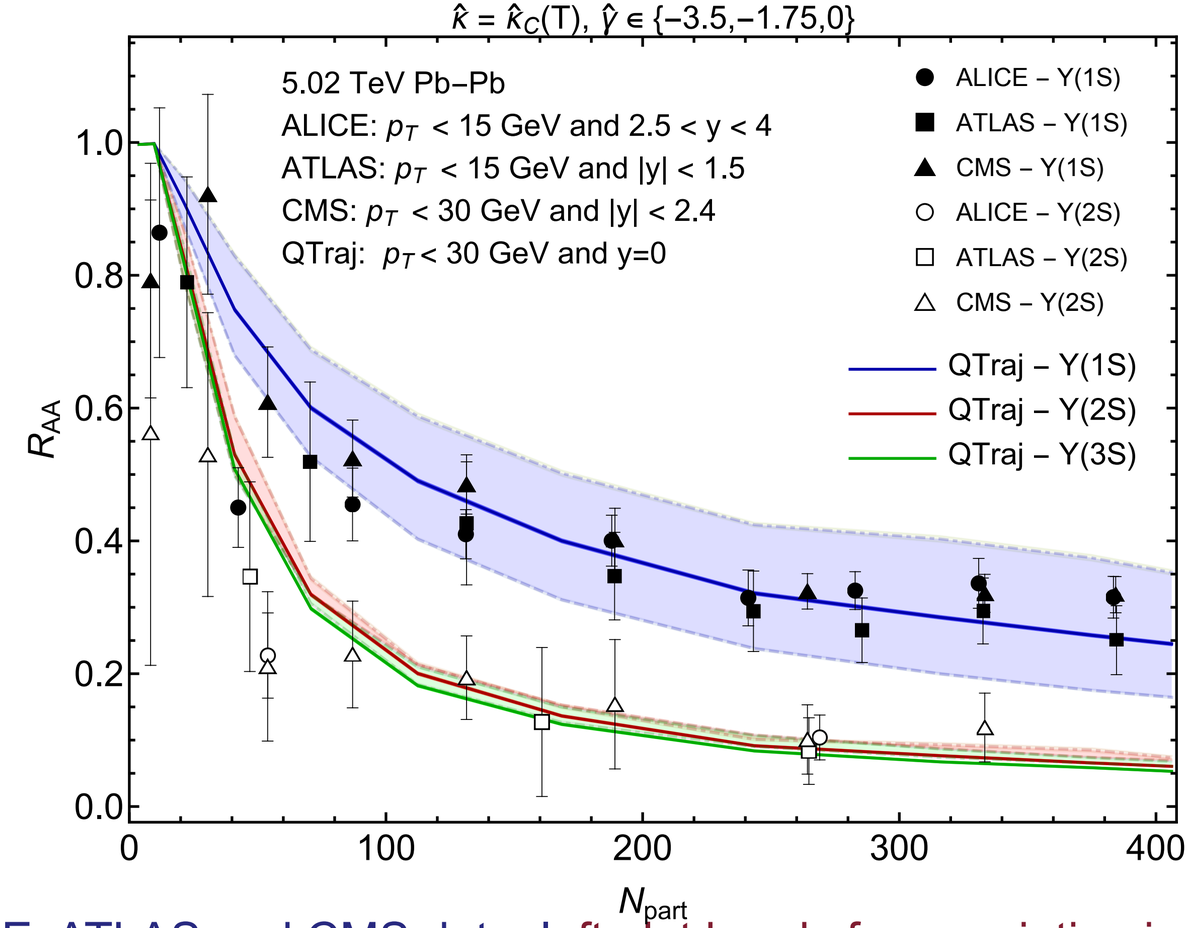

R_AA of singlet Bottomonium in comparison to ALICE, ATLAS and CMS data, left plot bands from variation in kappa, right plot variation in gamma —> we can use R_AA to learn about the QGP!

N.B. Escobedo , Strickland, Vairo, Vander Griend, Weber, 2012.01240

Differential quantities

Full diagnostic of the medium in terms of objects with a proper field theoretical definition, evaluated on the lattice

N.B. Escobedo , Strickland, Vairo, Vander Griend, Weber, 2107.06222

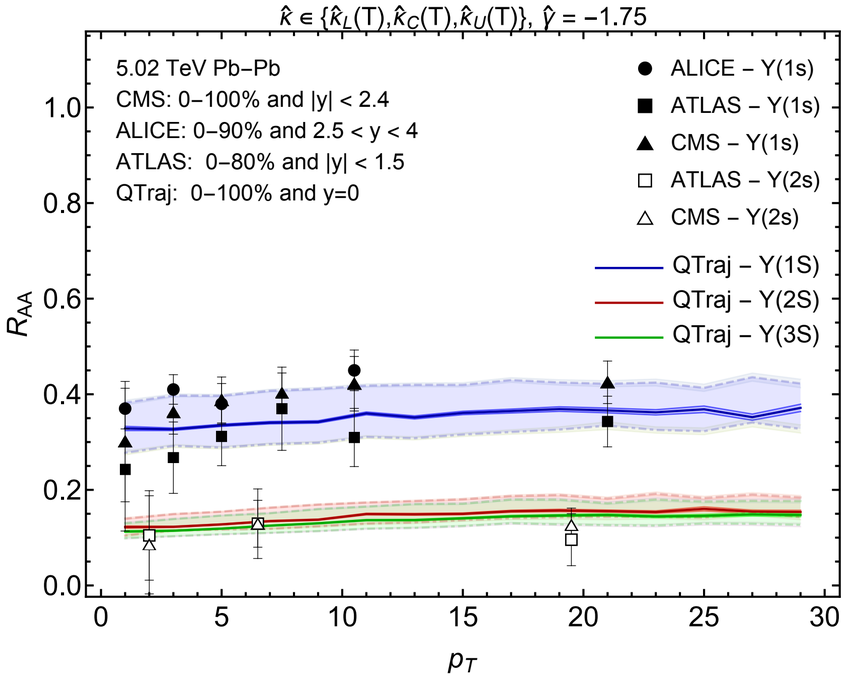

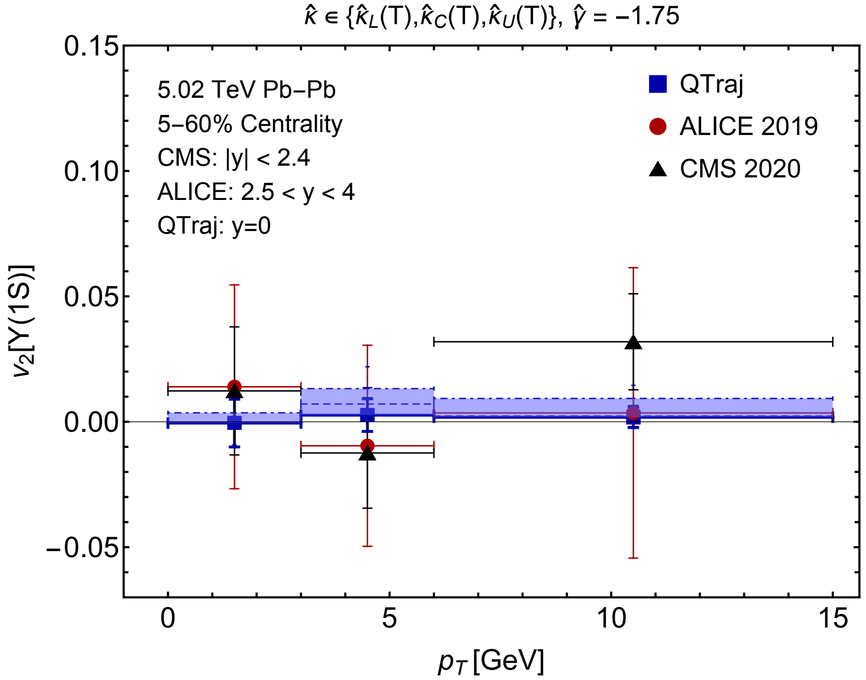

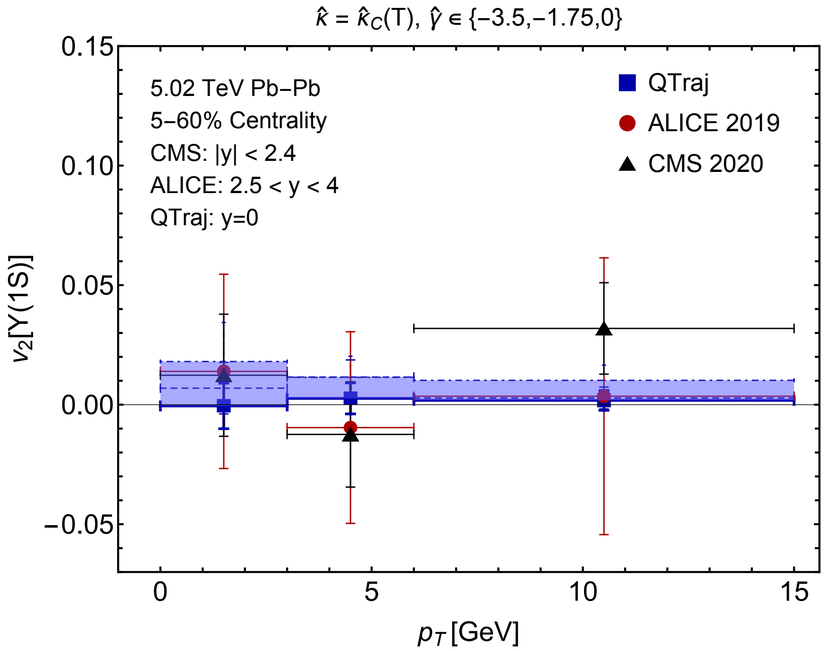

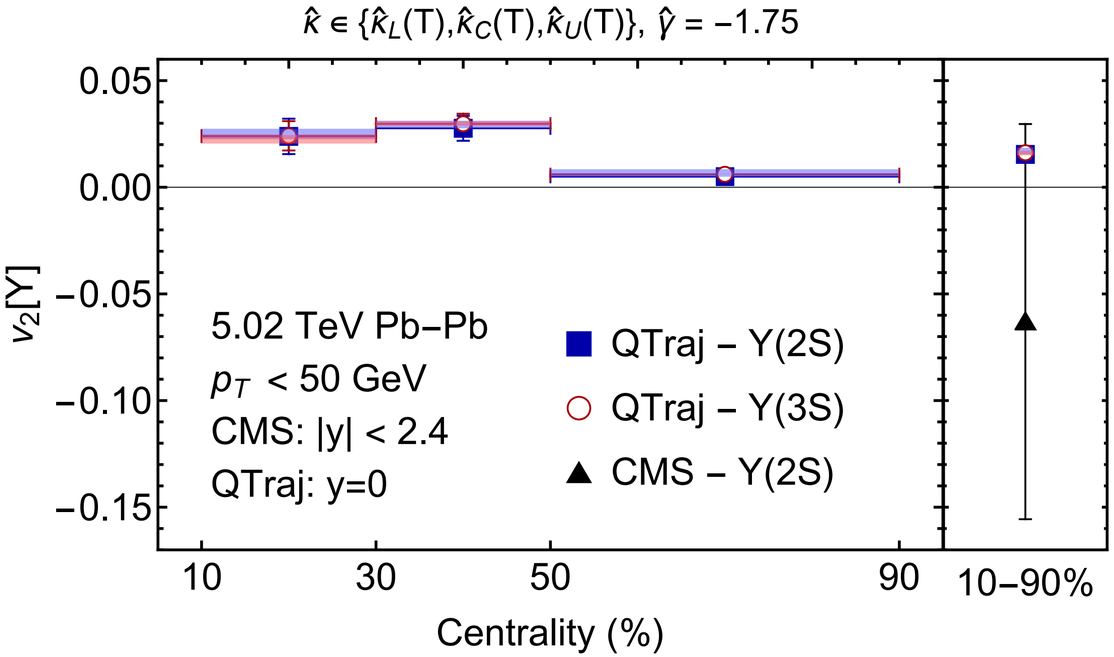

- This calculation with no free parameter can reproduce *inside errors* all the experimental data on bottomonia 1S 2S 3S:

- The band in our prediction depends on the indetermination on the transport coefficients

- Recombination is there but it is small for Y(1S) bottomonium

- The evolution equations we obtained do not make any special assumption on the medium

■ This calculation with no free parameter can reproduce *inside errors* all the experimental data on bottomonia 1S 2S 3S:

- R_AA as a function of N_part and as a function of p_T
- Ratios of R_AA, v_2

■ The band in our prediction depends on the indetermination on the transport coefficients

■ Recombination is there but it is small for Y(1S) bottomonium

■ The evolution equations we obtained do not make any special assumption on the medium

■ This calculation with no free parameter can reproduce *inside errors* all the experimental data on bottomonia 1S 2S 3S:

- R_AA as a function of N_part and as a function of p_T
- Ratios of R_AA, v_2

■ The band in our prediction depends on the indetermination on the transport coefficients

- Increasing kappa decreases survival for all states, while the impact of gamma varies from one state to the other
- More precise data could select the values of these coefficients and act as a direct diagnostic of the QGP

■ Recombination is there but it is small for Y(1S) bottomonium

■ The evolution equations we obtained do not make any special assumption on the medium

■ This calculation with no free parameter can reproduce *inside errors* all the experimental data on bottomonia 1S 2S 3S:

- R_AA as a function of N_part and as a function of p_T
- Ratios of R_AA, v_2

■ The band in our prediction depends on the indetermination on the transport coefficients

- Increasing kappa decreases survival for all states, while the impact of gamma varies from one state to the other
- More precise data could select the values of these coefficients and act as a direct diagnostic of the QGP

■ Recombination is there but it is small for Y(1S) bottomonium

- For Y(2S) and Y(3S) recombination is more relevant and it is interfering with dissociation
- We expect recombination to be much more important for charmonium

■ The evolution equations we obtained do not make any special assumption on the medium

■ This calculation with no free parameter can reproduce *inside errors* all the experimental data on bottomonia 1S 2S 3S:

- R_AA as a function of N_part and as a function of p_T
- Ratios of R_AA, v_2

■ The band in our prediction depends on the indetermination on the transport coefficients

- Increasing kappa decreases survival for all states, while the impact of gamma varies from one state to the other
- More precise data could select the values of these coefficients and act as a direct diagnostic of the QGP

■ Recombination is there but it is small for Y(1S) bottomonium

- For Y(2S) and Y(3S) recombination is more relevant and it is interfering with dissociation
- We expect recombination to be much more important for charmonium

■ The evolution equations we obtained do not make any special assumption on the medium

They could be used far from equilibrium or for a medium with a scale different from T-> use different methods to evaluate kappa and gamma (kinetic theory, classical simulations)

We focused on heavy quarks but there are other hard probes to which EFTs and open quantum system approach could be applied

example: jet quenching and qhat

A systematic treatment of a complex phenomenon like jet quenching is possible in an EFT framework owning to the hierarchy of scales that characterize the system. These are the typical SCET scales, Q, $Q\lambda$, $Q\lambda^2$, with $\lambda = T/Q$, which characterize the propagation of a very energetic parton in the medium and the thermal scales that characterize the medium itself, T, m_D, magnetic mass.

$$\hat{q} = \frac{\langle k_\perp^2 \rangle}{L} = \frac{1}{L}\int \frac{d^2k_\perp}{(2\pi)^2}\, k_\perp^2\, P(k_\perp)$$

$P(k_\perp)$ is the probability that after propagating through the medium for a distance L the hard parton acquires transverse momentum $k_\perp$,

$\hat{q}$ is the jet quenching parameter, i.e. the mean square transverse momentum picked up by the hard parton per unit distance traveled,

can be written in terms of a light cone Wilson Loop

M. Benzke,N.B., M. Escobedo, A, Vairo 1208.4253

A. Kumar, A. Majumder, J. Weber 2010.14463

- Idilbi Scimemi PL B695 (2011) 463

Idilbi Majumder PR D80 (2009) 054022

The gauge invariant expression of $\hat{q}$ allows for the use of lattice data.

The contribution from the scale g^2T may be extracted from the behaviour of the Wilson loop, $\sim e^{-LV}$, in three-dimensional QCD. - Laine arXiv:1208.5707

Correlators needed from the lattice for the NREFTs at zero and finite T

We need to calculate several gauge invariant correlators with chromoelectric and chromomagnetic fields:

Correlators needed from the lattice for the NREFTs at zero and finite T

We need to calculate several gauge invariant correlators with chromoelectric and chromomagnetic fields:

- for decays, spectra: time correlators of E and B fields
- for production: time correlators of electric and magnetic fields with a more complex structure of wilson line going to infinity
- for X Y Z states: static energies for hybrids and tetraquarks, i.e. generalized Wilson loops, time nonlocal correlators of several E and B field (for the spin stricture), three point functions of a magnetic field between singletand hybrid (mixing between quarkonium and hybrids), gluelump masses
- for quarkonium in medium : transport coefficients, the heavy quark momentum diffusion coefficient and its dispersive counterpart, kappa and gamma <EE> and <BB> correlators at finite T

Correlators needed from the lattice for the NREFTs at zero and finite T

We need to calculate several gauge invariant correlators with chromoelectric and chromomagnetic fields:

- for decays, spectra: time correlators of E and B fields
- for production: time correlators of electric and magnetic fields with a more complex structure of wilson line going to infinity
- for X Y Z states: static energies for hybrids and tetraquarks, i.e. generalized Wilson loops, time nonlocal correlators of several E and B field (for the spin stricture), three point functions of a magnetic field between singletand hybrid (mixing between quarkonium and hybrids), gluelump masses
- for quarkonium in medium : transport coefficients, the heavy quark momentum diffusion coefficient and its dispersive counterpart, kappa and gamma <EE> and <BB> correlators at finite T

NOTICE that all these objects are not depending on flavour, they are low energy objects, we need even the quenched determinations—> so they are simple

Correlators needed from the lattice for the NREFTs at zero and finite T

We need to calculate several gauge invariant correlators with chromoelectric and chromomagnetic fields:

- for decays, spectra: time correlators of E and B fields
- for production: time correlators of electric and magnetic fields with a more complex structure of wilson line going to infinity
- for X Y Z states: static energies for hybrids and tetraquarks, i.e. generalized Wilson loops, time nonlocal correlators of several E and B field (for the spin stricture), three point functions of a magnetic field between singletand hybrid (mixing between quarkonium and hybrids), gluelump masses
- for quarkonium in medium : transport coefficients, the heavy quark momentum diffusion coefficient and its dispersive counterpart, kappa and gamma <EE> and <BB> correlators at finite T

NOTICE that all these objects are not depending on flavour, they are low energy objects, we need even the quenched determinations—> so they are simple

BUT…..

Example of the QCD force

The force as a Wilson loop with a chromoelectric field

A direct computation of the force that avoids interpolating the static energy and taking numerically the derivative is possible from the expression of a rectangular Wilson loop, $W_{r\times T}$, with a chromoelectric field insertion on a quark line:

insertion of a single E into a static Wilson loop

physical object

$$F(r) = \frac{d}{dr} E_0(r) = \lim_{T\to\infty} -i \frac{\langle \mathrm{Tr}\{\mathrm{P}\, W_{r\times T}\, \hat{\mathbf{r}}\cdot g\mathbf{E}(\mathbf{r},t^*)\}\rangle}{\langle \mathrm{Tr}\{\mathrm{P}\, W_{r\times T}\}\rangle}$$

An equivalent expression can be written using a Polyakov loop instead of a Wilson loop.
At fixed t^* for $T\to\infty$, the rhs is independent of t^*.
The force is mass renormalon free and finite after charge renormalization.

- Brambilla Pineda Soto Vairo PRD 63 (2001) 014023
  Vairo MPLA 31 (2016) 34, 1630039

Lattice analysis of 2111.07916

For a study of concept, we have computed the Wilson loop and Polyakov loop with a chromoelectric field on three quenched QCD ($n_f = 0$) ensembles.

ensemble	β	$(L/a)^3 \times T/a$	r_0/a	a in fm
A	6.284	$20^3 \times 40$	8.333	0.060
B	6.451	$26^3 \times 50$	10.417	0.048
C	6.594	$30^3 \times 60$	12.500	0.040

- `TUMQCD coll. 2111.07916`

Renormalization constant Z_E

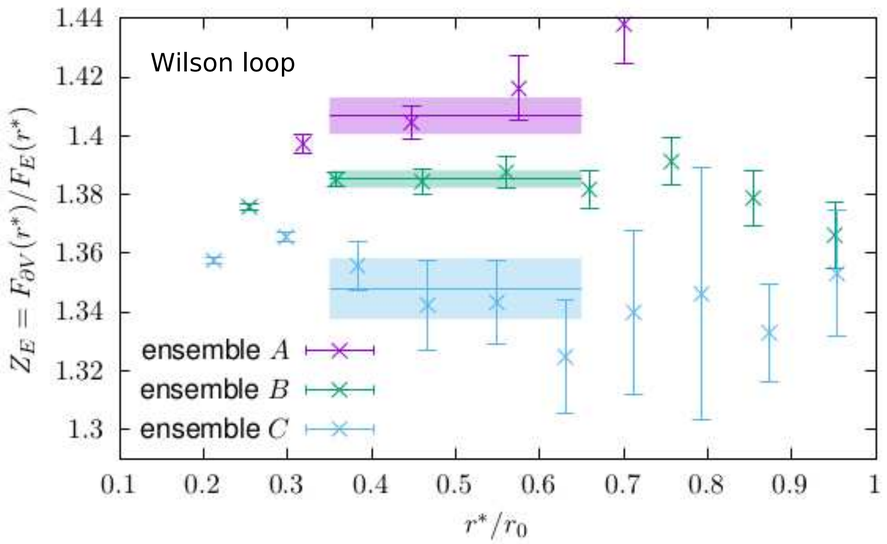

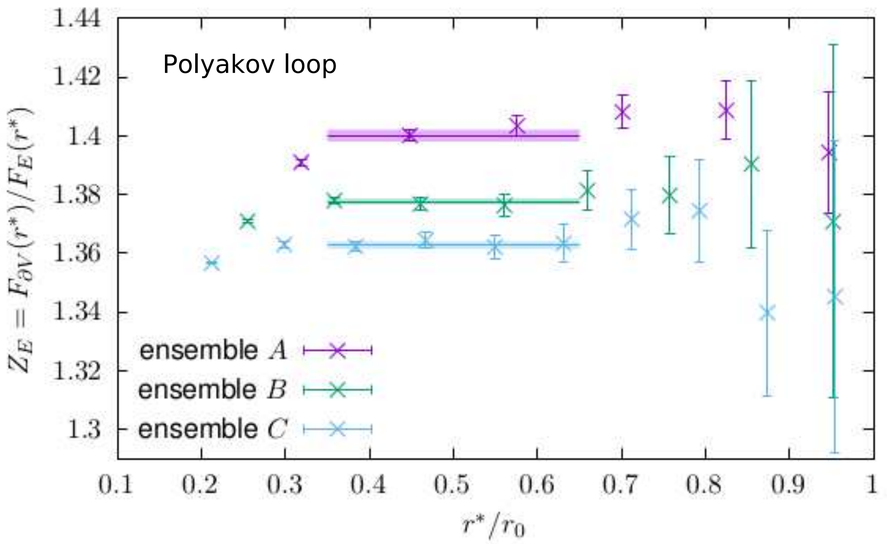

The convergence of the direct force towards the continuum, i.e. the derivative of the static potential, is slow. The ratio of the two determinations is an r independent constant Z_E that may be computed once forever at some fixed (arbitrary) distance r^* ($r_0 \approx 0.5$ fm).

ensemble	a in fm	Z_E from Wilson loops	Z_E from Polyakov loops
A	0.060	$1.4068(63)$	$1.4001(20)$
B	0.048	$1.3853(30)$	$1.3776(10)$
C	0.040	$1.348(11)$	$1.3628(13)$

Direct force vs lattice data

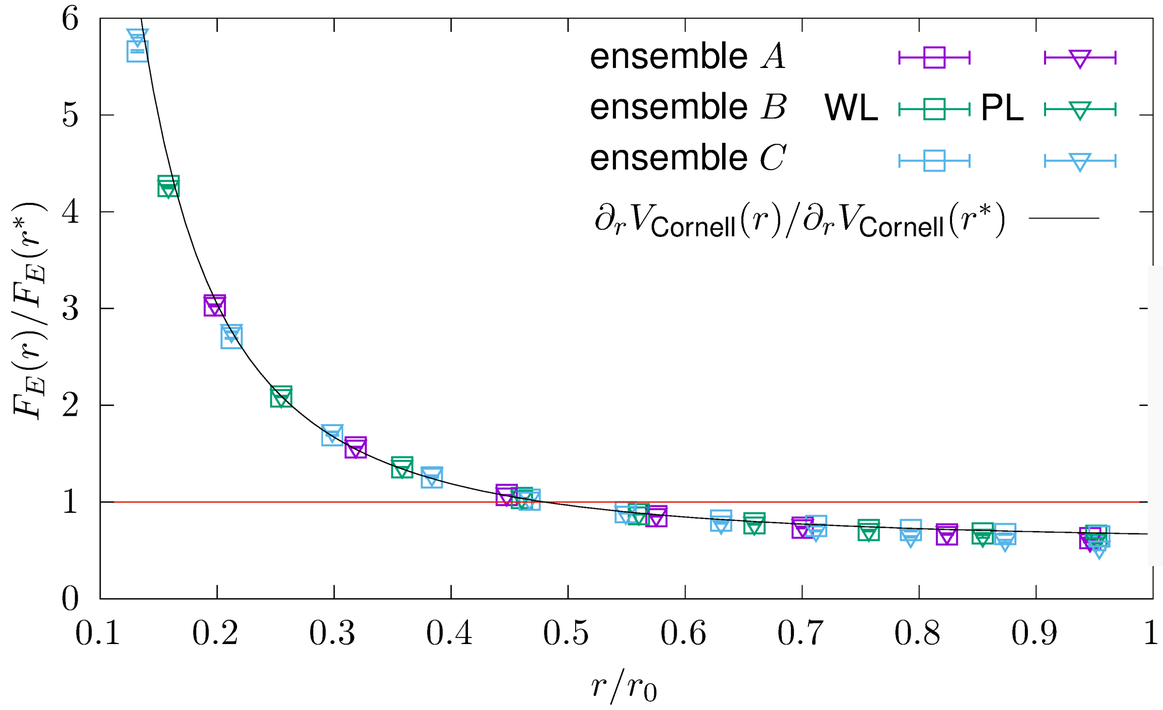

- Remove Z_E by dividing with measurement at $r^* = 0.48 r_0$
- Proof of concept:
  - Both derivative of potential and direct force agree
  - Both Wilson loop and Polyakov loops agree

Once normalized by Z_E the direct force agrees well with the Cornell parameterization based on quenched lattice data of the QCD static energy.
We have chosen $r^* = 0.48\, r_0 \approx 0.24$ fm.

- TUMQCD coll. 2111.07916

Gradient flow

The converge towards the continuum limit may be improved by using gradient flow.

Gradient flow consists in replacing the gluon fields $gA_\mu(x)$ by the flowed fields $B_\mu(x;t)$, where B_μ is defined through the flow equation

$$\begin{aligned} \frac{\partial}{\partial t} B_\mu(x;t) &= D_\nu G_{\nu\mu} + D_\mu \partial_\nu B_\nu \\ G_{\mu\nu} &= \partial_\mu B_\nu - \partial_\nu B_\mu + [B_\mu, B_\nu], \quad D_\mu = \partial_\mu + [B_\mu, \cdot] \end{aligned}$$

with the initial condition $B_\mu(x;t=0) = gA_\mu(x)$.

The new theory reduces to QCD in the limit of zero flow time t. But at any finite t it typically shows a much better behaviour than QCD in the ultraviolet (large momenta). We expect that the theory at finite flow time converges faster towards the continuum.

- Lüscher JHEP 08 (2010) 071, Lüscher Weisz JHEP 02 (2011) 051

The potential from gradient flow up to NLO

In the $\overline{\mathrm{MS}}$ scheme, we find at NLO in momentum space ($\bar{t} \equiv \boldsymbol{q}^2 t$)

$$\tilde{V}(\boldsymbol{q};t) = -\frac{4\pi\alpha_{\mathrm{s}}(\mu)C_F e^{-2\boldsymbol{q}^2 t}}{\boldsymbol{q}^2}\left\{1+\frac{\alpha_{\mathrm{s}}(\mu)}{4\pi}\left[\beta_0\log(\mu^2/\boldsymbol{q}^2)+a_1+C_A\,W^F_{\mathrm{NLO}}(\bar{t})\right]\right\}$$

The leading order term decreases like $e^{-2\boldsymbol{q}^2 t}$ for large momentum transfer $\boldsymbol{q}^2$.
Also the NLO one, which is analytically known, decreases exponentially like $e^{-\boldsymbol{q}^2 t}$.

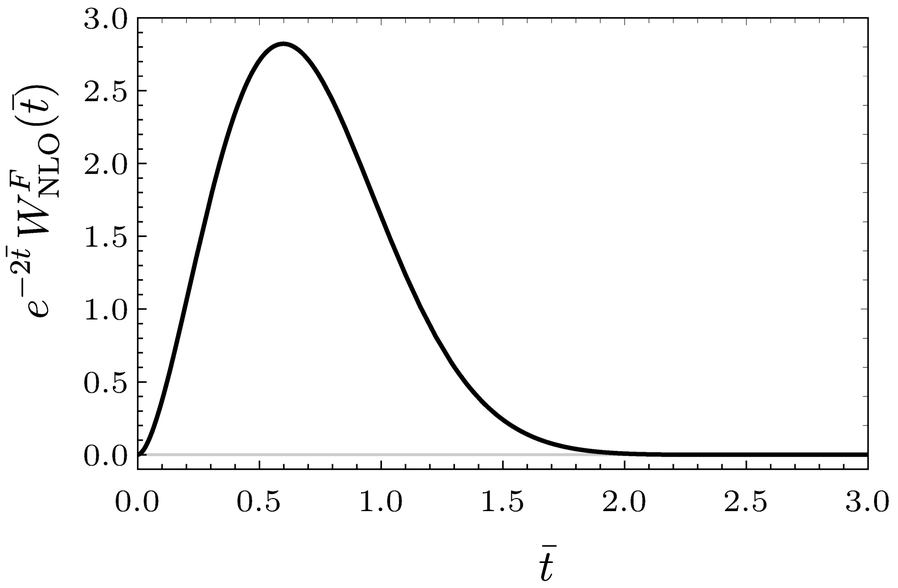

The force from gradient flow at NLO

In the $\overline{\rm MS}$ scheme, we find at NLO in coordinate space

$$F(r;t) = \frac{\alpha_{\rm s}(\mu) C_F}{r^2}\left[\left(1+\frac{\alpha_{\rm s}}{4\pi}a_1\right)\mathcal{F}_0(r;t) + \frac{\alpha_{\rm s}}{4\pi}\beta_0\mathcal{F}^L_{\rm NLO}(r;t;\mu) + \frac{\alpha_{\rm s} C_A}{4\pi}\mathcal{F}^F_{\rm NLO}(r;t)\right]$$

The functions $\mathcal{F}_0(r;t)$, $\mathcal{F}^L_{\rm NLO}(r;t;\mu)$ and $\mathcal{F}^F_{\rm NLO}(r;t)$ are analytically known.

- Brambilla Chung Vairo Wang 2111.07811

The force from gradient flow at NLO

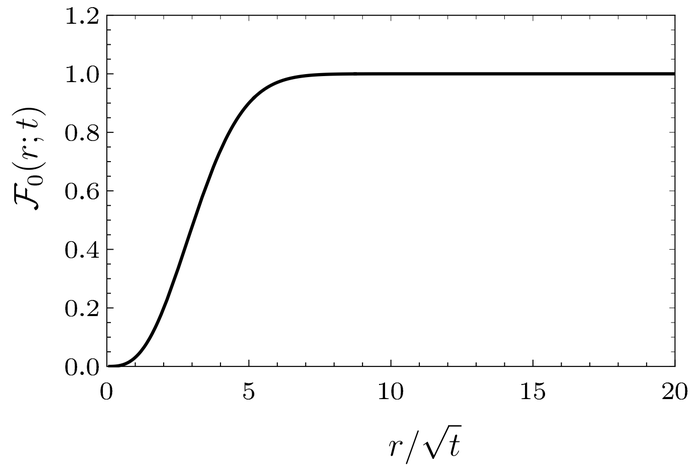

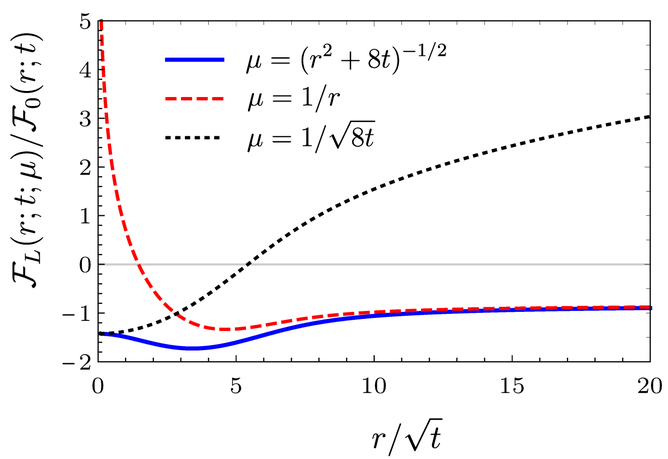

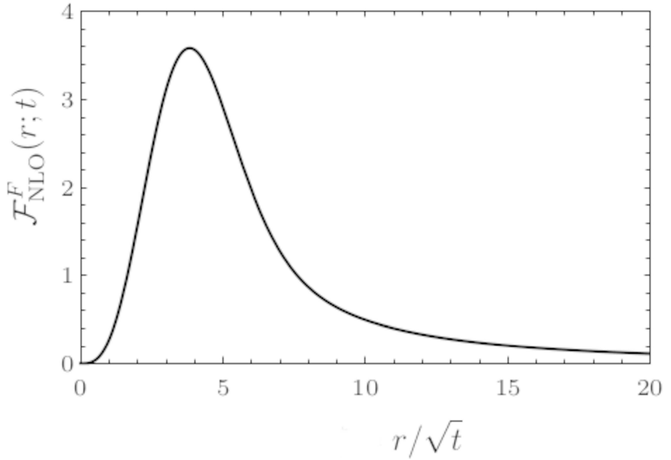

Lattice analysis of 2111.10212

For a preliminary study, we have computed the Wilson loop with a chromoelectric field in gradient flow on three quenched QCD ($n_f = 0$) ensembles.

β	$N_\sigma \times N_t$	a[fm]	# configurations
6.284	20×40	0.060	1949
6.481	26×56	0.046	1999
6.594	30×60	0.040	1997

- Brambilla Leino Mayer-Steudte Vairo 2111.10212

Renormalization constant Z_E with gradient flow

at zero flow time we reobtain the previous result for Z_E

At finite flow time the renormalization constant Z_E is about 1.

$$Z_{\mathrm{E}}(a) = \frac{F_{\partial V}(r^*, a)}{F_E(r^*, a)},$$

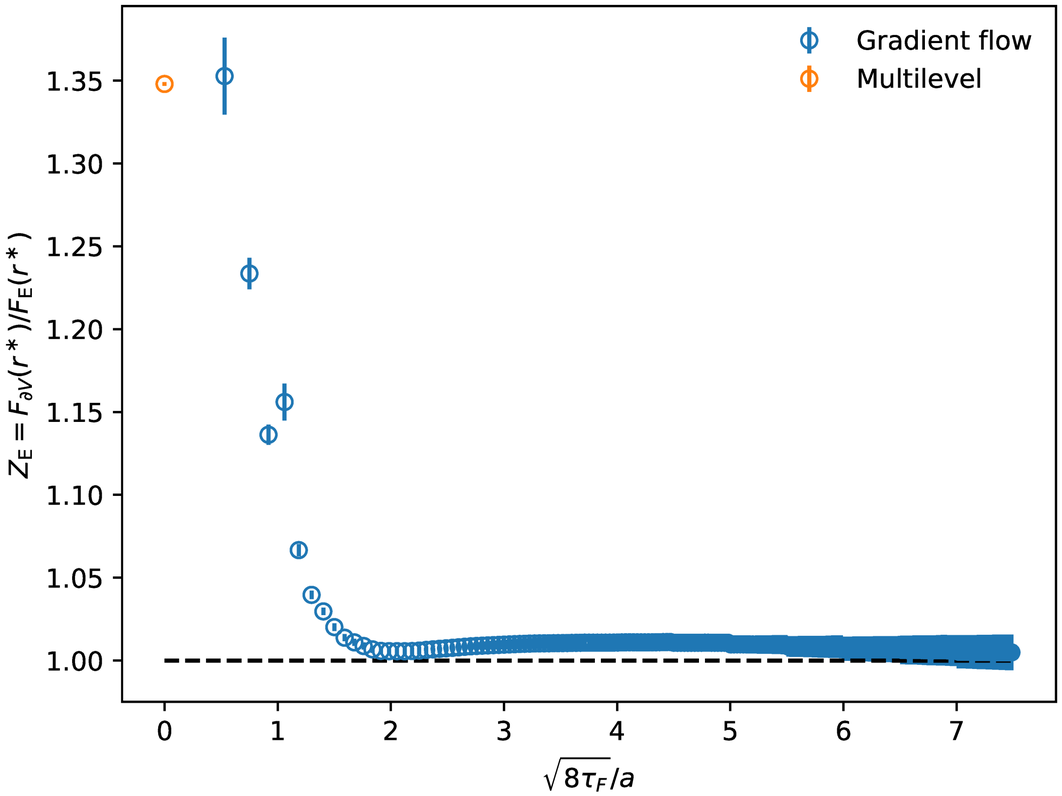

- Brambilla Leino Mayer-Steudte Vairo 2111.10212

for each flow time find the plateau in r*

Renormalization constant Z_E with gradient flow

at zero flow time we reobtain the previous result for Z_E

At finite flow time the renormalization constant Z_E is about 1.

$$Z_{\mathrm{E}}(a) = \frac{F_{\partial V}(r^*, a)}{F_E(r^*, a)},$$

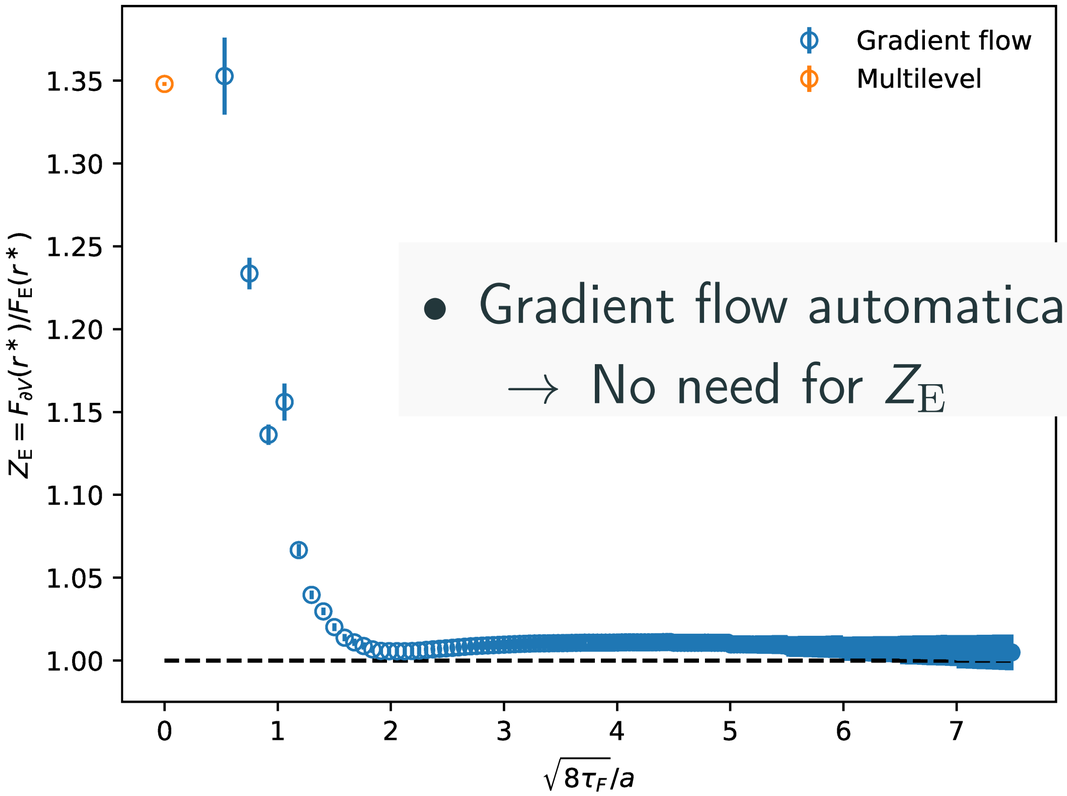

- Gradient flow automatically renormalizes the force at finite flowtime
  $\rightarrow$ No need for Z_{E}

○ Brambilla Leino Mayer-Steudte Vairo 2111.10212

for each flow time find the plateau in r*

Direct force vs lattice data with gradient flow

Cornell potential from previous lattice data on the Wilson and Polyakov loop

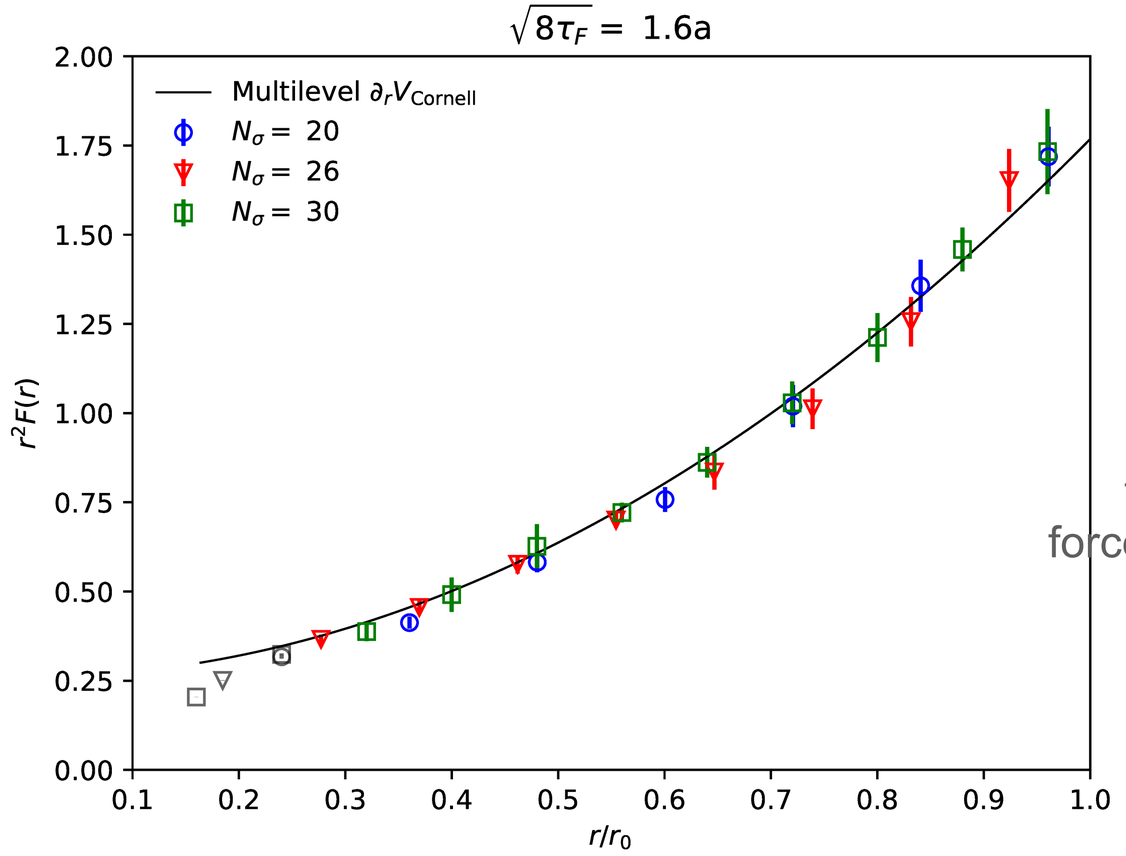

despite the lack of continuum
and zero flow time limit the force
from gradient flow seems to agree with the
force measured from the derivative of the potential
calculated previously

- Brambilla Leino Mayer-Steudte Vairo 2111.10212

These correlators depending on electric and magnetic field may be better calculated with gradient flow

- better convergence, less noisy

- no need of change of scheme, all the calculation regarding that can be done in msbar in continuum

R. Harlander , F. Lange 2201.08618 , A. 1808.09837
E. Mereghetti,C. Monahan, M. Rizik, A. shindler, P Stoffer 2111.11449

- requires dedicated perturbative calculations

In this way the lattice may obtain all the input that are needed for NREFTs calculations

Free energies and Polyakov loop/Polyakov loop correlator: EFTs and lattice

Bibliography: lattice

(1) A. Bazavov, N. Brambilla, P. Petreczky, A. Vairo and J. Weber [TUMQCD coll.]
Color screening in 2+1 flavor QCD
arXiv:1804.10600

(2) A. Bazavov, N. Brambilla, P. Petreczky, A. Vairo and J. Weber [TUMQCD coll.]
Polyakov loop in 2+1 flavor QCD from low to high temperatures
Phys. Rev. D93 (2016) 114502 arXiv:1603.06637

Polyakov loop average in a thermal ensemble at a temperature T

$$P(T)|_R \equiv \frac{1}{d_R}\langle \mathrm{Tr}\ L_R\rangle = e^{-F_Q/T} \qquad (\mathrm{R} \equiv \text{color representation})$$

$d_A = N^2-1$, $d_F = N$ and $L_R(\mathbf{x}) = \mathcal{P}\exp\left(ig\int_0^{1/T} d\tau A^0(\mathbf{x},\tau)\right)$

Polyakov loop correlator

$$P_c(r,T) \equiv \frac{1}{N^2}\langle \mathrm{Tr}L_F^\dagger(\mathbf{0})\mathrm{Tr}L_F(\mathbf{r})\rangle = e^{-F_{Q\bar{Q}}/T}$$

Bibliography: perturbation theory

with EFTs EQCD and pNRQCD

(1) M. Berwein, N. Brambilla, P. Petreczky and A. Vairo
Polyakov loop correlator in perturbation theory
Phys. Rev. D96 (2017) 014025 arXiv:1704.07266

(2) M. Berwein, N. Brambilla, P. Petreczky and A. Vairo
Polyakov loop at next-to-next-to-leading order
Phys. Rev. D93 (2016) 034010 arXiv:1512.08443

M. Berwein, N. Brambilla and A. Vairo
Renormalization of Loop Functions in QCD
Phys. Part. Nucl. 45 (2014) 656 arXiv:1312.6651

M. Berwein, N. Brambilla, J. Ghiglieri and A. Vairo
Renormalization of the cyclic Wilson loop
JHEP 1303 (2013) 069 arXiv:1212.4413

N. Brambilla, J. Ghiglieri, P. Petreczky and A. Vairo
The Polyakov loop and correlator of Polyakov loops at next-to-next-to-leading order
Phys. Rev. D82 (2010) 074019 arXiv:1007.5172

Physics of the screening static properties

Free energies: EFTs and lattice, study of phase transitions

- The Polyakov loop has been computed up to order g^5.
- The (subtracted) $Q\bar{Q}$ free energy has been computed at short distances up to corrections of order $g^7(rT)^4$, g^8.
- The (subtracted) $Q\bar{Q}$ free energy has been computed at screening distances up to corrections of order g^8.
- The singlet free energy has been computed at short distances up to corrections of order $g^4(rT)^5$, g^6.
- The singlet free energy has been computed at screening distances up to corrections of order g^5.

- Lattice calculations are consistent with weak-coupling expectations.
- Crossover temperature to the quark-gluon plasma is $153^{+6.5}_{-5}$ MeV from the entropy of the Polyakov loop.
- Screening sets in at $rT \approx 0.3$-0.4 (observable dependent), consistent with a screening length of about $1/m_D$.
- Asymptotic screening masses are about $2m_D$ (observable dependent).
- First determination of the color octet $Q\bar{Q}$ free energy.

the free energy is not the object to be taken as the potential in the Schroedinger equation

(the singlet free energy may provide a good approximation of the real part of the potential)

Polyakov loop correlator in pNRQCD

In an EFT/pNRQCD framework $P_c(r,T)$ can be put in the form

$$P_c(r,T) = \frac{1}{N^2}\left[e^{-f_s(r,T,m_D)/T} + (N^2-1)e^{-f_o(r,T,m_D)/T} + \mathcal{O}\left(\alpha_{\rm s}^3(rT)^4\right)\right]$$

$f_s = Q\bar{Q}$-color singlet free energy, $f_o = Q\bar{Q}$-color octet free energy
to be matched from the singlet and octet pNRQCD propagators

$$\frac{\langle S(\mathbf{r},\mathbf{0},1/T)S^\dagger(\mathbf{r},\mathbf{0},0)\rangle}{\mathcal{N}} = e^{-V_s(r)/T}(1+\delta_s) \equiv e^{-f_s(r,T,m_D)/T}$$

$$\frac{\langle O^a(\mathbf{r},\mathbf{0},1/T)O^{a\,\dagger}(\mathbf{r},\mathbf{0},0)\rangle}{\mathcal{N}} = e^{-V_o(r)/T}\left[(N^2-1)\langle P_A\rangle + \delta_o\right] \equiv (N^2-1)e^{-f_o(r,T,m_D)/T}$$

where δ_s and δ_o stand for thermal loop corrections to the singlet/octet propagators

$F_{Q\bar{Q}}$ on the lattice and pNRQCD

- low temperatures, $T \ll V_s$ (or $rT \ll \alpha_s$):

$$P_c \approx \frac{e^{-V_s/T}}{N^2}$$

- high temperatures, $T \gg V_s$ (or $rT \gg \alpha_s$):

P_c is a linear combination of $e^{-f_s/T}$ and $e^{-f_o/T}$.

A strict perturbative expansion in α_s corresponds to this regime.

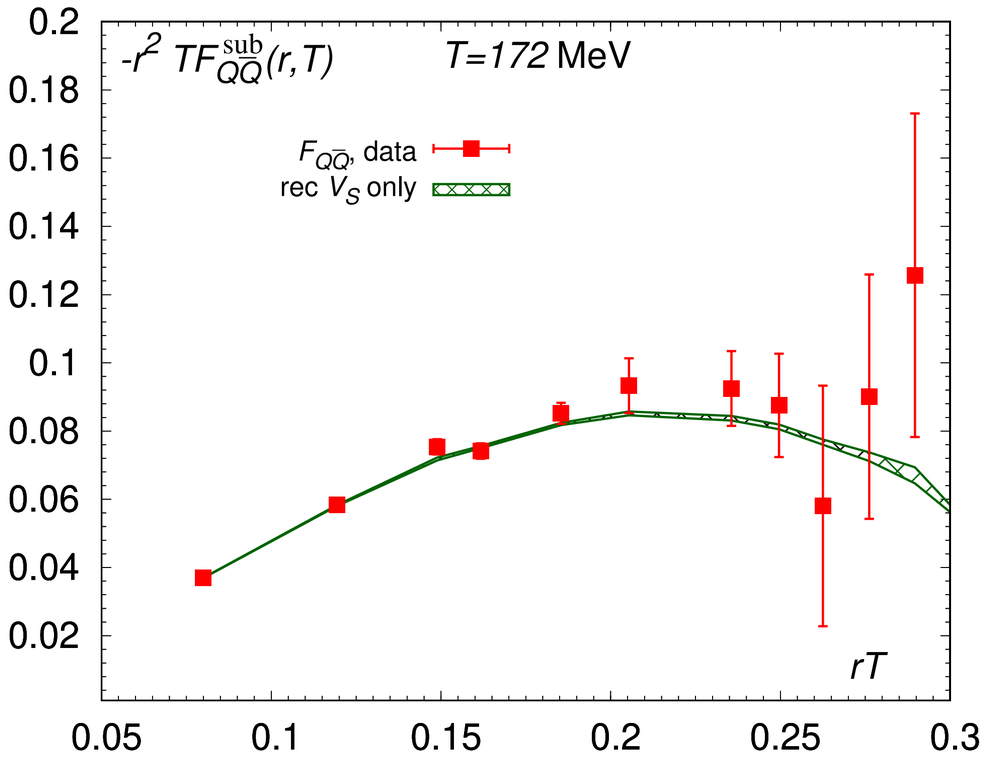

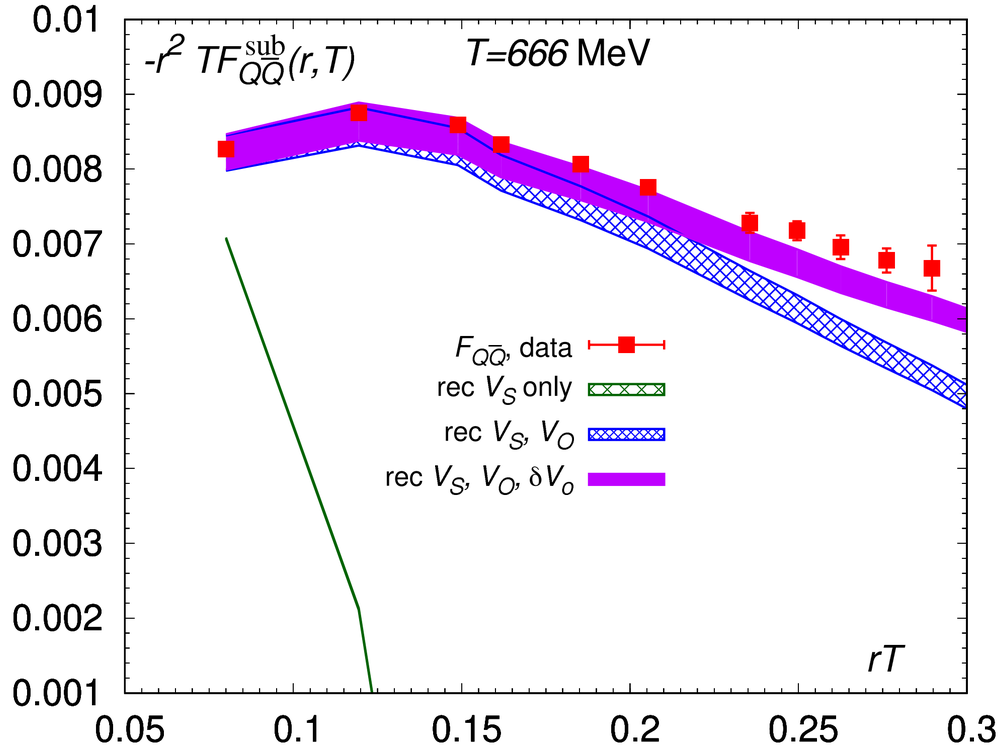

› TUMQCD coll. PR D98 (2018) 054511

Entropy vs 2+1 flavor lattice data

$$S_Q = -\frac{\partial F_Q(T)}{\partial T}$$

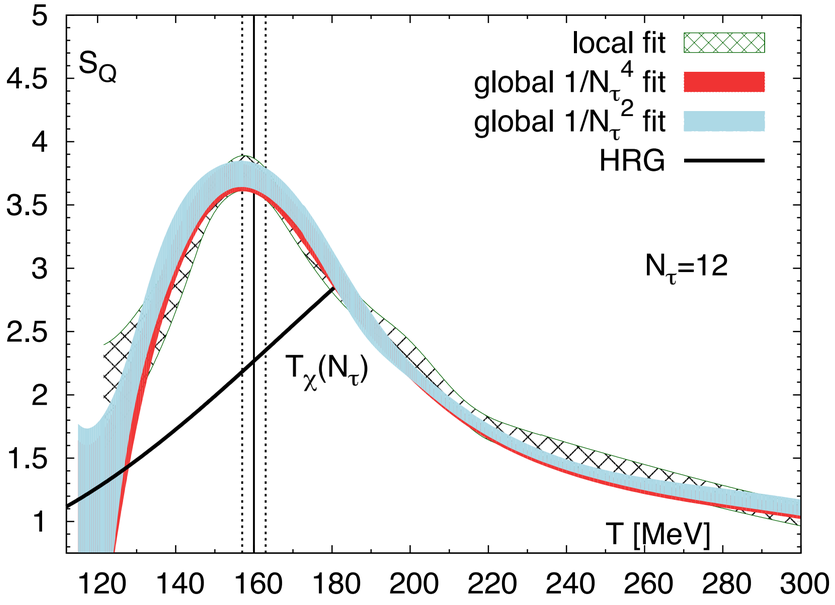

The entropy peaks around the chiral transition T, indicating that deconfinement and chiral transitions happen at similar T

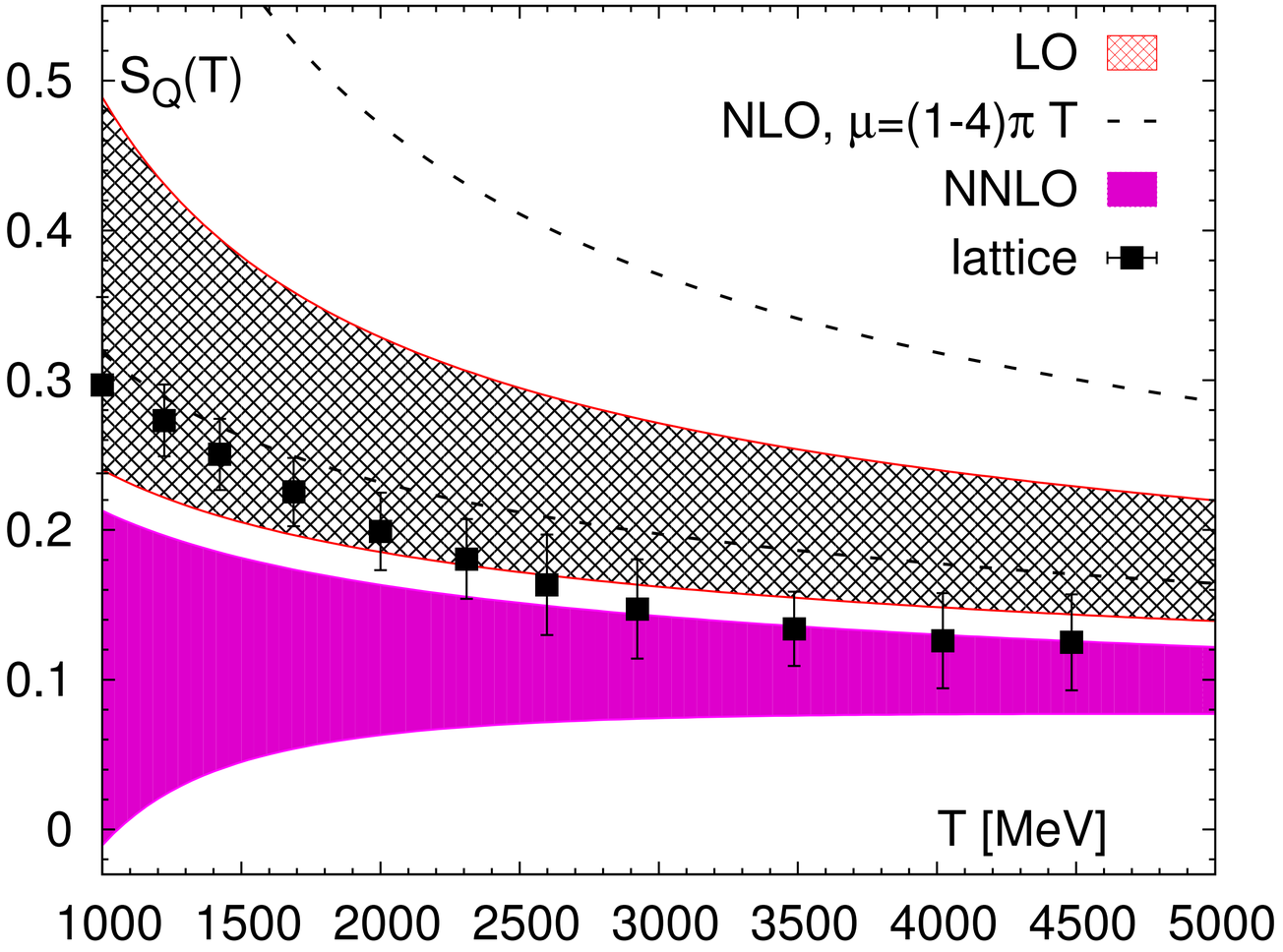

Position of the entropy peak: $T_S = 153^{+6.5}_{-5}$ MeV

- Bazavov Brambilla Ding Petreczky Schadler Vairo Weber PR D93 (2016) 114502

CONCLUSIONS

- Quarkonium suppression may be systematically studied with the use of **effective field theories** and **lattice QCD**
- **In equilibrium** properties like **dissociation width, cross section, mass shift…** have been computed as expansions in the small parameters of the system.
- **Out of equilibrium** properties, like octet recombination, can be studied by treating quarkonium as an open quantum system. Lattice input is crucial.

CONCLUSIONS

- Quarkonium suppression may be systematically studied with the use of **effective field theories** and **lattice QCD**
- **In equilibrium** properties like **dissociation width, cross section, mass shift...** have been computed as expansions in the small parameters of the system.
- **Out of equilibrium** properties, like octet recombination, can be studied by treating quarkonium as an open quantum system. Lattice input is crucial.

We have shown how the heavy quark-antiquark pair out-of-equilibrium evolution can be treated in the framework of pNRQCD. With respect to previous determinations:

- the medium may be a strongly-coupled plasma (not necessarily a quark-gluon plasma) whose characteristics are determined by lattice calculations;
- the total number of heavy quarks, i.e., $\mathrm{Tr}\{\rho_s\} + \mathrm{Tr}\{\rho_o\}$, is preserved by the evolution equations;
- the non-abelian nature of QCD is fully accounted for;
- the treatment does not rely on classical approximations.

The evolution equations follow from assuming the inverse size of the quark-antiquark system to be larger than any other scale of the medium and from being accurate at first non-trivial order in the multipole expansion and at first order in the heavy-quark density.

Under some conditions (large time, quasistatic evolution, quantum Brownian motion) the evolution equations are of the Lindblad form. Their numerical solution provides $R_{AA}[\Upsilon(nS)]$ and differential observables in good agreement with LHC data.

Outlook

- We need precise and unquenched determinations of the kappa and gamma transport coefficients

- Recombination effects are small for bottomonium for not for charmonium:
  we should go beyond the linear density approximation in that case

- We should investigate the effect of quarkonium moving with respect to the QGP and the anisotropy

- We should investigate the full master equations farther out of equilibrium: all the calculations holds
  if T is substituted by a generic scale

- We should investigate the full master equations farther Initial conditions may be tuned to account for
  pre equilibrium states like glasma

Lattice INPUT is crucial!

Outlook

- We need precise and unquenched determinations of the kappa and gamma transport coefficients

- Recombination effects are small for bottomonium for not for charmonium:
  we should go beyond the linear density approximation in that case

- We should investigate the effect of quarkonium moving with respect to the QGP and the anisotropy

- We should investigate the full master equations farther out of equilibrium: all the calculations holds
  if T is substituted by a generic scale

- We should investigate the full master equations farther Initial conditions may be tuned to account for
  pre equilibrium states like glasma

Inside EFT and OQS and with the help of the lattice quarkonium holds the promise to be a golden probe of QGP!

Lattice INPUT is crucial!

Backup

$v_2[\Upsilon(1S)]$ vs. Centrality

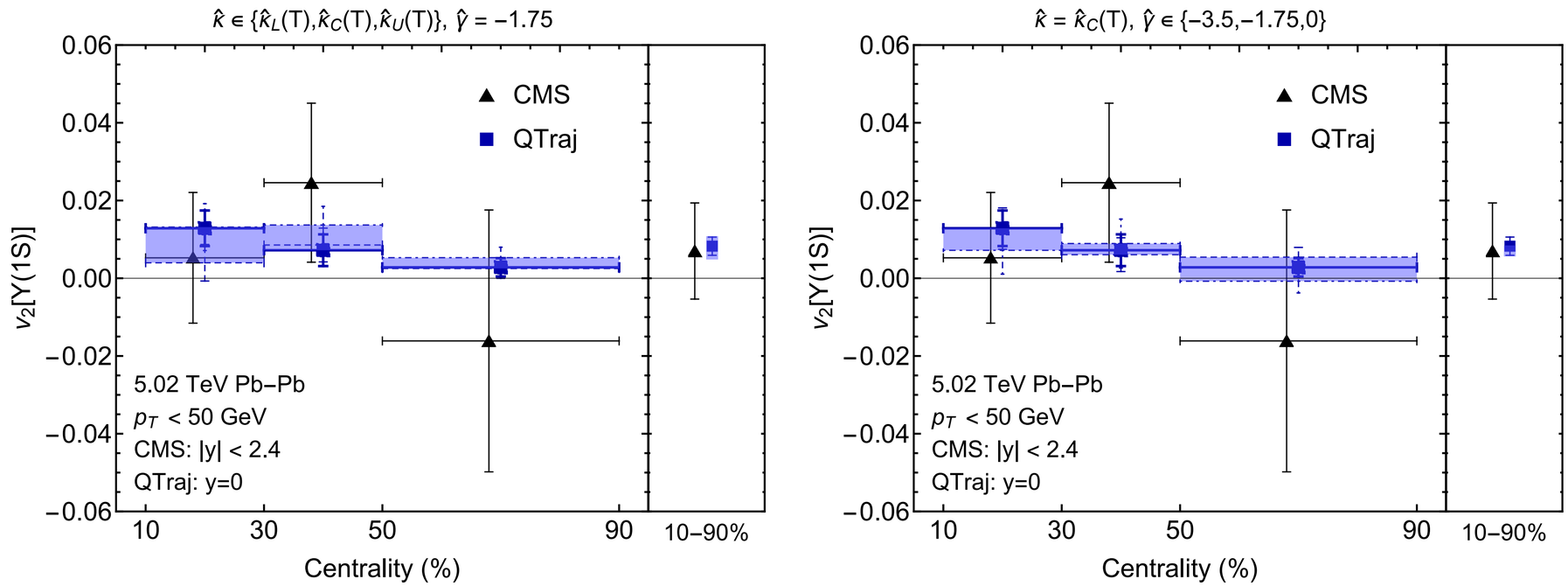

Figure: The elliptic flow v_2 of the $\Upsilon(1S)$ as a function of centrality compared to experimental measurements. The bands in the left plot represent variation of $\hat{\kappa}$ at fixed $\hat{\gamma} = -1.75$; the bands in the right plot represent variation of $\hat{\gamma}$ at fixed $\hat{\kappa} = \hat{\kappa}_C$.

$v_2[\Upsilon(1S)]$ vs. p_T

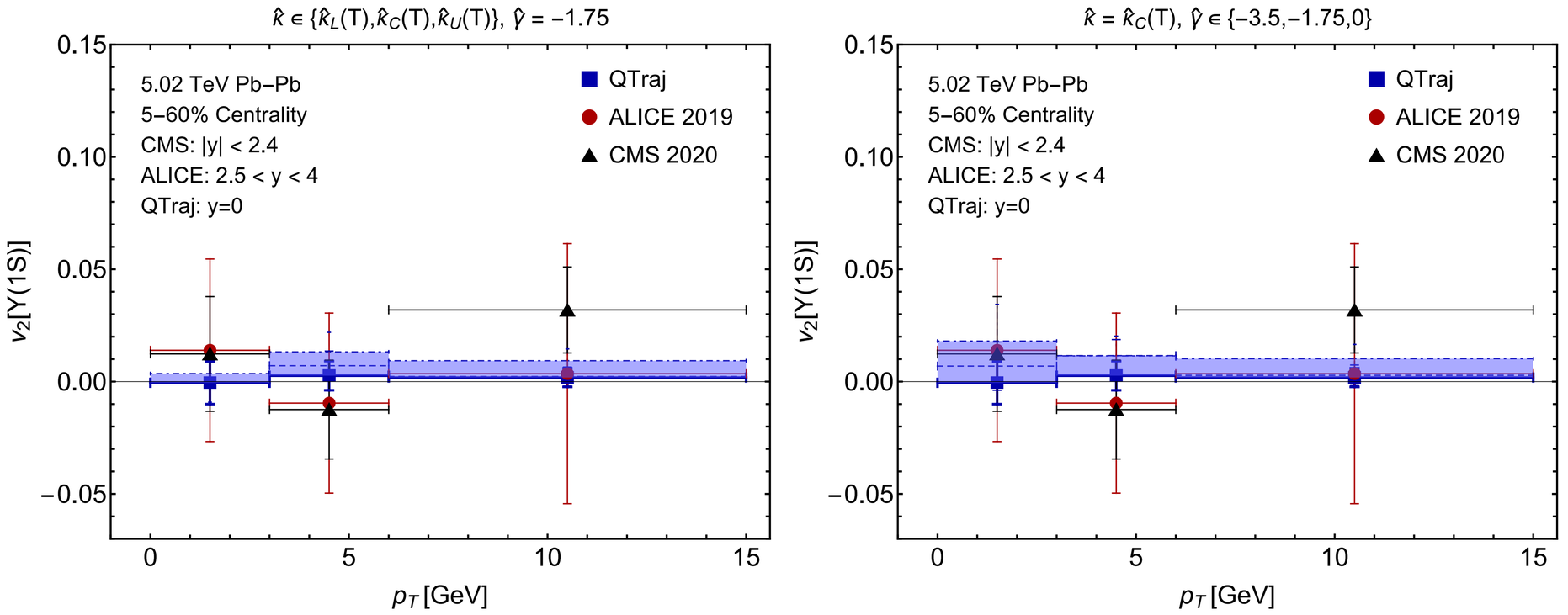

Figure: The elliptic flow v_2 of the $\Upsilon(1S)$ as a function of p_T compared to experimental measurements. The bands in the left plot represent variation of $\hat{\kappa}$ at fixed $\hat{\gamma} = -1.75$; the bands in the right plot represent variation of $\hat{\gamma}$ at fixed $\hat{\kappa} = \hat{\kappa}_C$.

Double Ratio 2S vs. p_T

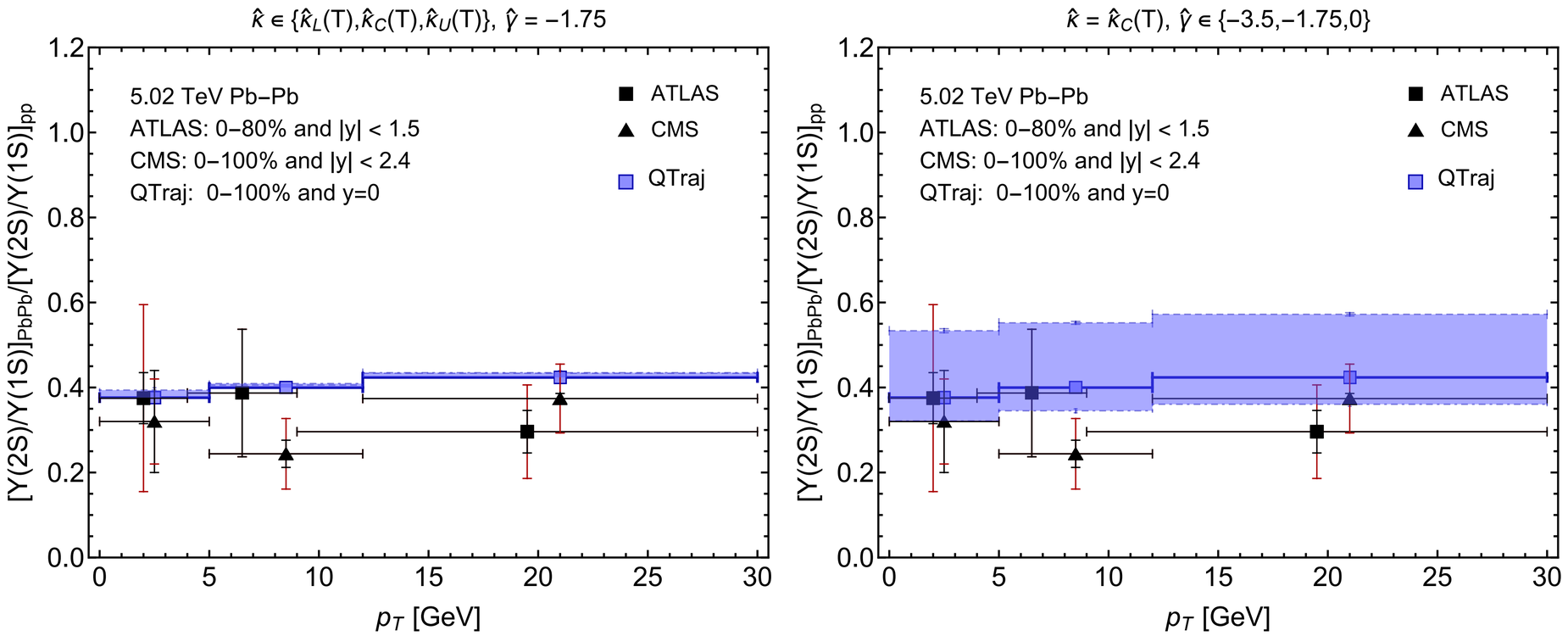

Figure: The double ratio of the nuclear modification factor $R_{AA}[\Upsilon(2S)]$ to $R_{AA}[\Upsilon(1S)]$ as a function of p_T compared to experimental measurements. The bands in the left plot represent variation of $\hat{\kappa}$ at fixed $\hat{\gamma} = -1.75$; the bands in the right plot represent variation of $\hat{\gamma}$ at fixed $\hat{\kappa} = \hat{\kappa}_C$. The black and red bars in the experimental data represent statistical and systematic uncertainties, respectively.

Double Ratio $2S$ vs. Centrality

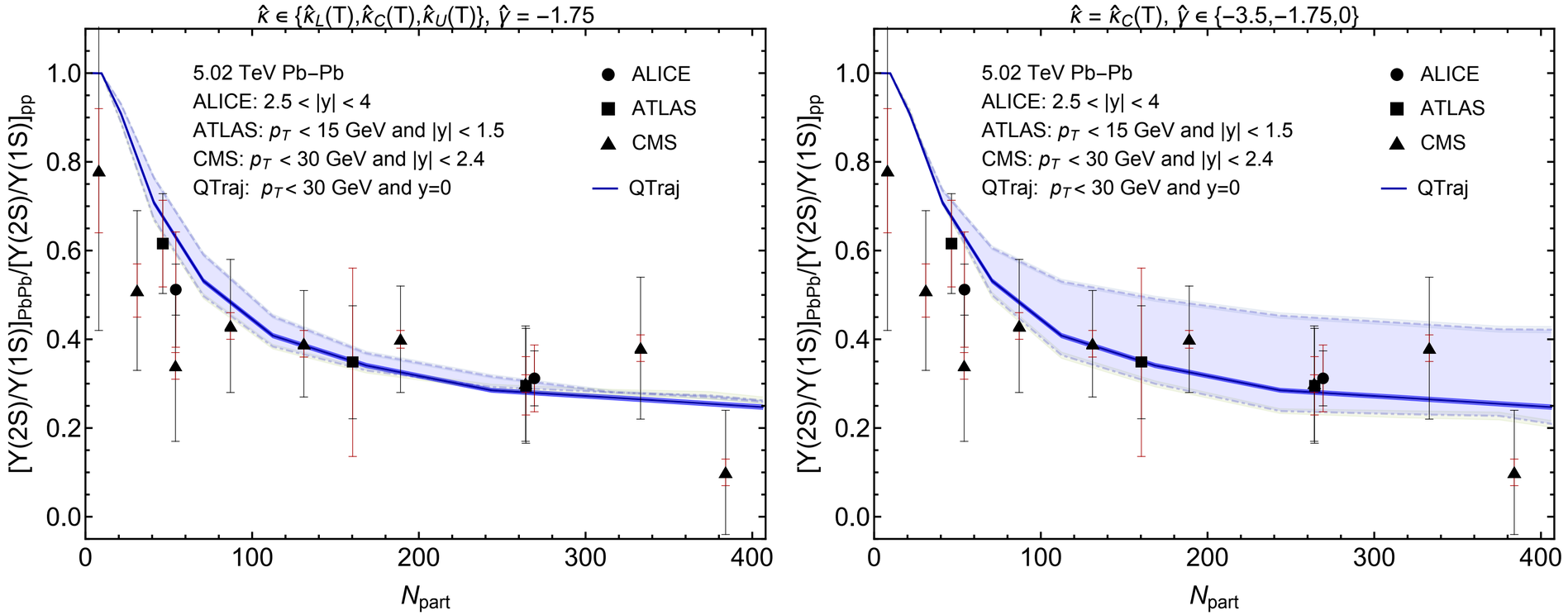

Figure: Ratio of $R_{AA}(2S)$ to $R_{AA}(1S)$ computed in QTraj compared to experimental results.

Double Ratio $3S$ vs. Centrality

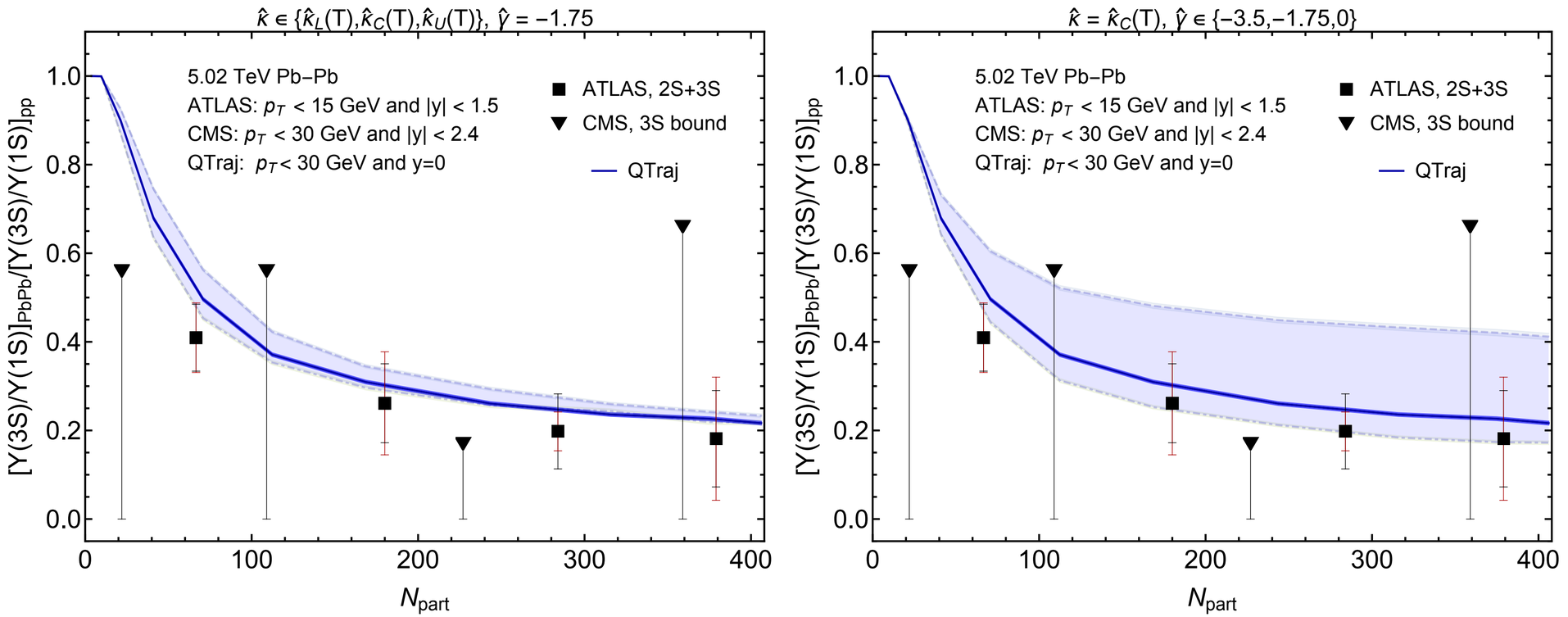

Figure: Ratio of $R_{AA}(2S)$ to $R_{AA}(1S)$ computed in QTraj compared to experimental results.

$v_2[\Upsilon(2,3S)]$ vs. Centrality

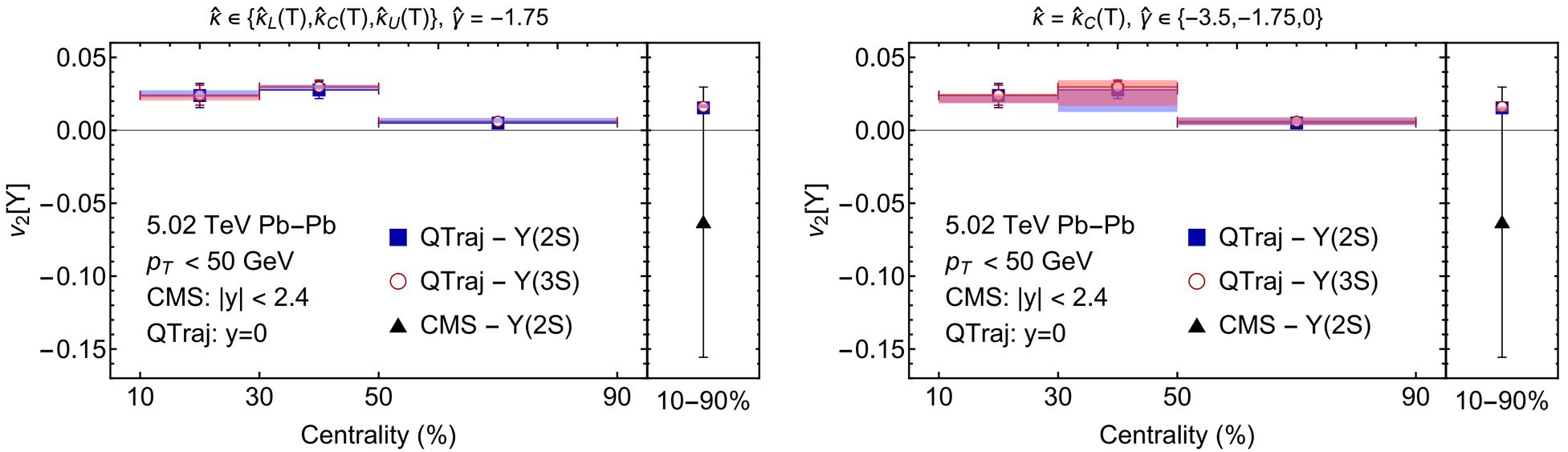

Figure: The elliptic flow v_2 of the $\Upsilon(2S)$ and $\Upsilon(3S)$ as a function of centrality compared to experimental measurements. The bands in the left plot represent variation of $\hat{\kappa}$ at fixed $\hat{\gamma} = -1.75$; the bands in the right plot represent variation of $\hat{\gamma}$ at fixed $\hat{\kappa} = \hat{\kappa}_C$.

The TUMQCD lattice calculation of kappa

N. B. , V. Leino, P. Petreczky, A. Vairo 2020

quenched with the multilevel algorithm in a window of T never attempted up to now

- Perform simulations in very wide range of temperatures
- See if we can connect to perturbation theory at high temperature
- Observe the temperature dependence of κ

T/T_c	$N_\mathrm{t} \times N_\mathrm{s}^3$	β	N_conf
1.1	12×48^3	6.407	1350
	16×48^3	6.621	2623
	20×48^3	6.795	2035
	24×48^3	6.940	2535
1.5	12×48^3	6.639	1801
	12×32^3	6.639	1557
	12×24^2	6.639	1000
	16×48^3	6.872	2778
	20×48^3	7.044	2081
	24×48^3	7.192	2496
2.2	12×48^3	6.940	1535
3	12×48^3	7.193	1579
	16×48^3	7.432	1553
	20×48^3	7.620	1401
	24×48^3	7.774	1663
6	12×48^3	7.774	1587
	16×48^3	8.019	1556
	20×48^3	8.211	1258
	24×48^3	8.367	1430
10	12×48^3	8.211	1807
	12×32^3	8.211	1737
	12×24^3	8.211	1000
	16×48^3	8.458	2769
	20×48^3	8.651	2073
	24×48^3	8.808	2423
10000	12×48^3	14.194	1039
	16×48^3	14.443	1157
	20×48^3	14.635	1139
	24×48^3	14.792	1375
20000	12×48^3	14.792	1948

TABLE I. Parameters of the lattice calculations.